

THIS REPORT HAS BEEN DELIMITED  
AND CLEARED FOR PUBLIC RELEASE  
UNDER DOD DIRECTIVE 5200.20 AND  
NO RESTRICTIONS ARE IMPOSED UPON  
ITS USE AND DISCLOSURE.

DISTRIBUTION STATEMENT A

APPROVED FOR PUBLIC RELEASE;  
DISTRIBUTION UNLIMITED.

# SECRET

## Services Technical Information Agency

Reproduced by

**DOCUMENT SERVICE CENTER**

**KNOTT BUILDING, DAYTON, 2, OHIO**

Best Available Copy

WHEN GOVERNMENT OR OTHER DRAWINGS, SPECIFICATIONS OR OTHER DATA ARE USED FOR ANY PURPOSE OTHER THAN IN CONNECTION WITH A DEFINITELY RELATED PROCUREMENT OPERATION, THE U. S. GOVERNMENT THEREBY INCURS NO LIABILITY, NOR ANY OBLIGATION WHATSOEVER; AND THE FACT THAT THE GOVERNMENT MAY HAVE FORMULATED, FURNISHED, OR IN ANY WAY SUPPLIED THE DRAWINGS, SPECIFICATIONS, OR OTHER DATA IS NOT TO BE REGARDED BY ANY OTHER PARTY AS IN ANY MANNER LICENSING THE HOLDER OR ANY OTHER PERSON, CORPORATION, OR CONVEYING ANY RIGHTS OR PERMISSION TO MANUFACTURE, REPRODUCE, OR ANY PATENTED INVENTION THAT MAY IN ANY WAY BE RELATED THERETO.

# UNCLASSIFIED

FC

109858601

WADC TECHNICAL REPORT 54-222

**A FUNDAMENTAL STUDY OF NATURAL AND SYNTHETIC  
FILMS ON MAGNESIUM AND ITS ALLOYS**

*THE DOW CHEMICAL COMPANY*

*AUGUST 1954*

*Best Available Copy*

WRIGHT AIR DEVELOPMENT CENTER

WADC TECHNICAL REPORT 54-222

**A FUNDAMENTAL STUDY OF NATURAL AND SYNTHETIC  
FILMS ON MAGNESIUM AND ITS ALLOYS**

*THE DOW CHEMICAL COMPANY*

*AUGUST 1954*

AERONAUTICAL RESEARCH LABORATORY

CONTRACT No. AF 33(038)-16655

PROJECT No. 7351

TASK No. 70608

WRIGHT AIR DEVELOPMENT CENTER  
AIR RESEARCH AND DEVELOPMENT COMMAND  
UNITED STATES AIR FORCE  
WRIGHT-PATTERSON AIR FORCE BASE, OHIO

## FOREWORD

This report was prepared by The Dow Chemical Company under Supplemental Agreement No. S2(520286) to USAF Contract No. AF 33(038)-16655. The contract was carried out under Project No. 7351, Metallic Materials, Task No. 70608, A Fundamental Study of Natural and Synthetic Films on Magnesium and its Alloys, and was administered under the direction of the Aeronautical Research Laboratory, Directorate of Research, Wright Air Development Center. Mr. E. J. Hassell served as project engineer.

## ABSTRACT

The development is described of techniques for the study of the films which are formed on magnesium during surface treatments or corrosion. Among the techniques described are electrical resistance measurements on isolated films and on surface treated electrodes during aqueous exposures, anodic polarization studies on magnesium alloys in inhibited electrolyte systems, and the microstructural study of surface treatment and corrosion films. Many of the properties of a film become understandable when the microstructural details of the film are known. Thus the hardness and abrasion resistance of the Dow No. 14, Dow No. 17 and H.A.E. films are related to their partial vitrification during the anodic treatment. By way of contrast, the Dow No. 7 film is a thin, smooth layer of a hydrous gel. Because of its structure it is susceptible to electrolytic permeation and to dehydration. Inadequacies in the protective abilities of the hydroxide films on magnesium stem from the spontaneous exfoliation of these films. Chromate ion inhibits the corrosion of magnesium by engendering the formation of a film which does not exfoliate.

## PUBLICATION REVIEW

The publication of this report does not constitute approval by the Air Force of the findings or the conclusions contained herein. It is published only for the exchange and stimulation of ideas.

FOR THE COMMANDER :



LESLIE B. WILLIAMS  
Colonel, USAF  
Chief, Aeronautical Research Laboratory  
Directorate of Research

## TABLE OF CONTENTS

	<u>Page No.</u>
INTRODUCTION . . . . .	1
SUMMARY OF RESULTS . . . . .	1
I. Electrical Impedance Measurements on Surface Treatment Films . . . . .	1
II. The Anodic Polarization of Magnesium Alloy Electrodes in Salt-Chromate Electrolytes . . . . .	2
CONCLUSIONS . . . . .	4
I. Electrical Impedance Measurements on Surface Treatment Films . . . . .	7
A. Measurements on Stripped Films . . . . .	7
B. Measurements Made Directly on Filmed Electrodes . . . . .	12
II. The Anodic Polarization of Magnesium Alloy Electrodes in Salt-Chromate Electrolytes . . . . .	19
A. Experimental . . . . .	19
B. Results . . . . .	22
III. The Study of Films with the Light and Elec- tron Microscopes . . . . .	31
A. General Techniques . . . . .	31
B. Specific Film Problems Studied with the Light and Electron Microscopes . . . . .	36
REFERENCES . . . . .	49

## LIST OF TABLES

<u>Table</u>	<u>Page No.</u>
I A Summary of the Resistances of Dow No. 14 Anodic Films Stripped from Pure Magnesium during Exposure to 0.1 N. Sodium Chloride Solution . . . . .	50
II A Summary of the Resistances of Dow No. 14 Anodic Films Stripped from FSl-O Alloy during Exposure to 0.1 N. Sodium Chloride Solution. (Film Thickness = 10 Microns) . . . . .	51
III A Summary of the Resistances of Filmed FSl Electrodes during Exposure to 0.1 N. Sodium Chloride Solution . . . . .	52
IV A Summary of the Resistances of Dow No. 7 Treated FSl Electrodes during Exposure to 0.5 N. Sodium Chloride Solution . . . . .	53
V A Summary of the Resistance of Dow's New Green, Anodic Treated FSl-O Electrodes during Exposure to 0.5 N. Sodium Chloride Solution. . . . .	54
VI Further Description of Elements in Polarizer Circuit Shown in Figure 18 . . . . .	55
VII Analyses of Alloys Discussed in This Report . . . . .	56
VIII Corrosion Rates of AZ31A-O Alloy Sheet in Aqueous Sodium Chloride-Sodium Chromate Solutions . . . . .	57
IX Characteristics of the Delay Effect during the Anodic Polarization of Magnesium Alloys in Sodium Chloride-Sodium Chromate Electrolyte . . . . .	58, 59, 60
X Characteristics of the Delay Effect during the Anodic Polarization of Magnesium Alloys in Sodium Bromide-Sodium Chromate Electrolyte . . . . .	61, 62, 63
XI Characteristics of the Delay Effect during the Anodic Polarization of Dow No. 7 Treated Magnesium Alloy in Sodium Chloride-Sodium Chromate Electrolyte . . . . .	64, 65

LIST OF TABLES (Cont.)

<u>Table</u>	<u>Page No.</u>
XII Summary of "Film Parameters" and Capacitances from Delay Data in the Electrolyte Systems NaCl-Na <sub>2</sub> CrO <sub>4</sub> - Aqueous and NaBr-Na <sub>2</sub> CrO <sub>4</sub> -Aqueous . . . . .	66,67
XIII The Effect of Current Density on the Delay Effect during the Anodic Polarization of Magnesium Alloys in 0.5 N. Sodium Chromate Solution . . . . .	68
XIV Summary at Two Current Density Levels of "Film Parameters" and Capacitances from Delay Data in 0.5 N. Na <sub>2</sub> CrO <sub>4</sub> Solutions . . . . .	69
XV The Thickness of Dow No. 7 Films on AZ31A Alloy as a Function of Alloy Condition and pH of the Dichromate Bath . . . . .	69

## LIST OF FIGURES

<u>Figure</u>	<u>Page No.</u>
1	Film Stripping Apparatus . . . . . 70
2	Cell for Measuring the Electrical and Osmotic Properties of Stripped Films . . . . . 71
3	Film Impedance Measuring Apparatus . . . . . 72
4	Circuit for Impedance Measurements on Films . . . . . 73
5	Variation of Cell Resistance with Frequency . . . . . 74
6	The Resistance of Stripped Dow No. 14 Films during Exposure to 0.1 N. Sodium Chloride Solution . . . . . 75
7	Impedance Cell No. 1 . . . . . 76
8	Impedance Cell No. 2 . . . . . 76
9	Impedance Cell No. 3 . . . . . 77
10	Electrical Characteristics of Dow No. 14 Treated FS Electrodes in Cell No. 1 . . . . . 78
11	Electrical Characteristics of Dow No. 14 Treated FS Electrode in Cell No. 2 . . . . . 79
12	Electrical Characteristics of an Acetic- Nitrate Pickled FS Electrode in Cell No. 2 . . . . . 80
13	The Resistance Characteristics of Cell No. 3 during Standardization with 0.5 N. Sodium Chloride Solution and Silver Electrodes . . . . . 81
14	Resistance Characteristics of Cell No. 3 when Two Dow No. 7 Treated FS1-H24 Alloy Electrodes Are in Series . . . . . 82
15	Resistance Characteristics of Cell No. 3 when Two Dow New Green Anodic Treated FS1-O Alloy Electrodes Are in Series. Electrode Pair No. 1 . . . . . 83
16	The Resistivity of Dow No. 7 Films on FS1 Alloy during Exposure to 0.5 N. Sodium Chloride Solution. . . . . 84

LIST OF FIGURES (Cont.)

<u>Figure</u>	<u>Page No.</u>
17 The Resistivity of Dow's New Green Anodic Treatment Films on FS1-0 Alloy during Exposure to 0.5 N. Sodium Chloride Solution . . . . .	85
18 Polarizer Circuit . . . . .	86
19 Cell for Polarization Studies . . . . .	87
20 Polarizer Apparatus . . . . .	88
21 Rotating Electrode for Polarization Measurements . . . . .	89
22 Polarization of Very High Purity Magnesium in 0.5 N. $\text{Na}_2\text{CrO}_4$ Saturated with $\text{Mg}(\text{OH})_2$ Showing the Effects of Polarization History . . . . .	90
23 Polarization of Very High Purity Magnesium in Salt-Chromate Solutions . . . . .	91
24 Polarization of Cell Magnesium in Salt- Chromate Solutions . . . . .	92
25 Polarization of AZ10A Alloy in Salt- Chromate Solutions . . . . .	93
26 Polarization of AZ31A Alloy in Salt- Chromate Solutions . . . . .	94
27 Polarization of AZ31B Alloy in Salt- Chromate Solutions . . . . .	95
28 Polarization of AZ63A Alloy in Salt- Chromate Solutions . . . . .	96
29 Polarization of Very High Purity Magnesium in Salt-Chromate Solutions . . . . .	97
30 Polarization of Cell Magnesium in Salt- Chromate Solutions . . . . .	98
31 Polarization of AZ10A Alloy in Salt- Chromate Solutions . . . . .	99
32 Polarization of AZ31A Alloy in Salt- Chromate Solutions . . . . .	100

LIST OF FIGURES (Cont.)

<u>Figure</u>	<u>Page No.</u>
33 Polarization of AZ63A Alloy in Salt-Chromate Solutions . . . . .	101
34 Corrosion Rate of AZ31A-O Alloy Sheet in Aqueous Sodium Chloride-Sodium Chromate Solutions . . . . .	102
35 Polarization of Very High Purity Magnesium in Sodium Bromide-Chromate Solutions . . . . .	103
36 Polarization of Cell Magnesium in Sodium Bromide-Chromate Solutions . . . . .	104
37 Polarization of AZ10A Alloy in Sodium Bromide-Chromate Solutions . . . . .	105
38 Polarization of AZ31A Alloy in Sodium Bromide-Chromate Solutions . . . . .	106
39 Polarization of AZ31B Alloy in Sodium Bromide-Chromate Solutions . . . . .	107
40 Polarization of AZ63A in Sodium Bromide-Chromate Solutions . . . . .	108
41 Polarization of Very High Purity Magnesium in Sodium Bromide-Chromate Solutions . . . . .	109
42 Polarization of Cell Magnesium in Sodium Bromide-Chromate Solutions . . . . .	110
43 Polarization of AZ10A Alloy in Sodium Bromide-Chromate Solutions . . . . .	111
44 Polarization of AZ31A Alloy in Sodium Bromide-Chromate Solutions . . . . .	112
45 Polarization of AZ31B Alloy in Sodium Bromide-Chromate Solutions . . . . .	113
46 Polarization of AZ63A Alloy in Sodium Bromide-Chromate Solutions . . . . .	114
47 Polarization of Dow No. 7 Treated AZ31A Alloy in Sodium Chloride-Chromate Solutions . . . . .	115
48 Polarization of Dow No. 7 Treated AZ31B Alloy in Sodium Chloride-Chromate Solutions . . . . .	116

LIST OF FIGURES (Cont.)

<u>Figure</u>	<u>Page No.</u>
49	Polarization of Dow No. 7 Treated AZ63A in Sodium Chloride-Chromate Solutions . . . . . 117
50	Polarization of Dow No. 7 Treated AZ31A Alloy in Sodium Chloride-Chromate Solutions . . . . . 118
51	Polarization of Dow No. 7 Treated AZ31B Alloy in Sodium Chloride-Chromate Solutions . . . . . 119
52	Polarization of Dow No. 7 Treated AZ63A in Sodium Chloride-Chromate Solutions . . . . . 120
53	Polarization Curves for Very High Purity Magnesium in 0.5 N. Na <sub>2</sub> CrO <sub>4</sub> Solution at Two Rates of Current Density Increase . . . . . 121
54	Polarization Curves for AZ31A Alloy in 0.5 N. Na <sub>2</sub> CrO <sub>4</sub> Solution at Two Rates of Current Density Increase . . . . . 122
55	Profile View at 1025X of Dow No. 14 Anodic Treatment on FS1-O Alloy . . . . . 123
56	Profile View at 1025X of Above Treatment That Has Been Interrupted at 85 Volts . . . . . 123
57	Profile Views of Dow No. 17 A.C. Anodic Treatment Films . . . . . 124
58	Profile Views of Dow D.C. Anodic Treatment Films . . . . . 125
59	Voltage Change with Time on Applying Dow No. 17 Treatment to AZ31A Alloy at 20 Amperes per Square Foot . . . . . 126
60	The Thickness of the Dow No. 17 Film on AZ31A Alloy as a Function of the Terminal Anodization Voltage . . . . . 127
61	The Thickness of the Dow No. 17 Film on AZ31A Alloy as a Function of Time of Anodi- zation at 20 Amperes per Square Foot . . . . . 128
62	Profile Views of the H.A.E. Treatment Film (Oblique Light) . . . . . 129

LIST OF FIGURES (Cont.)

<u>Figure</u>	<u>Page No.</u>
63 Profile Views of the H.A.E. Treatment Film (Polarized Light) . . . . .	129
64 Fading of Dow No. 7 Treatment Films on Ex- posure to 3 Percent Sodium Chloride Solution . . .	130
65 Profile Views of Dow No. 7 Treatment Films after Exposure to 3 Percent Sodium Chloride Solution . . . . .	131
66 Top Surface Views of Dow No. 7 Treatment Films after Exposure to 3 Percent Sodium Chloride Solution . . . . .	132
67 Top Surface View of a Dow No. 7 Treatment Film That Was Exposed Indoors for One Month and Then Exposed to Distilled Water for 15 Hrs. . .	133
68 Profile Views of Dow No. 7 Treatment Films Showing Manganese Precipitate Protruding into or Through the Film . . . . .	134
69 Top Surface Views of No. 7 Treatment Films Showing the Effect of Heating . . . . .	135
70 Profile Views of No. 7 Treatment Films Showing the Effect of Heating . . . . .	136
71 Electronmicrograph of the External Surface of a Dow No. 7 Treatment Film . . . . .	137
72 Electronmicrograph of the External Surface of a Dow No. 7 Treatment Film . . . . .	138
73 Electronmicrograph of the External Surface of a Dow No. 7 Treatment Film . . . . .	139
74 Electronmicrograph of the External Surface of a Dow No. 7 Treatment Film . . . . .	140
75 Electronmicrograph of the External Surface of a Dow No. 7 Treatment Film . . . . .	141
76 Electronmicrograph of the External Surface of a Dow No. 7 Treatment Film . . . . .	142
77 Profile Views of the Iridite Treatment Film on Magnesium . . . . .	143

LIST OF FIGURES (Cont.)

<u>Figure</u>	<u>Page No.</u>
78 Electronmicrographs of the Surface of Very High Purity Magnesium after Exposure to Distilled Water (Five-Minute Exposure) . . . . .	144
79 Electronmicrographs of the Surface of Very High Purity Magnesium after Exposure to Distilled Water (Twenty-Minute Exposure) . . . . .	144
80 Electronmicrographs of the Surface of Very High Purity Magnesium after Exposure to Distilled Water (One-Hour Exposure) . . . . .	145
81 Electronmicrographs of the Surface of Very High Purity Magnesium after Exposure to Distilled Water (Two-Hour Exposure) . . . . .	145
82 Electronmicrographs of the Surface of Very High Purity Magnesium after Exposure to Distilled Water (Four-Hour Exposure) . . . . .	146
83 Electronmicrographs of the Surface of Very High Purity Magnesium after Exposure to Distilled Water (Twenty-Four Hour Exposure) . . . . .	146
84 Electronmicrographs of the Surface of Very High Purity Magnesium after One Hour's Exposure to 0.5 N. $\text{Na}_2\text{CrO}_4$ Solution (Specimen Screen 2) .	147
85 Electronmicrographs of the Surface of Very High Purity Magnesium after One Hour's Exposure to 0.5 N. $\text{Na}_2\text{CrO}_4$ Solution (Specimen Screen 1) .	147
86 Electronmicrograph of the Surface of Very High Purity Magnesium after Exposure to 0.01 N. $\text{NaCl}$ -0.49 N. $\text{Na}_2\text{CrO}_4$ for One Hour . . . . .	148
87 Electronmicrograph of the Surface of Very High Purity Magnesium after Exposure to 0.2 N. $\text{NaCl}$ -0.3 N. $\text{Na}_2\text{CrO}_4$ for One Hour . . . . .	149
88 Electronmicrograph of the Surface of Very High Purity Magnesium after Exposure to 0.05 N. $\text{Na}_2\text{CrO}_4$ -0.45 N. $\text{NaCl}$ for One Hour . . . . .	150
89 Electronmicrograph of the Surface of Very High Purity Magnesium after Exposure to 0.01 N. $\text{Na}_2\text{CrO}_4$ -0.49 N. $\text{NaCl}$ for One Hour . . . . .	151

LIST OF FIGURES (Cont.)

<u>Figure</u>		<u>Page No.</u>
90	Electronmicrograph of the Surface of Very High Purity Magnesium after Exposure to 0.001 N. $\text{Na}_2\text{CrO}_4$ -0.499 N. NaCl for One Hour . . .	152
91	Electronmicrographs of the Surface of Very High Purity Magnesium after One Hour's Exposure to 0.5 N. NaCl Solution (Specimen Screen 3) . .	153
92	Electronmicrographs of the Surface of Very High Purity Magnesium after One Hour's Exposure to 0.5 N. NaCl Solution (Specimen Screen 4) . .	153
93	Electronmicrographs of the Surface of Very High Purity Magnesium after One Hour's Exposure to 0.5 N. NaCl Solution . . . . .	154
94	Electronmicrographs of the Surface of Very High Purity Magnesium after One Hour's Exposure to 0.5 N. NaCl Solution . . . . .	154

A FUNDAMENTAL STUDY OF NATURAL AND SYNTHETIC  
FILMS ON MAGNESIUM AND ITS ALLOYS

INTRODUCTION

In common with the other base metals, the chemical reactivity of magnesium is greatly influenced by the nature of the films at the solid-reactant interface. In its dual role as both a structural material and a chemical, magnesium makes many and diverse demands on its films. It is the purpose of this work to deepen our understanding of the deposition and performance of some of these films.

SUMMARY OF RESULTS

I. Electrical Impedance Measurements  
on Surface Treatment Films

1. Dow No. 14 films as thin as 3 microns have been stripped by selectively dissolving the host metal in a Grignard reaction.
2. Attempts to strip Dow No. 17 films and thin corrosion films in the above manner invariably lead to rupture of the film section.
3. A 12 micron thick film which had been formed on pure magnesium by the Dow No. 14 anodic treatment had an electrical resistance of 16-20 ohms-cm<sup>2</sup> when stripped and exposed to aqueous 0.1 N. sodium chloride solution.
4. The resistance of three sections of the above film agreed within  $\pm 2$  ohms-cm<sup>2</sup>.
5. A film formed by the above treatment which had been interrupted at a film thickness of 7 microns had an electrical resistance of 4-6 ohms-cm<sup>2</sup> under the above conditions.
6. A film formed by the above treatment which had been interrupted at a film thickness of 3-4 microns had an electrical resistance of 3-5 ohms-cm<sup>2</sup> under the above conditions.
7. A 10 micron thick film which had been formed on FS1-0 alloy by the above treatment had an electrical resistance of 15-22 ohms-cm<sup>2</sup> under the above conditions.
8. The above film has a capacitance of approximately 0.03  $\mu$ f/cm<sup>2</sup>.

9. Both the 12 micron thick film from pure magnesium and the 10 micron thick film from FS1-0 alloy show a gradual increase in resistance for about the first ten hours of exposure to the electrolyte.

10. The resistance to alternating current of Dow No. 7, Dow No.14 and Dow No.17 treated FS1 alloy electrodes are approximately linear functions of the reciprocal of the frequency between 2,000 and 8,000 cycles per second.

11. The area resistivity of a Dow No. 14 film of ten microns thickness is approximately 100 ohms-cm<sup>2</sup> when exposed in situ on FS1-0 alloy to 0.1 N. sodium chloride solution.

12. The above film increases in resistivity during exposure under the above conditions.

13. The area resistivity of a Dow No. 7 film of 2.0 microns thickness is approximately 10 ohms-cm<sup>2</sup> when exposed on FS1-H24 alloy under the above conditions.

14. The area resistivity of a Dow No. 7 film of 2.2 microns thickness is approximately 5 ohms-cm<sup>2</sup> when exposed on FS1-H24 alloy to 0.5 N. sodium chloride solution.

15. The above film decreases in resistivity during exposure under the above conditions.

16. The area resistivity of a Dow No. 7 film of 1.4 microns thickness is approximately 3 ohms-cm<sup>2</sup> when exposed on FS1-0 alloy to 0.5 N. sodium chloride solution.

17. The above film decreases in resistivity during exposure under above conditions.

18. The area resistivity of a Dow No. 17 film of 1.5 mils nominal thickness is approximately 10 ohms-cm<sup>2</sup> when exposed on FS1-0 alloy to 0.5 N. sodium chloride solution.

19. The above film decreases in resistivity during exposure under the above conditions.

## II. The Anodic Polarization of Magnesium Alloy Electrodes in Salt-Chromate Electrolytes

1. The partial replacement of 0.5 N. sodium chloride solution by 0.5 N. sodium chromate solution causes a depression in the potential of six magnesium alloys of up to 0.1 volt, but causes no significant polarization until the solution is richer than 0.4 N. in sodium chromate.

2. At 0.45 N. sodium chromate, the six alloys all show anodic polarization, but the potentials oscillate wildly.

3. With electrolytes richer in chromate than the above, extensive and reproducible anodic polarization occurs.

4. In the above electrolyte system, chromate concentrations as low as 0.001 N. significantly inhibit the corrosion of AZ31A-O alloy.

5. At chromate levels greater than 0.1 N., the corrosion is nearly completely inhibited during 14 day stagnant immersion.

6. Films displaying first order interference tints are produced at 0.45 N. sodium chromate. These tints are unique to a narrow region of electrolyte composition.

7. Chromate inhibition over the range of concentrations studied leads to a decrease in both the area and the depth of attack.

8. The six magnesium alloys show very weak anodic polarization in 0.5 N. sodium bromide solution.

9. Slightly more pronounced polarization occurs on the partial replacement of the above solution with 0.5 N. sodium chromate to give a total chromate concentration of 0.2 N.

10. Extensive polarization occurs in the sodium bromide-sodium chromate system at about the same chromate concentration as it does in the sodium chloride-sodium chromate system.

11. Three alloys which were given the No. 7 treatment and then subjected to polarization measurements in the electrolyte system sodium chloride-sodium chromate show essentially the same polarization behavior as untreated electrodes at chromate concentrations of 0.45 N. to 0.5 N.

12. The No. 7 treated electrodes also show significant anodic polarization at chromate concentrations as low as 0.1 N.

13. The above electrodes show no significant polarization in chromate free 0.5 N. sodium chloride.

14. With all of the above systems in the regions where severe anodic polarization occurs, as the current density is increased at a uniform rate, the potential moves in the cathodic direction very rapidly and then partially recovers to give a definite minimum in the current density-potential curve.

15. Doubling the rate of current density increase decreases the time and increases the current density at which the potential minimum is reached.

16. The above procedure does not significantly change the total charge that has been transported when the minimum is reached.

17. The above charge is of the proper magnitude to account for the formation of an ion monolayer at the electrode surface.

### CONCLUSIONS

1. The measurement of the properties of stripped films is largely confined to thick anodic films.

2. Dow No. 14 films which have been stripped by a Grignard reaction and exposed to aqueous sodium chloride solution show no evidence of a "barrier layer" which possesses unusual electrical properties.

3. The thickness of the above films has no significant effect on their volume resistivities.

4. There is no substantial difference in volume resistivities between Dow No. 14 films stripped from AZ31A-O alloy and those stripped from pure magnesium.

5. Stripped Dow No. 14 films show excellent stability in their electrical properties on continued exposure to dilute aqueous sodium chloride.

6. The measurement of film resistances directly on filmed electrodes by a.c. bridge methods using variable frequency signals is suitable for indicating the order of this property and for showing its more prominent trends with time.

7. The above measurement is not suitable for showing marginal differences in films.

8. The increase in resistance of Dow No. 14 films with time of exposure to 0.1 N. sodium chloride solution is due to film sealing by a hydration process.

9. The decrease in resistance of the Dow No. 7 film with time of exposure to 0.5 N. sodium chloride solution is due to the diffusion of electrolyte into the gel structure of the film.

10. There is no significant difference in the volume resistivity of the Dow No. 7 film when formed on AZ31A-H24 alloy from that of the same type of film when formed on AZ31A-0 alloy.

11. The decrease in resistance of the Dow No. 17 film with time of exposure to 0.5 N. sodium chloride solution is due to the permeation of electrolyte into voids in this exceedingly porous film.

12. The anomalously low resistivity of the above film is also due to the aforementioned porosity.

13. At concentrations less than 0.45 N. in the presence of 0.05 N. sodium chloride or sodium bromide, sodium chromate acts partially but not exclusively as an anodic inhibitor for magnesium alloys.

14. As the sodium chromate concentration is further increased at the expense of either of the above halides, sodium chromate acts as a severe anodic inhibitor for magnesium alloys.

15. Sodium chromate is a safe, contractive inhibitor for the corrosion of AZ31A-C alloy in sodium chloride solution.

16. Chromate engendered films less than 500 Å thick can cause severe anodic polarization.

17. The inhibition of the corrosion of AZ31A-0 alloy in sodium chromate-sodium chloride electrolyte can be produced by films less than 500 Å thick.

18. The delay effect is caused by the charging and discharging of an ion monolayer which is protected by a more massive film.

19. The Dow No. 14, Dow No. 17 and H.A.E. films are ceramic films which are formed by the fusion of glass producing oxides and/or oxy-salts deposited during the anodization.

20. The propensity of the Dow No. 17 and H.A.E. films for oils and waxes is due to their exceedingly porous structures.

21. Both the a.c. and the d.c. modifications of the Dow No. 17 treatment produce films by the same high efficiency process.

22. The Dow No. 7 film is a gel.

23. Variations in the color of the above films as the alloy is changed or as the pH of the dichromate boil is changed are largely due to differences in film thickness.

24. The cracking of the above film during extended room temperature aging or during heating is due to the loss of water of gelation.

25. The darkening and loss of translucency of the above film during moderate heating is largely due to the loss of water of gelation.

26. The decrease in thickness and fading of the above film during its exposure to initially neutral aqueous solutions is due to its dissolution which may be largely preferential in chromate ion.

27. The inferiority of an early Iridite treatment to the Dow No. 7 treatment may be due to the poorer continuity of the film produced by the former and by the manner in which the etching action of the bath leaves the film poorly supported by the metal.

28. The hydroxide films formed on very high purity magnesium in distilled water or sodium chloride solution are subject to an exfoliation process which robs them of part of their ability to protect the metal.

29. The addition of sodium chromate to the above solutions engenders films of greater physical stability toward exfoliation and in this manner aids in protecting the metal.

30. The existence of columnar growths on the films formed during corrosion in chromate inhibited sodium chloride solution is evidence that such inhibition is partially anodic in mechanism.

## I. Electrical Impedance Measurements on Surface Treatment Films

### A. Measurements on Stripped Films

Since the corrosion of magnesium in electrolytic environments proceeds by an electrochemical mechanism, it is reasonable to expect that at least a portion of the contribution of a surface treatment film in decreasing corrosion is due to its ability to decrease local action currents by increasing the resistance of the local action circuit. From this viewpoint, the electrical resistivity of the film during exposure to the corrosion environment becomes an important property of the film. Following this line of reasoning, Burwell and May<sup>1</sup> made resistivity measurements on various anodic films which they stripped from aluminum. The approach to be described here represents the application of their techniques to films that have been stripped from magnesium.

#### 1. Experimental

##### a. The Preparation of Films for Measurement

The Dow No. 14 a.c. anodic treatment films discussed in this report were prepared according to the directions given in Dowmetal Bulletin No. DM 103b. A thin sheet of the alloy desired was given an acetic-nitrate pickle of one-half mil per side, and then anodized in the No. 14 bath until the desired thickness was obtained. The thickness was controlled by the terminal anodization voltage and was measured under the microscope by methods which will be described later.

A section of the anodized sheet was then cemented with water glass to the flat-ground end of a one inch length of nine millimeter glass tubing. The external film and most of the metal was then dissolved away in dilute hydrochloric acid. Then the mounted sample was desiccated thoroughly over Drierite.

The remainder of the magnesium was then selectively dissolved from the film by a Grignard reaction in the apparatus shown in Figure 1. The reagents used were a solution of n-butyl bromide in diethyl ether. It is essential that the dissolution reaction proceed gently, and to this end, it is necessary to initiate the reaction below the customary reflux temperature. By rigorously excluding moisture from the system through the use of dry reagents, a drying tube, and Drierite in the reaction vessel, and by always retaining some of the Grignard compound from the previous reaction to initiate the one in progress, the complete dissolution of the metal can be made to occur without visible turbulence.

On completion of the reaction, the level of the reaction mixture was lowered well below the film, and the film was rinsed in place with anhydrous ether from the orifice (b). This is necessary to remove any residual n-butyl magnesium bromide dietherate which will hydrolyze to deposit magnesium hydroxybromide on the film when it is exposed to moisture.

By the above stripping technique, free Dow No. 14 films as thin as three microns can be obtained intact. Attempts to strip thinner films such as those from the Dow No. 7 treatment invariably lead to film rupture.

Prior to the "taming" of the Grignard reaction for this purpose, attempts were made to selectively

dissolve the magnesium from the film in etherial solutions of hydrogen bromide and of hydrogen iodide. However, the rate of solution of magnesium was too slow in these reagents to be practical. Grignard reactions employing allyl bromide and ethyl bromide were also explored. The latter worked about as well as n-butyl bromide. The reaction with allyl bromide, however, tended to become too vigorous.

The tube on which the film was mounted was then joined with Pyseal cement to the cell shown in Figure 2 so that the film was midway between the platinum electrodes. The cell was then filled with a 0.1 N. solution of sodium chloride to complete the electrolytic circuit. The filling of the cell was complicated by a tendency for air to become entrapped near the upper electrode and by the inability of the more fragile films to withstand even slight pressures without rupturing. The difficulty from air entrapment was partially alleviated by making the glass surfaces non-wetting near the electrode by the judicious use of a silicone grease. Even very careful filling of the cell, however, resulted in an extremely high "mortality" rate for the thinner films.

#### b. The Technique of Measurement

The instrumentation and the circuit for the the impedance measurements are shown in Figure 3 and Figure 4, respectively. The components of the circuit are:

- (1) A Hewlett-Packard, Model 200, Audio Oscillator.
- (2) A General Radio, Model 650A, Impedance Bridge.
- (3) A. Dumont, Type 208B, Cathode Ray Oscillograph.

(4) A Thorardson, Model T-20A25, Interstage Transformer.

(5) A decade condenser to cover the capacitance range of 0.0005 to 1

(6) A General Radio, Type 539A, Variable Air Condenser with a range of 50 to 550

The measurement cell is thermostated in transformer oil to reduce stray capacitance. The thermostat bath is maintained at  $25 \pm 0.05$  degrees Centigrade.

The impedance measurements are made over a range of audio frequencies. Each measurement is made by adjusting the resistance of the bridge and the parallel capacitance of the decade and air condensers until the oscillographic detector shows the amplitude of the signal across the bridge arms to be a minimum. At a signal frequency of one kilocycle per second or higher, the ripple in the cathode-ray trace at balance is barely noticeable even at the maximum amplification of the oscilloscope.

The repetition of such measurements for the film in place and the film removed permit the calculation of the film resistance and capacitance from the following expressions:

$$R_f = R_2 - R_1 \quad (1.)$$

$$C_f = \frac{R_2^2 C_2 - R_1^2 C_1}{(R_2 - R_1)^2} \quad (2.)$$

where R is resistance, C is capacitance, and the subscripts f, 2 and 1 refer to film, value measured with film intact, and value measured with film removed respectively.

## 2. Results

The frequency characteristics of the resistance measurements discussed here are illustrated in Figure 5. This graph is based on measurements made on a Dow No. 14 film of 12 micron thickness which had been stripped from pure magnesium. It is typical of the behavior experienced during all of these measurements. The use of semi-logarithmic paper tends to de-emphasize the manner in which the measured resistance become nearly independent of frequency at high frequencies, and the manner in which the resistance increases rapidly with decreasing frequency. This behavior can only be explained in terms of increasing polarization of the bright platinum electrodes with decreasing frequency. Not only does this behavior decrease the accuracy of the calculated film resistance by increasing the gross error in the resistance measurements, but being a polarization phenomenon, it is current sensitive and thus influenced by the difference in current flowing at a fixed potential across the bridge when the film is removed. For these reasons, all resistance readings made at frequencies less than 1000 cycles per second have been discarded, and even the values at 1000 and 2000 cycles are regarded with suspicion in some cases.

The variations in resistance during exposure to 0.1 N. sodium chloride solution for Dow No. 14 films of different thicknesses which have been stripped from both pure magnesium and FS1 alloy are shown in Tables I and II and Figure 6. The curves for the area resistivities are designed to show two things: (1) the general resistivity levels of the films, and (2) the increase in resistivity of these films during the first ten hours of exposure. To assure that the second trend was preserved in the mean curve, the mean curve has not been fitted to the individual data of the various sections, but instead is the mean of the curves for the various sections.

The increase in the resistivity of these thicker films is probably due to a small amount of pore sealing due to a hydration reaction. It can not be said that this sealing is specific to the film, for it could also be caused by the hydrolysis of some residual Grignard complex remaining in the film from the stripping operation.

The volume resistivities of the films are given in Tables I and II. Since these values are roughly independent of film thickness, it is safe to surmise that the stripped Dow No. 14 films do not possess any "barrier layers" of unusual electrical properties. It is also interesting to note that there is no significant difference in the volume resistivities of Dow No. 14 films formed on FSl-O alloy from those formed on pure magnesium.

Attempts were also made to obtain the capacitances of the stripped films. At low frequencies, the results were chaotic because of the large polarization of the platinum electrodes. At higher frequencies, the distributed capacitance of the cell is large in respect to the capacitance of the film. Thus, even at high frequencies, the results are only valid for indicating the order of magnitude. For the ten micron films stripped from FSl-O alloy, the capacitance was about  $0.03 \mu f/cm^2$ .

#### B. Measurements Made Directly on Filmed Electrodes

In view of the difficulty in obtaining stripped sections of thin films without rupturing them, and in view of the difficulty in relating the properties of a stripped film to the properties of the same film on the host metal, it was decided to make resistance measurements directly on filmed electrodes. This approach has certain inherent difficulties, the most serious of which is the inability to properly assess the contribution of the metal electrode itself.

In general, when alternating current is passed thru an electrolytic cell, the measured resistance ( $R_m$ ) is given by

$$R_m = R_o + R_p \quad (1.)$$

where  $R_o$  is the true ohmic resistance of the circuit and  $R_p$  is a "polarization resistance" which is frequency dependent. The relationship between  $R_p$  and the frequency ( $f$ ) is at least partially described by the expression

$$R_p = kf^{-n} \quad (2.)$$

where  $k$  and  $n$  are constants.<sup>2</sup> It can thus be seen that

$$\lim_{f \rightarrow \infty} R_m = R_o \quad (3.)$$

Such an extrapolation has been used very successfully in determining electrolytic conductivities with cells having polarizable electrodes.<sup>3</sup>

In actuality, the determination of electrolytic conductivities has the advantage that the cell constant can be so chosen that  $R_o$ ,  $R_p$ , and thus errors in extrapolation can be made small in respect to the ohmic contribution being sought. In the case of the measurements to be described here, both the ohmic resistance of the film and the polarization resistance of the host electrode are defined by the same interfacial area. Thus there is no stratagem by which the above advantage can be obtained if it does not already exist for the filmed electrode under consideration.

The sole work reported in the literature on this approach to film study is that of Wormwell and Brasher<sup>4</sup> in which they were unsuccessful in interpreting impedance measurements made on anodized aluminum electrodes with 1000 cycles per second alternating current. They suggested that comparable measurements over a frequency range might yield interpretable results.

## 1. Experimental

The impedance measurements on the filmed electrodes were made in the same manner and with the same instrumentation as that discussed in connection with the stripped film measurements.

The surface treatment procedures for the electrodes discussed in this section are as follows:

a. The Dow No. 14 film on F51-0 alloy was prepared in exactly the same manner as the corresponding film discussed in the preceding section.

b. The Dow No. 7 films on F51-0 alloy and F51-H24 alloy were prepared according to the directions given in Dowmetal Bulletin No. DM 95A. The modification was used which employs the acid fluoride activating dip and magnesium fluoride in the dichromate boil. Pretreatment consisted of a No. 320 aloxite grind.

c. The Dow No. 17 film was prepared according to the directions in Dowmetal Bulletin No. DM 141. The modification using alternating current was employed, and the film was the full green film that is obtained at about 85 volts a.c.

Three different cell designs were used during these measurements. These cells are shown in Figures 7, 8 and 9. The cells are numbered in the order of their evolution.

The manner of operation of Cell No. 1 is obvious from Figure 7. Lead wires are spot-welded to two sections of the same filmed sheet, and these sections are cemented to the ends of the cell with Pyseal cement. The cell is then filled with the electrolyte. This cell is 1.26 cm in internal diameter by 2.6 cm long. The resistance of the electrolytic path is calculated from these dimensions and the conductivity of the electrolyte.

In Cell No.1, a considerable amount of hydrogen from the corrosion of the electrodes was entrapped in the cell in such a manner as to partially shield the electrodes.

It was hoped to remedy this in Cell No. 2 by dissipating the hydrogen thru holes in the platinum electrode. Instead, the bubbles agglomerated and would not pass thru the holes. This made the situation even less tolerable, for the disposition of the cell permitted the hydrogen to mask off much of the platinum electrode. For reasons that will be discussed later, there was actually more hydrogen produced in Cell No. 2 than there was in Cell No. 1.

Because the above holes were likely to render the current distribution non-uniform in the vicinity of the platinum electrode, the contribution of the electrolyte resistance to the total resistance was determined by measurements with a platinum electrode replacing the filmed magnesium electrode.

In Cell No. 3, reliance was placed on the throwing power of the film to obtain uniform current distribution over the electrodes. Any hydrogen formed was free to leave the cell as the bubbles detached from the electrode surface. It was also designed with close electrode spacing to place the film resistance in better relation to the electrolyte resistance, and the electrode areas were made small to bring the total cell resistance into the optimum region of the bridge. The electrodes for this cell were prepared by wrapping strips of the filmed alloy with Scotch Brand electroplaters tape in which small circular holes had been cut with a cork borer. These holes were only 0.137 inch in diameter. The strip

was then mounted so that the only portion of the filmed metal exposed to the electrolyte was at one of the circular holes.

It was originally planned to make duplicate measurements during the same run by alternately measuring the resistance between each of two filmed electrodes and the central, silver electrode. It was found, however, that despite the moderately high resistance of the bridge, the current produced by the silver-magnesium couple formed in this manner was sufficient to cause appreciable hydrogen evolution. This discovery explained the rather copious hydrogen evolution in Cell No. 2, where the higher potential of the platinum-magnesium couple could be expected to make the matter even worse.

To eliminate this difficulty in Cell No. 3, it was only necessary to measure across the two oppositely disposed filmed electrodes. This was equivalent to measuring across two of the single cells in series. To obtain the electrolytic contributions to the total cell resistance, the resistance of each of the single cells was measured with the filmed electrode replaced by an equivalent silver electrode.

## 2. Results

Because of the inadequacy of the theory and the paucity of experience for this type of measurement, it was planned to make a cursory initial investigation to see if it merited further exploitation. These early experiments looked very promising. Thus, the curves shown in Figure 10 indicate that the resistance of a Dow No. 14 treated electrode approaches its limiting value comparatively rapidly. Furthermore, since its resistance behavior can be expressed by

$$R_m = R_o + kf^{-1} \quad (4.)$$

within the accuracy of measurement, it is a simple matter to extrapolate to this limiting value. The results shown in Figure 12 for an acetic nitrate pickled electrode were also encouraging since the resistance of the pickle film can be expected to be very small.

In the above cases, however, the electrolyte resistance was a sufficiently large portion of the total resistance that the contributions of the filmed electrodes were partially masked. In Cell No. 3, the resistance of the filmed electrode was made larger in respect to the electrolyte resistance. The current density over the electrode was also made much higher than it had been in the earlier cells. Under these conditions, it can be seen in Figure 13, 14 and 15 that small deviations occur from Equation 4.

In addition to the above phenomenon, two other disquieting processes were occurring at the filmed electrodes. Firstly, electrodes which had been given either the Dow No. 7 treatment or the Dow No. 17 treatment were able to partially rectify the bridge signal for periods of a few minutes. This rectification did not appear to start or stop at any particular frequency, nor did interrupting the current appear to have any noticeable effect. Although the rectification was very imperfect, it did make balancing the bridge nearly impossible while it continued.

In attempting to discover what process was causing the rectification, the potentials of the electrodes were measured against a calomel electrode immediately after the alternating signal had been interrupted.

It was found that an electrode with a No. 7 treatment could shift as much as 0.4 volts in the passive direction from its active value of 1.57 volts against saturated calomel, and then slowly recover its original active value. However, there did not appear to be any correlation between the onset of rectification and the appearance of the passive

potentials. The No. 17 treated electrodes also showed an occasional potential shift of much smaller magnitude, e.g., about 0.1 volts. Thus the electrodes are showing an anomalous response to the signal.

Because of these difficulties, it is not likely that the resistance values obtained from these measurements are sufficiently valid to show marginal differences in films. In general, they should show the order of magnitude of the film resistance, and it is reasonable to expect them to indicate the more prominent trends during continued exposure to the electrolyte.

The results are summarized in Tables III, IV and V and in Figures 16 and 17. The results in Table III for the resistance of the Dow No. 14 film during exposure to 0.1 N. sodium chloride solution are interesting since they show the same increase in resistance with time that the stripped Dow No. 14 films did. It is also interesting to note that the resistivity of the film when exposed in this manner is approximately five times as great as that of the same film when it is stripped and exposed to the same environment.

In Figure 16, it can be seen that the Dow No. 7 film experiences a decrease in resistance during exposure to 0.5 N. sodium chloride solution. Subsequent structural study shows this film to be a gel. It is reasonable to expect this decrease to be the result of the diffusion of electrolyte into the gel structure. It is also interesting to note in Table IV that the volume resistivity of the Dow No. 7 film is essentially the same when it is formed on FS1-H24 alloy as it is when formed on FS1-O alloy. The differences shown in Figure 16 are primarily the consequence of differences in the film thicknesses.

In Figure 11, it can be seen that the Dow No. 17 film also decreases in resistance during exposure to 0.5

N. sodium chloride solution. This would appear to be a logical manifestation of the permeation by electrolyte of the voids of its exceedingly porous structure. It had been anticipated that this film would show a high area resistivity, since it had a nominal thickness of 1.5 mils. That its resistivity is only about twice that of the No. 7 film must again be ascribed largely to its porous structure.

## II. The Anodic Polarization of Magnesium Alloy Electrodes in Salt-Chromate Electrolytes

In the film resistance measurements of the preceding section, it was found that filmed electrodes could respond to the bridge signals to give passive potentials. It seems reasonable to expect that this polarization was brought about by the anodic portion of the signal. This in turn indicated that the anodic polarization of filmed electrodes might yield interesting information about the manner in which the film performed. Because of the extreme importance of the chromate conversion type films in the protection of magnesium, and because a member of this class showed the greatest polarization in the resistance measurements, the work in this section is directed toward a study of the Dow No. 7 film. Since much of the utility of the above film may stem from its ability to supply chromate ion to the metal surface, most of the work to be discussed here deals with anodic polarizations in solutions bearing a chromate and a corrosion stimulating salt.

### A. Experimental

Since the automatic polarization apparatus is described in considerable detail in Figures 18 through 21 and Table VI, it will suffice to state the manner in which it operates and the operation it performs.

By interposing a very large resistance in series with the polarization cell, the latter is made to have a negligible effect on the current flow through the polarization circuit.

The polarization current can then be precisely regulated by a synchronous motor driven, helical potentiometer. When the above synchronous motor is meshed with the chart drive selsyn of the recording potentiometer, the polarization current becomes the ordinate of the strip chart. The potential of the measuring electrode system is then recorded while the helical potentiometer and the chart are synchronously driven. Thus the polarization curve is determined automatically.

The polarizer is characterized by extreme flexibility. It has two current ranges, 0 to 100 microamperes and 0 to 1000 microamperes. It has both single and double sweep programming. Under single sweep programming, the instrument progresses through the selected current range once and then stops. Under double sweep programming, the instrument moves across the current range once, stops, and then covers the range in the opposite direction. Double sweep programming is particularly useful in showing hysteresis effects.

The instrument has sweep rates of 5 minutes and 30 minutes per single sweep. It can be stopped at any time during the program without destroying the synchronization, or the mechanical linkage between the helical potentiometer and its drive motor can be disengaged to permit manual control or the determination of time-potential curves at constant current density. Furthermore, the polarizing current can be cut in or out at any time to study transient effects.

The recording potentiometer is a modified Brown "Electronic". It has sensitivities of 0.1 volt, 1 volt, and 2 volts for full scale deflection, and it has an overall range of 3 volts.

Provision has been made for very simple calibration of the polarizer circuit. With the current range set at 0 to 100 microamperes and the recording potentiometer set at 0.1 volt full scale, the potential drop across the 1,000 ohm

resistor  $R_g$  of Figure 6 is recorded during a current sweep. If the instrument is functioning properly, the trace will be a line with unit slope. Similarly, the 0 to 1000 microampere sweep should give a linear trace when the potential drop across  $R_g$  is recorded at a sensitivity of 1 volt full scale.

The cell arrangement and electrode arrangement are so clearly depicted in Figures 19 through 21 that little further discussion is necessary. For convenience, the exposed area of the electrode is one square inch. If a peak current density greater than 1 milliamperere per square inch is desired, it is a simple matter to decrease the area of the electrode by wrapping it with electroplaters tape. The electrode and its holder can be rotated during measurements to minimize any shielding effects of the salt-bridge tip.

It should be pointed out that this instrument has been neither developed nor constructed under the auspices of this project. The instrument has proven its value during several years' use in the Dow Laboratories. It is mentioned here because it has been serviced and put into operation to perform polarization experiments of interest to the project.

With the exception of the electrodes which were given the Dow No. 7 treatment, the electrodes were No. 400 Aloxite ground, rinsed in distilled water, and then aged for ten minutes in the electrolyte. This procedure gave stable and reproducible potentials. A series of double sweeps was then made for each alloy in each electrolyte. The electrodes were permitted to rest for ten minutes between each double sweep program. Most measurements were made with the electrode rotating. Several measurements made on stationary electrodes indicated that rotation had no significant effect on the electrode behavior.

The Dow No. 7 treatment was applied to the electrodes in the same manner as has been described earlier in this report. Prior to the treatment, the electrodes were No. 400 Aloxite ground. These electrodes were also aged in the electrolyte for ten minutes prior to the measurements.

Over most of the range of electrolyte compositions, a saturated calomel electrode was used in conjunction with a saturated potassium chloride solution bridge. In the range of low chloride or low bromide concentrations, however, a saturated potassium nitrate solution bridge was used to avert the possibility of sufficient chloride ion diffusing into the electrolyte to invalidate the results.

Analyses or specifications for the alloys discussed in this section are given in Table VII.

## B. Results

### 1. Polarization Characteristics in the Electrolyte System Sodium Chloride-Sodium Chromate

Although the addition of moderate amounts of sodium chromate to the sodium chloride electrolyte depresses the potential of all the electrodes appreciably, no significant polarization occurs until the ratio of chromate to chloride is greater than 4 to 1 for a total normality of one-half. The curves obtained in the range of polarizing concentrations are interesting and complicated. A typical family of such curves is shown in Figure 22.

The curve obtained with increasing current density shows an interesting drop and then recovery in potential that is reminiscent of the delay effect frequently encountered in the magnesium primary cell. This phenomenon will be discussed in greater detail later. The curve obtained on decreasing the current density obeys a logarithmic relationship as can be seen in Figures 23 through 28.

Since the polarization with decreasing current density shows the simpler behavior, it is these values that are used in showing the effect of electrolyte composition on the polarization in Figures 20 through 24. The extrapolation between 0.4 N. sodium chromate and 0.49 N. sodium

chromate is unfortunate since this is the region where the greatest changes in the potential must occur. However, data obtained at 0.45 N. sodium chromate could not be treated in the same manner as the other data because the potential oscillated wildly over most of the current density range. This same difficulty was encountered intermittently throughout the passivating electrolytes, but perseverance eventually gave stable and treatable potential behavior in most cases.

In order to relate the above polarization experiences with the protective ability of chromates in the presence of chlorides, the corrosion rates of AZ31A-0 alloy sheet was determined in the above electrolyte system. These rates were determined from the weight loss during the 14 day stagnant immersion of 1.5 inch by 1.5 inch by 0.125 inch coupons which had been acetic nitrate pickled from 1.5 to 2.0 mils per side. The samples were randomized before exposure to the electrolytes, and they were randomized again before the corrosion product was removed in boiling 20% chromic acid plus 1% silver nitrate.

As indicated in Table VIII and Figure 34, two separate exposures were made. The second series was necessary when it was found that inhibition was nearly complete during exposure to the first series of solutions. Although the same material was used for both series, and every effort was made to give both series the same pretreatment, results for the 0.5 N. sodium chloride solution control show that either a procedural error or a sampling error occurred. This lack of reproducibility only prevents direct interpolation between the two series. Since the samples in each series were randomized, their validity is indicated only by their deviations if no errors have been made in preparing the environments.

It can be seen from the curves of Figure 34 that even very small amounts of sodium chromate give some inhibition, and that the environments richer in chromate than 0.1 N. are

nearly completely protective during the 14 days. Yet the polarization data of Figure 32 indicates there is only a moderate depression in potential, e.g., about 0.1 volt and no observable polarization until the system is very rich in chromate. It is difficult to see how chromate can function exclusively as an anodic inhibitor and afford the observed level of protection without causing greater passivity in potential behavior. There can be little doubt, however, that much of its action is on the local anodes. It will be seen later, that chromate can engender the formation of films with greater physical stability than the conventional hydroxide film formed in its absence.

In addition to the weight loss data, the AZ31A-0 alloy coupons were inspected visually to determine if chromate is a "safe" inhibitor for magnesium. It was found that over the range of concentrations studied, increasing chromate leads to a decrease in both the area and the depth of attack. It thus falls into the category of what Mears calls the "Safe, Contractive Inhibitors".<sup>5</sup> This is also consistent with the view that the chromate inhibition is not purely anodic in mechanism.

At chromate concentrations greater than 0.45 N., the passive open circuit potentials and extensive polarization common to severe anodic inhibition do occur. And at 0.45 N. sodium chromate, the electrodes show erratic potential behavior. During the exposure of the AZ31A-0 alloy coupons to the chromate-chloride system, all four coupons exposed to the above electrolyte composition formed films possessing first order interference colors after about one week of exposure. None of the coupons exposed to the other electrolytes showed such films even after 14 days of exposure. This implies that the films formed at this composition have reached some maximum in thickness and/or uniformity. In the

case of the films formed at chromate concentrations greater than the above, the principal difference must be in thickness. At lower chromate levels, the answer is less obvious.

To produce first order interference colors the film must be in the order of 500 Å thick.<sup>6</sup> The absence of such colors in situations where the film has the requisite physical uniformity indicates the film to be less than 500 Å in thickness. Thus, the delay effect observed at the high chromate concentrations is due to a film less than 500 Å in thickness. Furthermore, chromate engendered films less than 500 Å in thickness can be completely protective.

Attempts to measure the rate of film growth in the 0.45 N. sodium chromate-0.05 N. sodium chloride electrolyte were unsuccessful because of the wide variation between samples for the time at which the colors appear and the difficulty in noticing the first colors in the presence of the yellow electrolyte. The time for the appearance of interference colors varied from less than one week to over two weeks.

## 2. Polarization Characteristics in the Electrolyte System Sodium Bromide-Sodium Chromate

The results from the polarization measurements in this system are shown in Figures 35 through 46. It can be seen that the open circuit potentials are depressed by approximately 0.1 volt by the substitution of bromide for chloride, and that very weak polarization can occur at quite low chromate levels, and even very weakly in the absence of chromate. This would indicate that bromide has a less deleterious effect on the anode film than chloride. Such differences have long been surmised from the fact that bromides are distinctly less potent corrosion activators than chlorides.

Severe passivation occurs at the same chromate to halide ratios as it did in the sodium chloride-sodium chromate

system, and the individual polarization curves at these ratios are nearly identical in shape for both systems. The odd shapes of the potential-electrolyte composition curves at 0.45 N. chromate stem from attempts to utilize the data at this composition despite the erratic oscillation of potentials.

### 3. Polarization Characteristics of Dow No. 7 Treated Electrodes in the Electrolyte System Sodium Chloride-Sodium Chromate

At high ratios of chromate to chloride, the individual polarization curves of the Dow No. 7 treated electrodes show marked resemblance to those obtained for untreated electrodes in the same electrolyte. At ratios of chromate to chloride lower than those causing polarization of the untreated electrodes, the No. 7 treated electrodes continue to show marked polarization. Even at chromate concentrations as low as 0.1N., significant polarization occurs. However, there is no significant polarization in the uninhibited 0.5 N. sodium chloride solution. These effects are shown in Figures 47 through 52. No explanation can be offered at this time for these effects.

### 4. Some Interesting Characteristics of the Delay Effect and a Tentative Mechanism of Explain Them

It has been mentioned earlier that an interesting transient effect is observed during polarizations in the chromate rich regions of both electrolyte systems discussed here. This effect consists of a drop in potential followed by a partial recovery to yield a definite potential minimum. A family of curves which show the effect very clearly is given in Figure 22. The effect shows sufficient resemblance to the delayed action phenomenon of the magnesium primary cell to make it of practical as well as theoretical interest.

The nature of this delay type transient suggests that the filmed electrode may be acting as an electrolytic condenser. Let the drop from the open circuit potential to the minimum potential of the delay hump be considered the potential across such a condenser, and let the charge on the condenser be the total charge transported when the potential minimum is reached. The capacitance of the condenser is given by

$$c \equiv \frac{q}{v} \quad (1.)$$

where  $c$  is the capacitance in farads/cm<sup>2</sup>,  $v$  is the potential in volts, and  $q$  is the charge in coulombs/cm<sup>2</sup>. This charge can be readily calculated by integration of the current since the latter is a linear function of time; i.e.,

$$q = 1/2 it \quad (2.)$$

where  $q$  is the charge in coulombs/cm<sup>2</sup> of electrode area,  $i$  is the current density in amperes/cm<sup>2</sup>, and  $t$  is the delay time in seconds.

Capacitances calculated in this manner are given in Tables IX through XIV. These capacitances are extremely large. If the hypothetical condenser is considered to be a parallel plate condenser for which the plate separation is equivalent to a film thickness, the film must be extraordinarily thin and/or must have an unusually high dielectric constant.

While the capacitance concept does not appear to be particularly informative, it does serve to focus attention on the delay effect as a charge effect rather than a time effect. This in turn creates interest in the number of ions taking part in the charging process, which in turn leads to the following treatment of the process.

Assume that all of the ions transporting charge in the delay process accumulate in a layer in the vicinity of the electrode surface. The apparent area ( $a$ ) in cm<sup>2</sup> per ion

involved in such a process will be given by

$$a = \frac{n \mathcal{F}}{qN} \quad (3.)$$

where  $n$  is the number of electrons per ion transporting charge,  $\mathcal{F}$  is the Faraday,  $q$  is the charge density per unit apparent area in coulombs/cm<sup>2</sup>, and  $N$  is Avagadro's number. Restated in terms of the area actually operative in the charging process,

$$\tau = \frac{n \mathcal{F}}{qN} \rho \epsilon \quad (4.)$$

where  $\rho$  is a roughness factor; i.e., the ratio of true area to apparent or projected area, and  $\epsilon$  is an exclusion factor, i.e., the ratio of the area actually involved in the charging process to the true area. This term takes in account any areas denied to the process by inhomogeneities in the metal surface, by extraordinary film conditions, or by pre-charging due to local action currents.

If the ion layer is assumed to be built up of close packed spheres, it is also seen that

$$\tau = \frac{d^2 \sin 60^\circ \times 10^{-16}}{m} \quad (5.)$$

where  $m$  is the number of monolayers and  $d$  is the interionic distance in Å. Equating (4.) and (5.) and solving for the terms which are as yet unmeasured

$$d(mn\rho\epsilon)^{1/2} = \frac{\mathcal{F}}{qN \sin 60^\circ}^{1/2} \times 10^8 \quad (6.)$$

Substituting the values of the Faraday and Avagadro's number,

$$d(mn\rho\epsilon)^{-1/2} = 4.29 \times 10^{-2} q^{-1/2} \quad (7.)$$

The expression  $d(mn\rho\epsilon)^{-1/2}$  will be hereafter called the "film parameter" and denoted by "F". Such values calculated from the charge transported in the delay process are

given in Tables IX, X, XI, XII, XIII and XIV.

It is seen that the film parameter ranges from 0.8 Å in the case of very high purity magnesium to nearly 2.5 Å in the case of some alloys. If reasonable values are assumed for the interionic distance, ionic charge, surface roughness, and exclusion factor, it is obvious that the ion film will be at most a few layers thick. Thus if  $d = 3 \text{ \AA}$ ,  $m = 1$ ,  $n = 2$ ,  $\rho = 5$  and  $\epsilon = 0.9$ , then

$$F = 3 / \sqrt{1 \times 2 \times 5 \times 0.9} \\ = 1 \text{ \AA}$$

Since the energy necessary to form the first ion layer can be expected to be markedly smaller than the energy required to form any subsequent layer, it is reasonable to expect the process to be one of monolayer formation.

The ion monolayer hypothesis is still incomplete, however, for it explains neither the residual polarization on completion of the delay process for all of the electrodes, nor the increase in the potential drop experienced as the high purity magnesium electrodes are repeatedly polarized. These phenomena indicate that there is a solid film, as well as the ion film, in existence on the electrode. Furthermore, it is not unreasonable to expect that the ion film may owe its existence to the insulating properties of a more massive film. To complete the hypothesis then, and state it in its entirety:

The delay effect is caused by the formation of a monolayer of magnesium ions at the metal surface. These ions are prevented from hydration and subsequent diffusion from the surface by an insulating film. At completion of the charging process, the potential across the insulating film is sufficient to cause it to suffer dielectric breakdown, and this in turn permits the discharge of the ion monolayer.

A re-examination of the experimental data in terms of the completed hypothesis is enlightening. To do this, recourse will be made to the six trends that were considered to be significant before the monolayer hypothesis was conceived.

a. "The time to reach the minimum potential is the greatest when the heterogeneity of the metal surface is the least." The presence of a heterogeneity denies area to the charging process. Furthermore, heterogeneities lead to local action currents, which in turn lead to some degree of precharging of the ion monolayer.

b. "The above time is the greatest for pure sodium chromate solution and decreases with increasing chloride concentration for the alloys with the more homogeneous surfaces. Any such effect becomes less obvious for magnesium aluminum alloys." The electron micrographs of this report indicate small amounts of chloride ion cause the formation of local cells on very high purity magnesium. This should lead to some precharging. Any such precharging will be less noticeable on alloys where galvanic cells are also operating.

c. "The above time decreases with the number of consecutive polarization cycles to which the electrode has been subjected, except in the case of very high purity magnesium where any such trend is small." The anodic dissolution of magnesium serves to enrich the surface in impurities and alloying constituents. This denies area to the charging process and promotes self-charging by local action.

d. "Electrode rotation has no large effect on this time." This is true because the process is not under diffusion control.

e. "There is a significant increase with the number of cycles in the potential change from open circuit to the minimum in the case of very high purity magnesium." It

can be seen in Table IX that this potential is reaching a limiting value of about 1.5 volts at the third cycle. This indicates that the solid film has a limiting thickness which is not reached during the first two cycles.

f. "In the above case during the first cycle, and for the remainder of the alloys during all cycles, the potential change does not vary significantly from an average value of about 0.7 volts." This indicates that the solid film has reached its limiting thickness during the first cycle in the case of the alloys. The lower dielectric strength of the film in this case indicates either a thinner film or a less perfect one. The latter view would appear to be the more logical one. The greater speed with which films on the alloys reach their limiting thickness may be due to the assistance of local action currents in the film deposition process.

The ion monolayer mechanism predicts that the total charge transported to reach the potential minimum should be largely independent of the charging rate. To test this prediction, polarization runs were made on electrodes which had their area halved by being masked with electroplaters tape. This doubled the charging rate per unit of electrode area. The effect of this increased charging rate can be seen in Figures 53 and 54 and Tables XIII and XIV. As predicted by the hypothesis, the "film parameters" remain essentially the same for each alloy irrespective of the charging rate.

### III. The Study of Films with the Light and Electron Microscopes

#### A. General Techniques

##### 1. Topographical Examination with the Light Microscope

Essentially the same techniques are used for the topographical examination of films as are used in metallography. Most of the interesting films on magnesium are

either micro-crystalline or amorphous. This permits the profitable use of polarized light to study the homogeneity of color of the film, for under these conditions, the film appears in its true colors.<sup>7</sup> In general, the use of non-polarized light causes the film colors to be washed out.

Oblique light is useful in revealing the surface texture of the film. In general, this utility is limited to a few films which possess comparatively coarse surface textures; e.g., the films formed during high voltage anodization.

Film surfaces are characterized by much greater absorption and dispersion of the incident light than are metal surfaces. At high magnifications, even with a high intensity source such as the carbon arc, it is necessary to make very long exposures to get decent photomicrographs.

## 2. Topographical Examination with the Electron Microscope

Many of the important films on magnesium have textures that are too fine to be resolved under the light microscope. To study these textures, it is necessary to use the much greater resolution inherent in the electron microscope. Because the electron microscope requires surface replicas for study, its use involves two major risks:

- a. The replica may not faithfully reproduce the surface from which it was taken.
- b. The replication process may change the surface under study.

To meet the needs of this project and other Dow projects, considerable work has been done in our laboratories on replication techniques. Excellent techniques are now available as a result of this work. Since certain of the techniques have been used in this project, they are being described here. It should be pointed out, however, that they were not developed under the contract covering this project.

The standard method in the Metallurgical Laboratories for obtaining replicas from metal surfaces is the hot molded polystyrene technique of Heidenrich and Peck.<sup>8</sup> The molding is done in a conventional specimen mounting press at 2000 lbs./in.<sup>2</sup> and 160°C. The metal is then dissolved away from the plastic in dilute acid, and a silica film is sputtered on the plastic negative. The plastic is dissolved in ethyl bromide and the silica positive is floated upon the supporting screen. This technique is simple, rapid, and yields excellent detail. Unfortunately, the temperatures and pressures of the initial molding operation are too drastic to be completely safe with most surface treatment and corrosion films.

Because of these difficulties, work has been done on cold replica techniques. The first such technique consists of building up a heavy negative film by the successive application and drying of thin films of twenty percent polystyrene in benzene. This composite is then handled in exactly the same manner as the hot molded composite. Unfortunately, not only is this procedure time consuming, the replicas it yields are definitely inferior in detail to those formed by hot molding.

Much greater success has been obtained by making the initial replica with a catalyst conversion polyester resin. Because there are no satisfactory solvents for these resins, it is necessary to take a hot molded polystyrene impression from the polyester replica. The resulting polystyrene replica is then handled in the manner described above. The first polyester to be a success in this process was Paraplex F-43, a product of Rohm and Haas. This was later replaced by Minnesota Mining and Manufacturing's EC 1294 resin which is more consistent in withstanding the

pressures necessary for obtaining the polystyrene impression. The latter resin may also give marginally superior replicas. Both resins yield excellent replicas.

### 3. Profile Examination with the Light Microscope

In general, examination of a film in profile is much more informative than a topographical examination of the same film. Profile examination may yield the following significant information.

- a. The thickness of the film.
- b. Its uniformity of thickness.
- c. The roughness of its external surface.
- d. The amount of etch the metal received during the treatment which produced the film.
- e. The presence and distribution of phases in the film.
- f. Relations between phases in the film and phases in the host metal.
- g. Relations between film thickness and phases in the metal.
- h. The extent of "keying" of a point with the film.
- i. The presence of porosity in the film.

There are two major problems in studying films in profile. They are:

- a. Mounting and grinding the specimen without scuffing away the film or dragging the metal or mounting resin over the film, and
- b. Obtaining the proper contrast between the film and the metal, and the film and its support. This is particularly important in black and white photography.

Thin, dense films such as the chromate conversion coatings can be kept from scuffing by applying a paint

system over the film. After the paint has dried, several of such specimens can be wired or bolted together tightly to give a thick composite, which is then mounted in Lucite with a mounting press.

This procedure does not work as well on thick, porous films such as those produced by the Dow No. 17 treatment and the H.A.E. treatment, for the pressures involved in mounting may crack the films or cause them to spall. Instead, catalyst conversion resins such as Paraplex P-43 should be used. Because these resins shrink on curing, the support they afford the film is inferior to that of the first method. Although it has not been tried, it would appear that this can be remedied by rough grinding the specimen, sealing the shrinkage cracks with more of the resin, and then finishing the grinding.

The specimen is ground normal to the film. All grinding and polishing times are kept at a minimum to decrease dragging of the metal and the supporting resin over the film. This also helps to prevent scuffing of the film.

If the profile mount is to be used for film thickness measurements alone, it is advisable to aim for a maximum in contrast between the film and the supporting resin. If the film is dark in color, this is best done by using a light colored resin and either non-polarized light or sensitive tint. If the film is light in color, a dark resin and either plane polarized light or sensitive tint are preferable.

Where structural details within the film are to be observed, it is preferred to have slightly less contrast between the film and its support. In general, sensitive tint is a safe compromise in getting proper contrast between the film and the metal. As in the case of the topographical examination of films, plane polarized light is most useful in showing variations in film colors while oblique light is best for showing textures. Sensitive tint shows variations in

both color and texture at the same time, but to a lesser extent than either of the above individually.

B. Specific Film Problems Studied with the Light and Electron Microscopes

1. The Microstructures of Anodic Treatment Films

a. The Dow No. 14 Film

Profile views of this film are shown in Figures 55 and 56. The film is formed by the high voltage anodization of magnesium alloys in an alkaline bath containing sodium metaborate, sodium metasilicate, and a depolarizer. Alternating current is used. Anodization is generally continued until the film blocks the current at 110 volts. At this stage, the film has a mean thickness of about ten microns.

It can be seen that both surfaces of the film are moderately rough. Such roughness is common among the high voltage anodic treatments on magnesium, and, indeed, the No. 14 film is much smoother than both the No. 17 film and the H.A.E. film.

The No. 14 film is composed of two phases of different hardness. It is believed that the harder appearing outer phase is formed by the sintering of the film material as the potential across the film becomes sufficiently great to cause dielectric breakdown accompanied by a roving spark discharge over the face of the film. That the outer phase has actually been fused is further indicated by what appear to be spherical gas bubbles in the phase. This hard phase is probably a sodium-magnesium boro-silicate glass. Thus, the film is actually a ceramic coating. It is not surprising that it is noted for its hardness.

b. The Dow No. 17 Film

The Dow No. 17 film is formed by the anodic

oxidation of magnesium in an acidic bath containing sodium, ammonium, phosphate, dichromate, and fluoride ions. Either alternating or direct current can be used. The structures that are obtained at various terminal voltages of anodization are shown in Figure 57 for the a.c. treatment and Figure 58 for the d.c. treatment.

It can be seen that both modifications produce films that are extremely rough at the outer surface and moderately rough at the inner surface. Both films are also characterized by exceptional porosity. These properties make the film outstanding acceptors of oils, waxes, and other systems where little reliance can be placed on specific adhesive effects. It was also thought at one time that the excellent paint base properties of these films might stem from the paint "keying" to these open structures. However, the excellent performance of paint systems on the lower voltage films, which are much thinner and smoother than the full voltage treatment, indicates that specific adhesion between the film material and the paint is an important part of their paint base properties.

Just as in the case of the Dow No. 14 film, the No. 17 film also possesses small spherical gas bubbles indicative of fusion during the latter stages of the deposition process. Unlike the Dow No. 14 film, however, the No. 17 film shows no microstructural evidence of being a two phase film. This is surprising since the film appears to change in color from a light gray to a grayish green as the anodization voltage is increased. The low voltage films are exceedingly thin, however, and it is possible that the color is "washed out" by reflection from the metal surface. On the other hand, it is also possible that the under film was overlooked in the profile

studies because of its thinness and lack of contrast with the bulk of the film.

It is interesting to note, that once again we are dealing with a system that is capable of forming a glass. In fact, the bath used in this treatment contains the ions of microsmic salt,  $\text{NaNH}_4\text{HPO}_4$ , which is used in the phosphate bead tests of qualitative analysis. Furthermore, the film contains the chromic ion which gives it a green color, just as the chromic ion forms a green bead in the above test. And finally, the film is amorphous to X-ray diffraction.

The variation in film thickness with forming voltage for the No. 17 treatment is shown in Figure 60. Because of the roughness of the films, the thickness measurements are somewhat arbitrary. By scanning large cross sections of the film and disregarding sections of unusual porosity, however, reasonable thickness measurements can be made. The variation of thickness with forming voltage is a surprisingly simple relationship; namely, the thickness is an exponential function of forming voltage. The same type of variation is observed in the high voltage anodization of aluminum in oxalic acid.<sup>7</sup> The significance of this type of variation is not obvious, but it would appear to stem from the variation in the dielectric strength of the film with thickness.

If the anodization time to reach specified voltages is plotted against the potential (Figure 59), another exponential function is obtained. This immediately suggests a simple relationship between the time of anodization and the thickness of the film. As can be seen from Figure 61, not only is the relationship linear for both types of current, but it would appear to be the same linear relationship. This would indicate that the film

deposition occurs by the same process at the same efficiency for both types of current, and that the process and its efficiency does not change with time and potential.

### c. The H.A.E. Film

The H.A.E. treatment is a high voltage, alternating current, anodic treatment, which is applied in an alkaline bath containing potassium, sodium, phosphate, fluoride, aluminate and manganate ions. The film it produces has a light brown, faintly mottled appearance. Profile views of a typical film are shown in Figures 62 and 63. This film is intermediate between the No. 14 film and the No. 17 film in roughness. The full treatment produces a film of about the same thickness as the full No. 17 treatment. As one would guess from its porosity, the H.A.E. film resembles the No. 17 film in its propensity for waxes and oils.

Just as in the case of the No. 14 and No. 17 films, fusion in the H.A.E. film is indicated by the presence of a hard phase which contains spherical gas bubbles. Also, as in the case of the No. 14 and No. 17 baths, the H.A.E. bath contains a likely progenitor of glass formation. In this case, it is the phosphate ion.

## 2. The Microstructures of Chromate Corrosion Coatings

### a. The Dow No. 7 Film

#### (1) Its Thickness as a Function of the Temper Condition of AZ31A Alloy and the pH of the Dichromate Boil

In the Dow No. 7 treatment, a magnesium alloy is subjected to an activating bath which usually contains hydrofluoric acid or an acid fluoride. This is then followed by boiling in a weakly acidic sodium

dichromate solution which may also contain magnesium fluoride or calcium fluoride. During this process, there is some reduction of hexavalent chromium to trivalent chromium followed by the deposition of a thin film, which contains chromium in both of the above oxidation states.

The deposition of this film must depend on differences in potential over the surface of the alloy due to the different metallurgical phases, for alloys with fairly homogenous surfaces do not form any appreciable amount of film.

In the case of AZ61A alloy for which the treatment was originally designed, the treatment consistently produces a uniformly dark brown film. In the case of AZ31A alloy, the color will vary according to the temper of the alloy and the pH of the dichromate boil. If the alloy is homogenized and/or the pH of the dichromate boil is increased, the color of the film will change from a medium brown to a golden yellow. This change might conceivably stem from a decrease in the ratio of trivalent chromium to hexavalent chromium in the film, or it may be primarily due to differences in thickness of the film. It can be seen from the results of Table XV, that the film does experience a large decrease in thickness as the alloy is homogenized and as the pH of the dichromate boil is increased.

(2) Its Dissolution during  
Aqueous Exposures

The Dow No. 7 film also undergoes a moderately rapid change in color when it is exposed to sodium chloride solution. In this case, the color transition is from the initial medium brown to a pale gray-green after 24 hours of exposure. This change

in shade is illustrated in Figure 64. Profile examination of these films at 2000X indicate a decrease in film thickness to be partially responsible for the fading. (Figure 65) The film also tends to become more diffuse in appearance after such exposure. These phenomena are in accord with the decrease in electrical resistivity that occurs during the exposure of this film.

There is no obvious change in the appearance of the top surface of the film when examined under bright light at 500X. However, the same sections when viewed under polarized light show a significant decrease in the area of the darker portion of the film. (Figure 66) Polarized light also brings out clearly the frequency and extent of pits in the host metal by the amount and extent of white deposits of corrosion product. It is interesting to note that micro-pitting occurs on very brief exposure to the salt solution.

The exposure of an identically treated coupon to distilled water for 15 hours gave approximately the same fading as 15 hours' exposure to salt water. Top surface views of this film are shown in Figure 67. The cracks in the film are due to its dehydration during the one month aging period. The cause for this will be discussed shortly.

### (3) An Oddity in Its Distribution around Certain Precipitates

In general, the Dow No. 7 film is remarkable for the smoothness of both of its surfaces. Figure 68 reveals the distribution of the film around a hard precipitate at the metal surface. This precipitate is presumed to be a manganese aluminum compound. Part of the compound may exist due to the preferential dissolution of the magnesium rich phases during the chemical

treatment. At least in the case of Figure 68c, it would appear that some of the protrusion may stem from the slower abrasion of the hard magnesium rich phase during the grinding of the surface which preceded the chemical treatment. Although it is difficult to see because of the shadows cast by the precipitate particle, the outer film surface has attempted to remain planar despite the presence of the precipitate particle. Thus, the particle is covered in (a) but not in (b) and (c). In all cases, there do not appear to be any gaps in the film where the particle joins the hot metal. This deposition may be caused by high cohesion within the film, high specific adhesion between the film and the magnesium rich phases, and low specific adhesion between the film and the manganese rich phases.

#### (4) Its Cracking during Dehydration

It may be recalled that Figure 67 revealed that the No. 7 film may undergo micro-cracking during aging at room temperature. This cracking obviously stems from dehydration of the film. In Figures 69 and 70, it can be seen that the cracking can be made much more severe by heat. After one hour's heating at 156°C, the cracks become visible in profile. These cracks are only about 0.2 microns wide at the outer surface, and become vanishingly small at the metal film interface. It is difficult to visualize such a restrictive crack as being a serious site for corrosion.

Even after dehydration for over an hour at 232°C, the cracks are only about one micron wide at the outer surface and are still quite narrow at the metal-film interface. It is interesting to note that the stresses introduced in the film are released by cracking and not by detachment of the film from the metal. This is indicative of the outstanding adhesion of this film.

In addition to the cracking of the Dow No. 7 film during heating, the film also loses much of its translucency and becomes progressively darker in color. The cause for these phenomena will be discussed later.

(5) Its Microstructure as Revealed  
by the Electron Microscope

During the preparation of a hot molded polystyrene replica from the external surface of a Dow No. 7 film, much of the surface undergoes dehydration similar to that which has just been discussed. The result of such dehydration can be seen in Figure 71. In addition to the aforementioned cracking, the surface is largely covered by small craters which are produced by the rapid evolution of water from the film. In Figure 72 can be seen a section of the film where the dehydration has been so severe that the film has suffered partial collapse. Most of the film shown in Figure 73 and 74 has suffered little dehydration. These electronmicrographs reveal the cellular structure characteristic of the film. Figures 75 and 76 are from replicas made by a cold molding technique which should not cause dehydration. While this technique gives poor resolution, it does indicate what the structure looks like in the absence of dehydration.

The extent of the structural damage that occurs in the No. 7 film during dehydration indicates the fresh film to have an appreciable water content. The ease with which this water can be removed from the film indicates it to be loosely bound. That the film has a cellular structure is indicated by its external surface when fresh and by the manner in which it collapses during dehydration. All of these phenomena indicate the film to be a gel. This is further supported by its electron diffraction patterns which invariably indicate strong amorphism.

### b. The Iridite Treatment Film

The Iridite treatment yields a film on magnesium that resembles the Dow No. 7 film in appearance. However, the corrosion protection and performance as a paint base of the modification of the treatment to be discussed here is definitely inferior to the Dow No. 7 treatment. Obvious reasons for its poor performance can be seen in Figure 77. The film itself lacks the continuity of the Dow No. 7 film, and this lowers its protective value. Furthermore, the film is badly undercut by the severe etching action of the treatment solution, and it is to be expected that the adhesion of the film to the metal is poor. More favorable reports have been heard on the newer modifications of the treatment. No work has been done under this project on films formed in the modified treatment.

### 3. The Microstructures of the Corrosion Films Formed on Very High Purity Mg

Whereas the potency of the surface treatments that have been discussed thus far would appear reasonably capable of removing the initial films on the metal and then forming the film indigenous to the treatment, such behavior can not be relied on in the case of the environments to be discussed in this section. Fortunately, there are techniques available which will remove the films from very high purity magnesium to such an extent that no evidence for their existence can be found by the diffraction of low incidence electron beams. This would indicate that any films which are still extant are no thicker than a very few molecules. The procedure used to do this is as follows:

- a. Rough polish the metal under benzene.
- b. Etch for two hours in a solution of equal portions of 2 N. ammonium hydroxide and 2 N. ammonium chloride.

c. Rinse in an anhydrous solution of equal portions of methanol and acetone to which has been added one percent of formic acid.

d. Rinse in the above mixture without formic acid.

e. Rinse in thiophene free, anhydrous benzene.

f. Store in a dessicator over magnesium perchlorate.

This pretreatment was used for all of the specimens discussed in this section. The metal used was very high purity magnesium (Alloy No. 67535). Its analysis is given in Table VII.

(1) The Films Formed during  
Exposure to Distilled Water

The hydroxide films formed during exposure to distilled water are subject to a remarkable exfoliation process. The interesting structures arising from this process are shown in Figures 78 through 83. To gain a real appreciation of the structures, they must be viewed stereoscopically, and to this end, stereo pairs are included in each figure.

Before postulating a mechanism for the exfoliation process, it is necessary to decide if it occurs during the aqueous exposure or during the replication process. Since the replication process uses a resin which polymerizes at room temperature, the only portion of the process that can be suspected is an initial mild dessication at room temperature. While it is inconceivable that magnesium hydroxide could be dehydrated under these conditions, it is possible that the hydroxide structure could have harbored water between its layers, and that the exfoliation is due to loss of this water of absorption.

It is this writer's contention, however, that the exfoliation has occurred during the aqueous exposure. To support this contention, the following evidence is offered:

(a) The exfoliation is progressive. This is best shown in Figure 83 where appendages from previous curls are rolled up into a new curl.

(b) Many such appendages appear to have been subjected to electrolytic action.

(c) Areas from which the film has curled appear to have been subjected to a subsequent film formation.

(d) Specimens exposed to distilled water possess a "milky" appearing surface while still wet from the electrolyte. This would be an obvious consequence of film roughening by the exfoliation process.

A mechanism by which the observed exfoliation may occur is a common one in the field of the high temperature oxidation of metals. The film is under compressive stress because its site of deposition is controlled by a lower volume metal lattice. The total stress increases with increasing film thickness until the film finally cracks and detaches from the metal. The subsequent curling of the film would appear to be a manifestation of the layer structure of the hydroxide. This view is supported by the occurrence of nemalite, a fibrous brucite which has just such a curled sheet structure.

(2) The Films Formed during Exposure  
to the Electrolyte System Sodium  
Chloride-Sodium Chromate

The above mechanism immediately suggests that the above exfoliation process would not occur if the manner of deposition of the film was not controlled by the structure of the host metal. This would be the case if the film showed pronounced amorphism. The films deposited on magnesium from aqueous chromate solutions show such amorphism.

It can be seen in Figures 84 and 85 that the addition of chromate does practically stop exfoliation. Exfoliated sections like that shown in Figure 84 are very rare. This micrograph has been included to show that a solid film is involved in the chromate effect, for the films engendered by chromate are generally so thin and devoid of structure that they might be mistaken for the metal surface which they cover. Because of the absence of any of the criteria by which exfoliation was concluded to have occurred during the exposure to the distilled water, it is reasonable to believe that it occurred during the replication process in the case of the chromate engendered film.

Figures 86 through 94 show the manner in which the film structures change as the sodium chromate is replaced by increasing amounts of sodium chloride. The addition of even very small amounts of sodium chloride causes the formation of remarkable, columnar growths. These projections are remarkable in their high cylindrical symmetry, their small diameter, and their ability to reach high ratios of length to diameter before toppling. Diameters of less than 0.1 micron can be observed. Ratios of length to diameter of nearly ten to one can also be observed. They would appear to be a result of a hydrogen ion concentration cell. In view of the marked passivity obtained, at least at high chromate concentrations, it is reasonable to expect corrosion in salt-chromate solutions to be partially under anodic control. At each small local anode, magnesium ions go into solution and diffuse outward until they reach a region of sufficiently high pH to precipitate them as a hydroxide or basic salt. Since the solutions possess high bulk pH, the magnesium ion

can diffuse only a short distance before it is precipitated. Since the concentration gradients have rotational symmetry, the resulting structure has rotational symmetry. Comparable structures of macro size are sometimes observed around cathodes during the corrosion of magnesium in salt solutions in which its corrosion is largely under cathodic control.

Only small changes are observed as the concentration of chloride is further increased at the expense of chromate until very low concentrations of chromate are present; e.g., 0.05 N. in sodium chromate. At this level, the film is becoming considerably rougher and the columnar projections are showing greatly decreased incidence. Even as little as 0.001 N. sodium chromate has a definite stabilizing effect on the film. And finally 0.5 N. sodium chloride solution in the absence of chromate causes very severe exfoliation which is somewhat different in distribution from that obtained in distilled water.

## REFERENCES

1. R. L. Burwell and T. P. May in "Pittsburgh International Conference on Surface Reactions", Corrosion Pub. Co., Pittsburgh, Pa., 1948, pp. 10-20.
2. G. Jones and S. M. Christian, J. American Chemical Society, 57, 272 (1935).
3. S. Glasstone, "An Introduction to Electrochemistry", D. Van Nostrand Co., Inc., New York, (1942), p. 36.
4. H. Wormwell and F. M. Brasher, Iron and Steel Institute J. 164, 141-8 (1950).
5. R. B. Mears, Quoted in U. R. Evans, "Metallic Corrosion, Passivity, and Protection", E. Arnold and Co., London, 1937, p. 301.
6. U. R. Evans, "Metallic Corrosion, Passivity, and Protection", E. Arnold and Co., London, 1937, pp. 672-679.
7. L. V. Foster and J. E. Wilson, Proc. ASTM 38, 315-28 (1938).
8. R. D. Heidenrich and V. D. Peck, J. Appl. Phys. 14, 23 (1943).
9. M. Schenk, "Werkstoff Aluminum und Seine Anodische Oxydation", A. Francke A.G., Bern, 1947, p. 779.
10. Frankford Arsenal, "Recommended Practice for the Operation of the H.A.E. Process for Magnesium". (This is a brief bulletin without identifying numbers or dates.)

TABLE I

A Summary of the Resistances of Dow No. 14 Anodic Films Stripped from Pure Magnesium during Exposure to 0.1 N Sodium Chloride Solution

Film	Estimated Mean Thickness (Microns)	Time of Exposure (Hours)	Frequency Range (Kilocycles/sec.)	Average Resistance (Ohms-cm <sup>2</sup> )	Probable Error (Ohms-cm <sup>2</sup> )	Number of Values	Bulk Resistivity (Ohms-cm)
A-2	12	1.7	1-10	18.1	±0.4	10	15,000
"	"	21.3	1-10	20.3	±1.2	11	17,000
"	"	44.4	1-10	19.6	±0.5	10	16,000
A-3	12	0.2	1-8	15.7	±0.5	9	13,000
"	"	0.7	1-8	16.0	±0.6	9	13,000
"	"	0.9	1-8	16.1	±0.3	9	13,000
"	"	3.7	1-8	16.8	±0.4	9	14,000
"	"	6.8	1-8	17.4	±0.5	9	15,000
"	"	23.5	1-8	20.1	±0.5	9	17,000
A-4	12	2.2	1-8	19.2	±0.3	9	16,000
"	"	5.5	1-8	20.3	±0.4	9	17,000
"	"	22.6	1-8	19.3	±0.5	9	16,000
B-1	7	0.4	1-8	6.5	±0.4	9	9,000
"	"	2.2	1-8	5.2	±0.3	9	7,000
"	"	5.0	1-8	4.6	±0.3	9	7,000
"	"	21.5	1-8	4.3	±0.2	9	6,000
C-2	3-4	0.7	3-8	4.9	±0.7	6	16,000-12,000
"	"	4.8	3-8	4.6	±0.5	6	15,000-11,000
"	"	28.4	1-8	2.6	±0.5	9	9,000-7,000
"	"	95.9	1-8	2.5	±0.3	9	8,000-6,000

TABLE II

A Summary of the Resistances of Dow No. 14 Anodic Films Stripped from FSL-0 Alloy during Exposure to 0.1 N Sodium Chloride Solution. (Film Thickness = 10 Microns)

Film	Time of Exposure (Hours)	Frequency Range (Kilocycles/Sec.)	Average Resistance (Ohms-cm <sup>2</sup> )	Probable Error (Ohms-cm <sup>2</sup> )	Number of Values	Bulk Resistivity (Ohms-cm)
S-1	0.3	5-8	16.4	±0.1	9	16,000
"	0.8	5-8	16.9	±0.1	7	17,000
"	2.3	1-8	18.0	±0.3	15	18,000
"	4.6	2-8	18.4	±0.1	7	18,000
"	5.0	2-8	19.3	±0.1	7	19,000
"	24.1	1-8	22.4	±0.2	15	22,000
"	28.4	2-8	22.6	±0.2	7	23,000
S-2	0.4	5-8	15.3	±0.1	7	15,000
"	0.9	4-8	16.4	±0.1	9	16,000
"	2.0	4-8	17.3	±0.1	9	17,000
"	5.4	2-8	17.2	±0.2	13	17,000
"	5.5	2-8	16.8	±0.2	7	17,000
"	24.6	2-8	15.2	±0.3	13	15,000
"	28.2	3-8	15.0	±0.3	6	15,000

TABLE III

A Summary of the Resistances of Filmed F91  
Electrodes during Exposure to 0.1 N. Sodium Chloride Solution

Surface Treatment	Heat Treatment	Cell Number	Time of Exposure (Hours)	Resistance of Electrode (Ohms)	Film Resistivity (Ohms-cm <sup>2</sup> )	Bulk Resistivity of Film (Ohms-cm)
Dow No. 14	0	1	3.3	79	99	99,000
			5.9	70	84	84,000
			70.6	100	125	125,000
			95.4	103	128	128,000
			118.6	117	146	146,000
Dow No. 14	0	2	0.4	133	120	120,000
			1.5	85	77	77,000
Dow No. 7	H-24	2	0.3 to 2.1	12	11	55,000
Acetic Nitrate Pickled	0	2	0.1 to 0.2	0	0	--

TABLE IV

A Summary of the Resistances of Dow No. 7 Treated FSI Electrodes during Exposure to 0.5 N Sodium Chloride Solution

Alloy Condition	Electrode Arrangement	Time of Exposure (Hours)	Resistance (Ohms)	Surface Resistivity (Ohms-cm <sup>2</sup> )	Bulk Resistivity (Ohms-cm)
-0	Single	0.8	14	1.3	9,000
		1.9	16	1.5	11,000
		3.0	14	1.3	9,000
		22.1	12	1.1	8,000
-0	Series Pair No. 1	0.5	29	2.7	19,000
		1.3	23	2.2	16,000
		3.3	19	1.8	13,000
		5.9	19	1.8	13,000
-0	Series Pair No. 2	0.3	70	6.6	47,000
		0.4	54	5.1	36,000
		1.5	39	3.7	26,000
		3.0	39	3.7	26,000
-0	Series Pair No. 3	5.9	29	2.7	19,000
		3.0	37	3.5	25,000
		5.3	27	2.6	19,000
		0.6	39	3.7	17,000
-H24	Single	2.0	11	1.0	5,000
		2.9	17	1.6	7,000
		22.2	6	0.6	4,000
		0.2	81	7.7	36,000
-H24	Series Pair	0.4	72	6.8	31,000
		2.9	56	5.3	25,000
		6.0	43	4.1	19,000

TABLE V

A Summary of the Resistance of Dow's New, Green, Anodic Treated FSI-0 Electrodes during Exposure to 0.5 N Sodium Chloride Solution

<u>Electrode Arrangement</u>	<u>Time of Exposure (Hours)</u>	<u>Resistance (Ohms)</u>	<u>Surface Resistivity (Ohms-cm<sup>2</sup>)</u>
Series Pair No. 1	1.3	117	11.1
	3.7	109	10.3
	6.0	94	8.9
	23.8	35	3.3
Series Pair No. 2	1.3	1170	111
	2.0	67	6.4
	3.3	112	10.6

TABLE VI

Further Description of Elements  
in Polarizer Circuit Shown in Figure 18

<u>Resistance Number</u>	<u>Value in Ohms</u>
1	100 $\pm$ 1
2	600 (Rheostat)
3	10,000 (Helipot)
4	100,000
5	1,000 000
6	200 (Rheostat)
7	200 (Rheostat)
8	1,000 $\pm$ 10
9	10,000

<u>Ammeter Number</u>	<u>Range (Milliamperes)</u>	<u>Sensitivity per Division (Milliamperes)</u>
1	15	0.2
2	1	0.02
3	$\pm$ 0.025	0.001

Terminals 1 through 8 connect with the selsyn driving recorder chart.

TABLE VII  
Analyses of Alloys Discussed in This Report

ALLOY	%Al	%Zn	%Mn	%Ca	%Cu	%Fe	%Ni	%Pb	%Si	%Sn	%Ba	%K	%Na	%Sr	%C	%Cd
Very High Purity																
Mg No. 67535	<.0001	<.01	<.0001	.0015	<.0001	.0005	<.0003	<.0005	<.001	<.001	<.0001	.0006	.0009	<.0001	.0021	
Cell																
Mg No. 70812	.0004	<.01	.068	<.01	.0007	.027	.0004	<.0005	<.001	<.001						
AZ10A																
AZ31A																
AZ31B																
No. 74150	3.0	1.0	.54	<0.1	0.010	0.004	<.001	.003	.01	<.01						<.01
AZ63A																
No. 46732	6.3	3.0	.41		.012	.002	<.001	.019	.03	<.001						

TABLE VIII

Corrosion Rates of AZ31A-O Alloy Sheet in  
Aqueous Sodium Chloride-Sodium Chromate Solutions

<u>Normality of Na<sub>2</sub>CrO<sub>4</sub>*</u>	<u>Corrosion Rate (Mg/cm<sup>2</sup>/day)</u>	<u>No. of Samples</u>	<u>Mean Deviation</u>
<u>First Run</u>			
0.5	nil	4	--
0.49	nil	4	--
0.45	0.0016	4	0.0002
0.4	0.0025	4	0.0012
0.3	0.0024	4	0.0005
0.2	0.0051	4	0.0014
0.1	0.0061	4	0.0006
0.0	0.278	4	0.0015
<u>Second Run</u>			
0.1	0.060	3**	0.014
0.05	0.131	4	0.014
0.01	0.216	4	0.071
0.001	0.337	4	0.065
0.0	0.515	3**	0.040

\* Plus NaCl to make total concentration of 0.5 N.

\*\* The value for one sample was eliminated because its deviation was over 10 times the mean deviation for the other three.

TABLE IX

Characteristics of the Delay Effect during the Anodic Polarization of Magnesium Alloys in Sodium Chloride-Sodium Chromate Electrolyte

Run Sequence	Normality $\text{Na}_2\text{CrO}_4$	Magnesium Electrode Rotated?	Potential Drop (Volts)	Current Density at Min. ( $\text{mA}/\text{in}^2$ )	Charge Transferred at Min. (Coulombs/ $\text{cm}^2 \times 10^4$ )	$\frac{d}{(\text{m}\mu\epsilon)^{1/2}} = \frac{4.29 \times 10^{-2}}{q^{1/2}}$ ( $\text{\AA}$ units)	Capacitance (Farads/ $\text{cm}^2 \times 10^3$ )
1	0.500	Yes	0.81	0.35	28.3	0.79	3.5
1	0.499	"	0.87	0.28	18.2	1.02	2.1
1	0.490	"	0.90	0.24	13.2	1.19	1.5
1	0.490	"	0.70	0.25	14.5	1.15	2.1
2	0.500	"	1.30	0.35	28.3	0.79	2.2
3	0.500	No	1.53	0.31	22.4	0.90	1.5
3	0.499	Yes	1.50	0.27	17.0	1.06	1.1
3	0.490	"	1.62	0.25	14.5	1.15	0.9
<u>Very High Purity Magnesium</u>							
<u>Cell Magnesium</u>							
1	0.500	Yes	0.69	0.35	28.3	0.79	4.1
1	0.499	"	0.74	0.22	11.1	1.31	1.5
1	0.490	"	0.57	0.22	11.1	1.31	1.9
1	0.490	No	0.54	0.24	13.2	1.19	2.4
2	0.500	Yes	0.74	0.20	9.2	1.42	1.2
2	0.499	"	0.73	0.18	7.5	1.62	1.0
2	0.490	"	0.65	0.17	6.7	1.71	1.0

TABLE IX (Cont.)

Run Sequence	Normality Na <sub>2</sub> CrO <sub>4</sub>	Electrode Rotated?	Potential Drop (Volts)	Current Density at Min. (mA/in <sup>2</sup> )	Charge Transferred at Min. (Coulombs/cm <sup>2</sup> )x10 <sup>4</sup>	$d = \frac{4.29 \times 10^{-2}}{(\text{m}\mu\text{e})^{1/2}} = \frac{q^{1/2}}{(\text{\AA units})}$	Capacitance (Farads/cm <sup>2</sup> )x10 <sup>3</sup>
3	0.500	No	1.08	1.14	4.6	2.07	0.4
3	0.499	"	0.66	0.15	5.2	1.93	0.8
3	0.490	"	0.82	0.14	4.6	2.07	0.5
3	0.490	Yes	0.65	0.15	5.2	1.93	0.8
<u>AZ10A ALLOY</u>							
1	0.500	Yes	0.71	0.20	9.2	1.42	1.3
1	0.499	"	0.75	0.20	9.2	1.42	1.2
1	0.490	"	0.59	0.20	9.2	1.42	1.6
1	0.490	No	0.60	0.15	5.2	1.93	0.8
2	0.500	Yes	0.90	0.15	5.2	1.93	0.6
2	0.499	"	0.71	0.15	5.2	1.93	0.7
2	0.490	"	0.66	0.12	3.4	2.38	0.5
2	0.490	No	0.59	0.12	3.4	2.38	0.6
<u>AZ31A ALLOY</u>							
1	0.500	Yes	0.61	0.20	9.2	1.42	1.5
1	0.499	"	0.58	0.19	8.3	1.54	1.4
1	0.490	"	0.58	0.18	7.5	1.62	1.3
2	0.500	"	0.59	0.13	4.0	2.22	0.7
3	0.500	No	0.66	0.12	3.4	2.38	0.5
3	0.490	Yes	0.83	0.13	4.0	2.22	0.5

TABLE IX (Cont.)

Run Sequence	Normality Na <sub>2</sub> CrO <sub>4</sub>	Electrode Rotated?	Potential Drop (Volts)	Current Density at Min. (mA/in <sup>2</sup> )	Charge Transferred at Min. (Coulombs/cm <sup>2</sup> )x10 <sup>4</sup>	$\frac{d}{(m\mu\epsilon)^{1/2}} = \frac{4.29 \times 10^{-2}}{q^{1/2}}$ (Å units)	Capacitance (Farads/cm <sup>2</sup> )x10 <sup>3</sup>
<u>AZ31B ALLOY</u>							
1	0.500	Yes	0.66	0.25	14.5	1.15	2.2
1	0.499	"	0.52	0.19	8.3	1.54	1.6
1	0.490	"	0.72	0.18	7.5	1.62	1.0
1	0.490	No	0.55	0.19	8.3	1.54	1.5
2	0.500	Yes	0.67	0.14	4.6	2.07	0.7
2	0.490	"	0.66	0.14	4.6	2.07	0.7
2	0.490	No	0.69	0.13	4.0	2.22	0.6
3	0.500	"	0.67	0.15	5.2	1.93	0.8
3	0.499	Yes	1.06	0.12	3.4	2.38	0.3
<u>AZ63A ALLOY</u>							
1	0.500	Yes	0.65	--	--	--	--
1	0.490	"	0.58	0.24	13.2	1.19	2.3
1	0.490	No	0.58	--	--	--	--
2	0.500	Yes	1.03	0.23	12.1	1.25	1.2
2	0.490	"	0.83	0.18	7.5	1.62	0.9
2	0.490	No	0.57	0.12	3.4	2.38	0.6
3	0.500	"	1.10	0.14	4.6	2.07	0.4

TABLE X

Characteristics of the Delay Effect during the Anodic Polarization of Magnesium Alloys in Sodium Bromide-Sodium Chromate Electrolyte

Run Sequence	Normality $\text{Na}_2\text{CrO}_4$	Electrode Rotated?	Potential Drop (Volts)	Current Density at Min. (mA/in <sup>2</sup> )	Charge Transferred at Min. (Coulombs/cm <sup>2</sup> )x10 <sup>4</sup>	$\frac{d}{(\text{m} \rho \epsilon)^{1/2}} = \frac{4.29 \times 10^{-2}}{q^{1/2}}$ (Å units)	Capacitance (Farads/cm <sup>2</sup> )x10 <sup>3</sup>
<u>Very High Purity Magnesium</u>							
1	0.500	Yes	0.83	0.35	28.3	0.79	3.4
1	0.500	No	0.88	0.23	12.1	1.25	1.4
1	0.500	No	0.89	0.23	12.1	1.25	1.4
1	0.490	Yes	0.78	0.23	12.1	1.25	1.5
1	0.490	Yes	0.93	0.23	12.1	1.25	1.3
1	0.490	Yes	0.81	0.23	12.1	1.25	1.5
1	0.490	Yes	0.78	0.21	10.1	1.38	1.3
1	0.490	No	0.82	0.22	11.1	1.31	1.4
2	0.490	Yes	1.04	0.23	12.1	1.25	1.2
<u>Cell Magnesium</u>							
1	0.500	Yes	0.71	0.25	14.5	1.15	2.0
1	0.500	Yes	0.72	0.21	10.1	1.38	1.4
1	0.500	No	0.65	0.21	10.1	1.38	1.5
1	0.500	No	0.75	0.19	8.3	1.54	1.1
2	0.500	Yes	0.68	0.15	5.2	1.93	0.8
<u>AZ10A ALLOY</u>							
1	0.500	Yes	0.62	0.19	8.3	1.54	1.3
1	0.500	Yes	0.59	0.17	6.7	1.71	1.1

TABLE X (Cont.)

Run Sequence	Normality Na <sub>2</sub> CrO <sub>4</sub>	Electrode Rotated?	Potential Drop (Volts)	Current Density at Min. (mA/in <sup>2</sup> )	Charge Transferred at Min. (Coulombs/cm <sup>2</sup> )x10 <sup>4</sup>	$d = \frac{4.29 \times 10^{-2}}{q^{1/2}}$ (Å units)	Capacitance (Farads/cm <sup>2</sup> )x10 <sup>3</sup>
1	0.500	No	0.49	0.17	6.7	1.71	1.4
1	0.500	No	0.58	0.18	7.5	1.62	1.3
1	0.490	Yes	0.53	0.18	7.5	1.62	1.4
1	0.490	Yes	0.55	0.16	6.0	1.81	1.1
1	0.490	No	0.57	0.15	5.2	1.93	0.9
2	0.490	Yes	0.54	0.14	4.6	2.07	0.9
<u>AZ31A ALLOY</u>							
1	0.500	Yes	0.70	0.19	8.3	1.54	1.2
1	0.500	Yes	0.56	0.17	6.7	1.71	1.2
1	0.500	No	0.46	0.17	6.7	1.71	1.5
1	0.500	No	0.47	0.16	6.0	1.81	1.3
1	0.500	No	0.60	0.17	6.7	1.71	1.1
1	0.500	No	0.57	0.18	7.5	1.62	1.3
1	0.490	Yes	0.49	0.17	6.7	1.71	1.4
1	0.490	Yes	0.52	0.18	7.5	1.62	1.4
1	0.490	No	0.52	0.17	6.7	1.71	1.3
1	0.490	No	0.52	0.17	6.7	1.71	1.3
2	0.500	Yes	0.55	0.13	4.0	2.22	0.7
2	0.490	Yes	0.62	0.13	4.0	2.22	0.6

TABLE X (Cont.)

Run Sequence	Normality $\text{Na}_2\text{CrO}_4$	Electrode Rotated?	Potential Drop (Volts)	Current Density at Min. (mA/in <sup>2</sup> )	Charge Transferred at Min. (Coulombs/cm <sup>2</sup> )x10 <sup>4</sup>	$\frac{d}{(\text{m}\mu\text{e})^{1/2}} = \frac{4.29 \times 10^{-2}}{q^{1/2}}$ ( $\text{\AA}$ units)	Capacitance (Farads/cm <sup>2</sup> )x10 <sup>3</sup>
<u>AZ31B ALLOY</u>							
1	0.500	Yes	0.70	0.20	9.2	1.42	1.3
1	0.500	No	0.53	0.15	5.2	1.93	1.0
1	0.500	No	0.48	0.17	6.7	1.71	1.4
1	0.490	Yes	0.64	0.18	7.5	1.62	1.2
1	0.490	Yes	0.68	0.17	6.7	1.71	1.0
1	0.490	Yes	0.59	0.20	9.2	1.42	1.6
1	0.490	Yes	0.59	0.17	6.7	1.71	1.1
1	0.490	Yes	0.63	0.18	7.5	1.62	1.2
1	0.490	Yes	0.72	0.21	10.1	1.38	1.4
1	0.490	Yes	0.61	0.19	8.3	1.54	1.4
1	0.490	No	0.54	0.17	6.7	1.71	1.2
1	0.490	No	0.57	0.18	7.5	1.62	1.3
2	0.500	Yes	0.64	0.13	4.0	2.22	0.6
<u>AZ63A ALLOY</u>							
1	0.500	Yes	0.53	0.22	11.1	1.31	2.1
1	0.500	Yes	0.72	0.23	12.1	1.25	1.7
1	0.490	Yes	0.64	0.21	10.1	1.38	1.6
1	0.490	No	0.68	0.18	7.5	1.62	1.1
2	0.500	Yes	0.76	0.15	5.2	1.93	0.7
2	0.490	Yes	0.70	0.14	4.6	2.07	0.6

TABLE XI

Characteristics of the Delay Effect during the Anodic Polarization of Dow No. 7 Treated Magnesium Alloy in Sodium Chloride-Sodium Chromate Electrolyte

Run Sequence	Normality Na <sub>2</sub> CrO <sub>4</sub>	Electrode Rotated?	Potential Drop (Volts)	Current Density at Min. (mA/in <sup>2</sup> )	Charge Transferred at Min. (Coulombs/cm <sup>2</sup> )x10 <sup>4</sup>	$\frac{d}{(mn/\epsilon)^{1/2}} = \frac{4.29 \times 10^{-2}}{q^{1/2}}$ (Å units)	Capacitance (Farads/cm <sup>2</sup> )x10 <sup>3</sup>
<u>AZ31A Alloy</u>							
1	0.450	No	0.99	0.14	4.6	2.07	0.5
1*	0.400	No	0.34	0.10	2.3	2.78	0.7
2	0.500	Yes	0.68	0.13	4.0	2.22	0.6
2/	0.500	No	1.27	0.17	6.7	1.71	0.5
2	0.490	Yes	1.04	0.24	13.2	1.19	1.3
2	0.450	No	1.13	0.15	5.2	1.93	0.5
2*	0.400	No	0.89	0.23	12.1	1.25	1.4
3	0.500	Yes	1.19	0.18	7.5	1.62	0.7
3/	0.500	No	1.15	0.14	4.6	2.07	0.4
3	0.450	Yes	0.33	0.07	1.2	3.46	0.4
3*	0.400	Yes	1.03	0.17	6.7	1.71	0.7
4/	0.500	Yes	1.19	0.12	3.4	2.38	0.3
<u>AZ31B Alloy</u>							
1	0.500	No	0.30	0.16	6.0	1.81	2.0
1*	0.450	No	0.24	0.09	1.9	2.94	0.8
1*	0.400	No	0.36	0.10	2.3	2.78	0.7

\* Potential was oscillating sufficiently to make results uncertain.

/ Electrode was aged an extra 30 minutes before first run.

TABLE XI (Cont.)

Run Sequence	Normality $\text{Na}_2\text{CrO}_4$	Electrode Rotated?	Potential Drop (Volts)	Current Density at Min. (mA/in <sup>2</sup> )	Charge Transferred at Min. (Coulombs/cm <sup>2</sup> )x10 <sup>4</sup>	$\frac{d}{I^{1/2}}$ (mA <sup>1/2</sup> ε) = $\frac{4.29 \times 10^{-2}}{q}$ (Å units)	Capacitance (Farads/cm <sup>2</sup> )x10 <sup>3</sup>
2	0.500	Yes	0.62	0.14	4.6	2.07	0.7
2/	0.500	No	1.17	0.21	10.1	1.38	0.9
2	0.450	No	0.82	0.18	7.5	1.62	0.9
2*	0.400	No	0.76	0.16	6.0	1.81	0.9
3/	0.500	No	1.19	0.18	7.5	1.62	0.7
3	0.450	Yes	1.00	0.19	8.3	1.54	0.8
3*	0.400	Yes	0.88	0.15	5.2	1.93	0.6
<u>AZ63A ALLOY</u>							
2	0.490	No	0.86	0.15	5.2	1.93	0.6
2*	0.450	No	0.97	0.18	7.5	1.62	0.8
2*	0.400	No	0.64	0.27	17.0	1.06	2.7
2*	0.300	No	0.34	0.27	17.0	1.06	5.0
3	0.490	Yes	0.96	0.15	5.2	1.93	0.5
3*	0.450	Yes	1.11	0.19	8.3	1.54	0.8
3*	0.400	Yes	0.77	0.27	17.0	1.06	2.2
3*	0.300	Yes	0.57	0.25	14.5	1.15	2.5

\*Potential was oscillating sufficiently to make results uncertain.

/ Electrode was aged an extra 30 minutes before first run.

TABLE XII

Summary of "Film Parameters"\* and Capacitances from Delay Data in the Electrolyte Systems NaCl-Na<sub>2</sub>CrO<sub>4</sub>-Aqueous and NaBr-Na<sub>2</sub>CrO<sub>4</sub>-Aqueous

Run Sequence	Normality* NaCl	Normality* NaBr	$\frac{d}{(\text{msec})^{1/2}}$ in Å			Capacitance (Farads/cm <sup>2</sup> )x10 <sup>3</sup>		
			Avg.	No. of Values	Mean Deviation	Avg.	No. of Values	Mean Deviation
<u>Very High Purity Magnesium</u>								
1	0	0	1.0	4	0.2	2.4	4	1.0
1	0.01	0	1.0	1	-	2.1	1	-
1	0.1	0	1.2	2	<0.1	1.8	2	0.2
1	0	0.1	1.3	6	<0.1	1.4	6	<0.1
2	0	0	0.8	1	-	2.2	1	-
2	0	0.1	1.3	1	-	1.2	1	-
3	0	0	0.9	1	-	1.5	1	-
3	0.01	0	1.1	1	-	1.1	1	-
3	0.1	0	1.2	1	-	0.9	1	-
<u>Cell Magnesium</u>								
1	0	0	1.2	5	0.2	2.0	5	0.8
1	0.01	0	1.0	1	-	2.1	1	-
1	0.1	0	1.2	2	<0.1	1.8	2	0.3
2	0	0	1.7	2	0.3	1.0	2	0.2
2	0.01	0	1.6	1	-	1.0	1	-
2	0.1	0	1.7	1	-	1.0	1	-
3	0	0	2.1	1	-	0.4	1	-
3	0.01	0	1.9	1	-	0.8	1	-
3	0.1	0	2.0	2	<0.1	0.7	2	<0.2
<u>AZ10A Alloy</u>								
1	0	0	1.6	5	0.1	1.3	5	<0.1
1	0.01	0	1.4	1	-	1.2	1	-
1	0.1	0	1.7	2	<0.3	1.2	2	0.4
1	0	0.1	1.8	3	0.1	1.1	3	0.2

\* Plus Na<sub>2</sub>CrO<sub>4</sub> to make a total normality of 0.5.

TABLE XII (Cont.)

Run Sequence	Normality* NaCl	Normality* NaBr	$\frac{d}{(m\mu e)}^{1/2}$ in Å			Capacitance (Farads/cm <sup>2</sup> )x10 <sup>3</sup>		
			Avg.	No. of Values	Mean Deviation	Avg.	No. of Values	Mean Deviation
2	0	0	1.9	1	-	0.6	1	-
2	0.01	0	1.9	1	-	0.7	1	-
2	0.1	0	2.4	2	0	0.6	2	<0.1
2	0	0.1	2.1	1	-	0.9	1	-
<u>AZ31A Alloy</u>								
1	0	0	1.6	7	0.1	1.3	7	0.1
1	0.01	0	1.5	1	-	1.4	1	-
1	0.1	0	1.6	1	-	1.3	1	-
1	0	0.1	1.7	4	<0.1	1.4	4	<0.1
2	0	0	2.2	2	0	0.7	2	0
2	0	0.1	2.2	1	-	0.6	1	-
3	0	0	2.4	1	-	0.5	1	-
3	0.1	0	2.2	1	-	0.5	1	-
<u>AZ31B Alloy</u>								
1	0	0	1.6	4	0.3	1.5	4	0.4
1	0.01	0	1.5	1	-	1.6	1	-
1	0.1	0	1.6	2	<0.1	1.3	2	>0.2
1	0	0.1	1.6	9	0.1	1.3	9	>0.1
2	0	0	2.1	2	0.1	0.7	2	<0.1
2	0.1	0	2.1	2	0.1	0.7	2	<0.1
2	0	0.1	1.9	1	-	0.8	1	-
3	0	0	1.9	1	-	0.8	1	-
3	0.01	0	2.4	1	-	0.3	1	-
<u>AZ63A Alloy</u>								
1	0	0	1.3	2	<0.1	1.9	2	0.2
1	0.1	0	1.2	1	-	2.3	1	-
1	0	0.1	1.5	2	0.1	1.4	2	<0.3
2	0	0	1.6	2	<0.4	1.0	2	<0.3
2	0.1	0	2.0	2	0.4	0.8	2	<0.2
2	0	0.1	2.1	1	-	0.6	1	-

\* Plus Na<sub>2</sub>CrO<sub>4</sub> to make a total normality of 0.5.

TABLE XIII

The Effect of Current Density on the Delay Effect during the Anodic Polarization of Magnesium Alloys in 0.5 N. Sodium Chromate Solution

Run Sequence	Current Density Range (MA/in. <sup>2</sup> )	Potential Drop (Volts)	Current Density at Min. (MA/in. <sup>2</sup> )	Charge Transferred at Minimum (Coulombs/in. <sup>2</sup> )x10 <sup>4</sup>	$\frac{d}{(\text{mm}\rho e)} = \frac{1/2}{q} \frac{4.29 \times 10^{15}}{1/2}$ (Å Units)	Capacitance (Farads/in. <sup>2</sup> )x10 <sup>3</sup>
1	1.0	0.81	0.35	28.3	0.79	3.5
1	1.0	0.83	0.35	28.3	0.79	3.4
1	1.0	0.88	0.23	12.1	1.25	1.4
1	1.0	0.89	0.23	12.1	1.25	1.4
1	2.0	0.95	0.40	18.5	1.00	2.0
2	1.0	1.30	0.35	28.3	0.79	2.2
2	2.0	1.24	0.38	16.8	1.05	1.4

Very High Purity Magnesium

AZ31A ALLOY

1	1.0	0.61	0.20	9.2	1.42	1.5
1	1.0	0.70	0.19	8.3	1.54	1.2
1	1.0	0.56	0.17	6.7	1.71	1.5
1	1.0	0.46	0.17	6.7	1.71	1.3
1	1.0	0.47	0.16	6.0	1.81	1.1
1	1.0	0.60	0.17	6.7	1.71	1.3
1	1.0	0.57	0.18	7.5	1.62	1.0
1	2.0	0.82	0.27	8.4	1.48	0.7
2	1.0	0.59	0.13	4.0	2.22	0.7
2	1.0	0.55	0.13	4.0	2.22	0.7
2	2.0	0.71	0.24	6.7	1.66	0.9

TABLE XIV

Summary at Two Current Density Levels of "Film Parameters" and Capacitances from Delay Data in 0.5 N.  $\text{Na}_2\text{CrO}_4$  Solutions

Run Sequence	Current Density Range (MA/in. <sup>2</sup> )	$\frac{d}{(mm\mu\epsilon)^{1/2}}$ in Å			Capacitance (Farads/in. <sup>2</sup> )x10 <sup>3</sup>		
		Avg. Values	No. of Values	Devi- ation	Avg. Values	No. of Values	Devi- ation
<u>Very High Purity Magnesium</u>							
1	1.0	1.0	4	0.2	2.4	4	1.0
1	2.0	1.0	1	-	2.0	1	-
2	1.0	0.8	1	-	2.2	1	-
2	2.0	1.0	1	-	1.4	1	-
<u>AZ31A Alloy</u>							
1	1.0	1.6	7	0.1	1.3	7	0.1
1	2.0	1.5	1	-	1.0	1	-
2	1.0	2.2	2	0	0.7	2	0
2	2.0	1.7	1	-	0.9	1	-

TABLE XV

The Thickness of Dow No. 7 Films on AZ31A Alloy as a Function of Alloy Condition and pH of the Dichromate Bath\*

Condition	pH of Bath	Film Thickness (Microns)	Number of Measurements	Mean Deviation (Microns)
-H24	4.1	2.2	28	0.3
-H24	4.7	2.1	35	0.3
-H24	5.1	1.7	32	0.3
-0	4.1	1.4	28	0.2
-0	4.7	1.4	15	0.4
-0	5.1	1.1	15	0.2

\* Surface pretreatment consisted of polishing the sheet with No. 320 aloxite paper to remove surface contamination and then treating it for five minutes with MF (a mixture of alkali acid fluorides) activator.

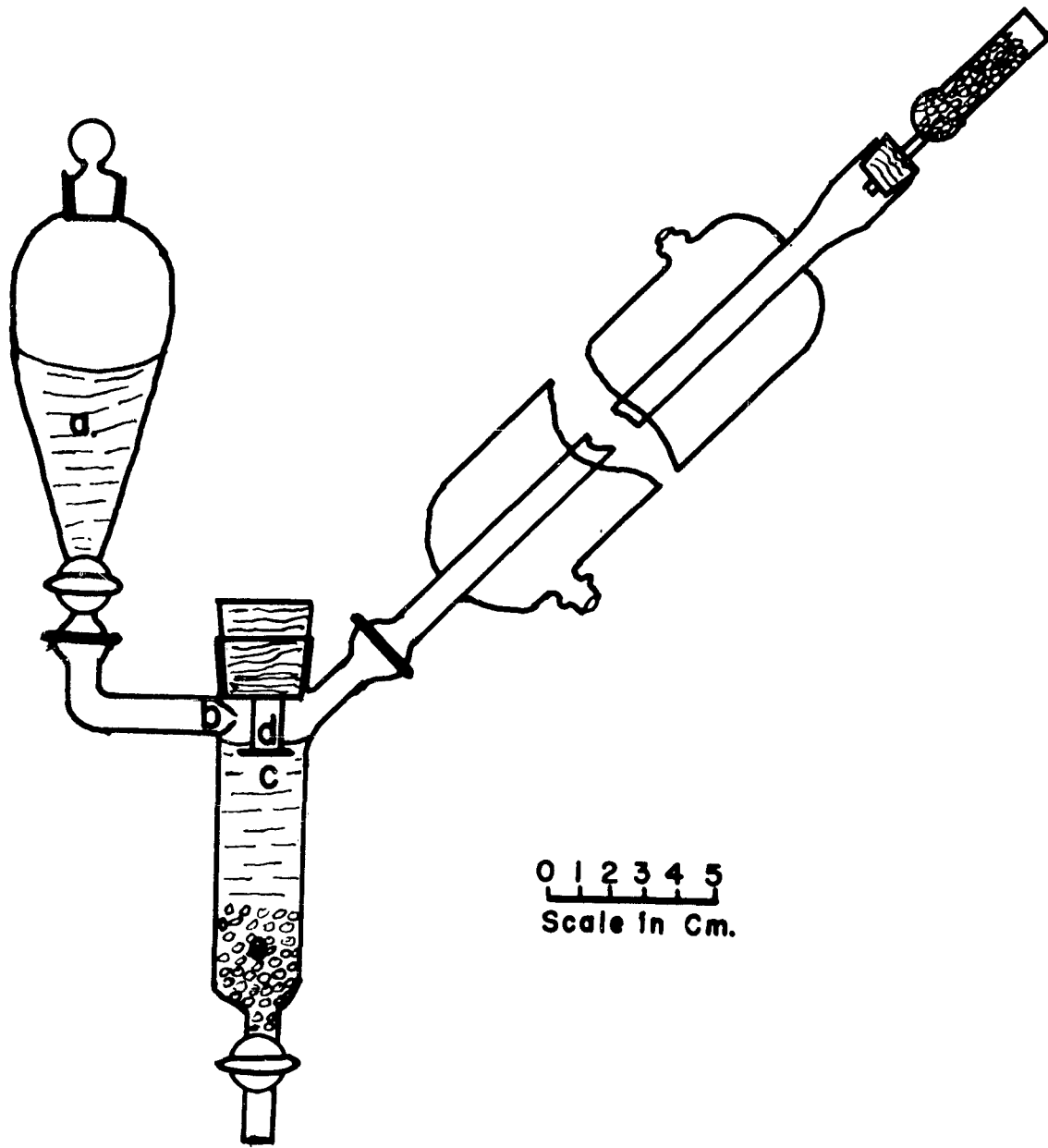


Figure 1. Film Stripping Apparatus.

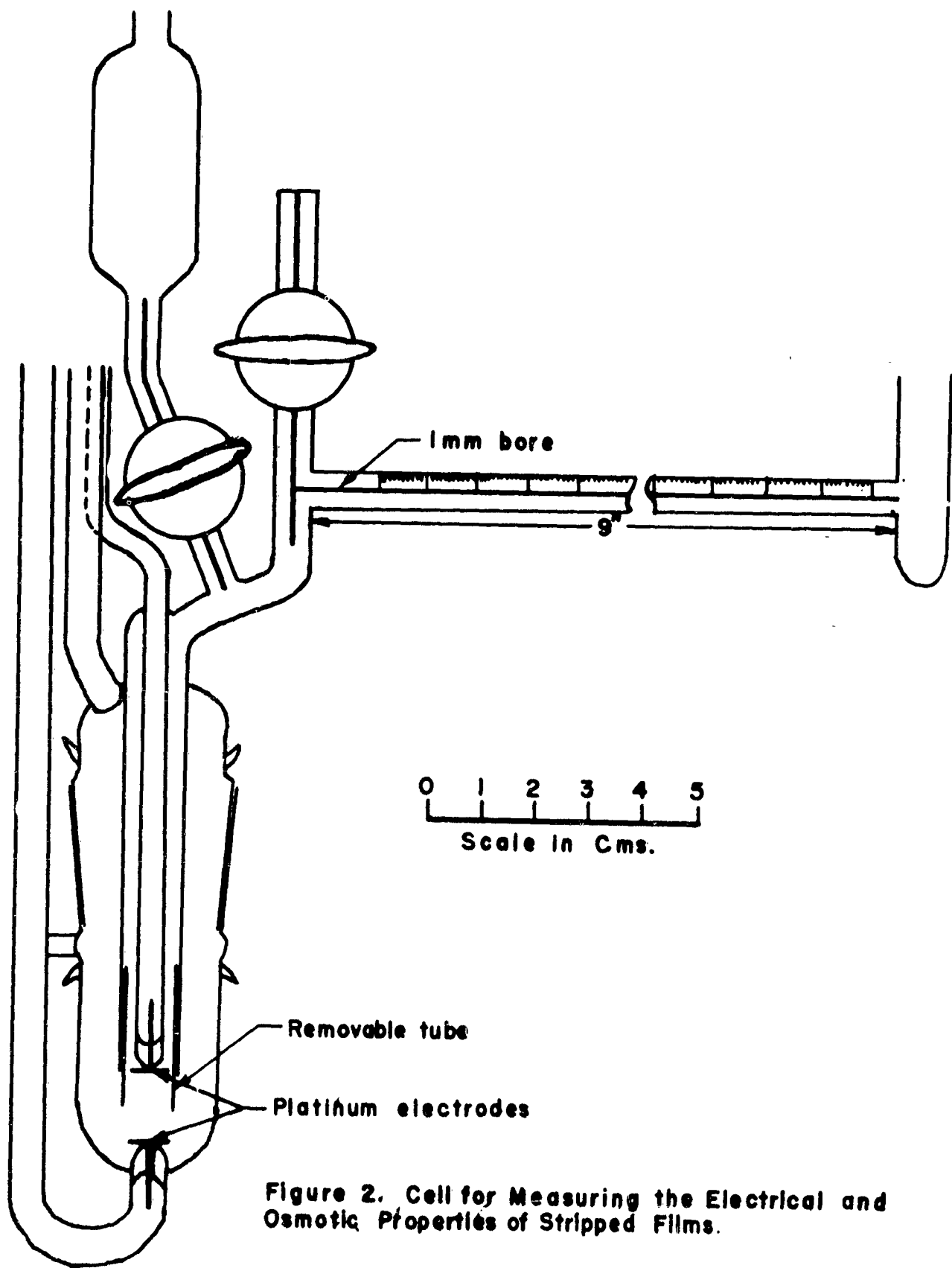
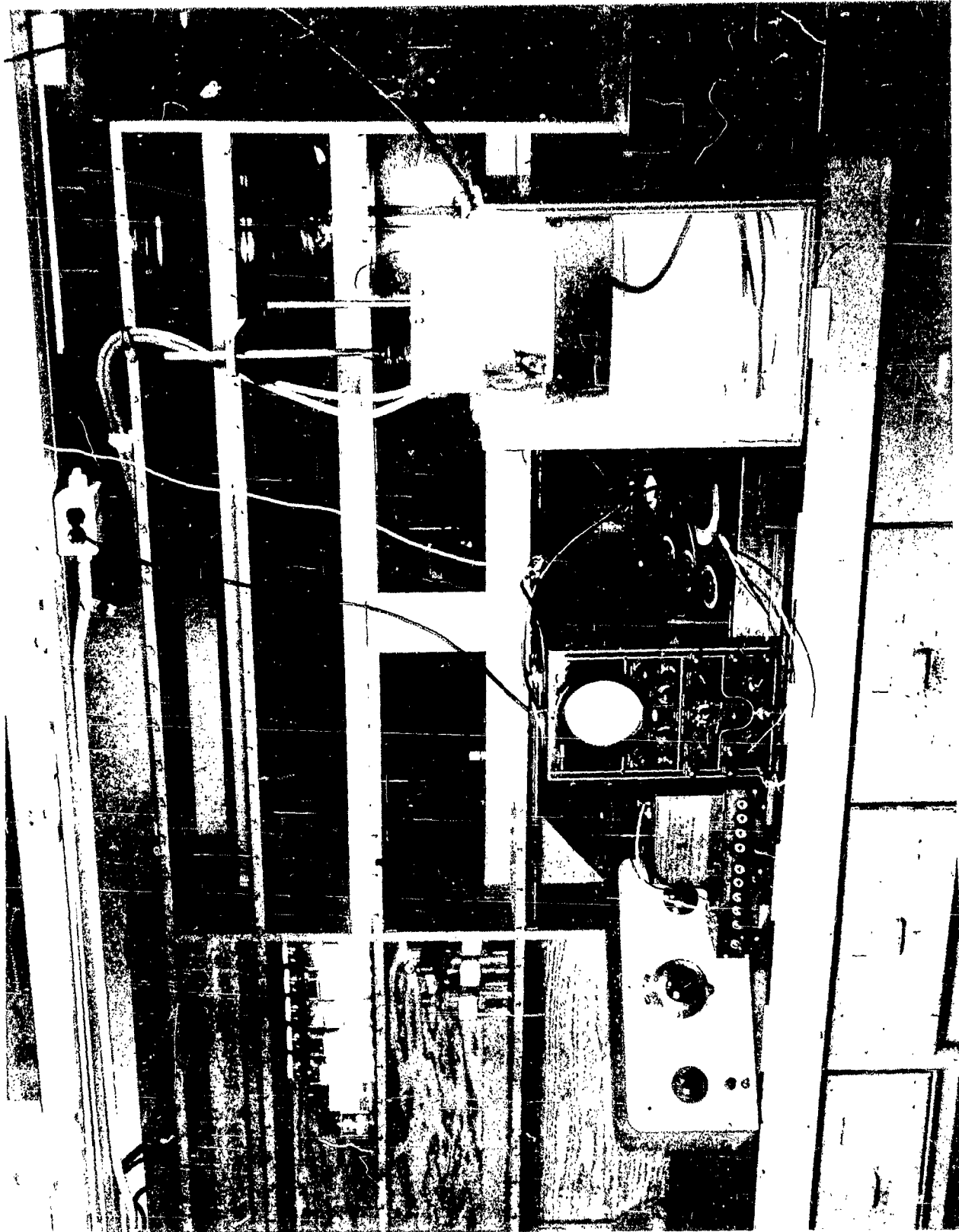


Figure 2. Cell for Measuring the Electrical and Osmotic Properties of Stripped Films.



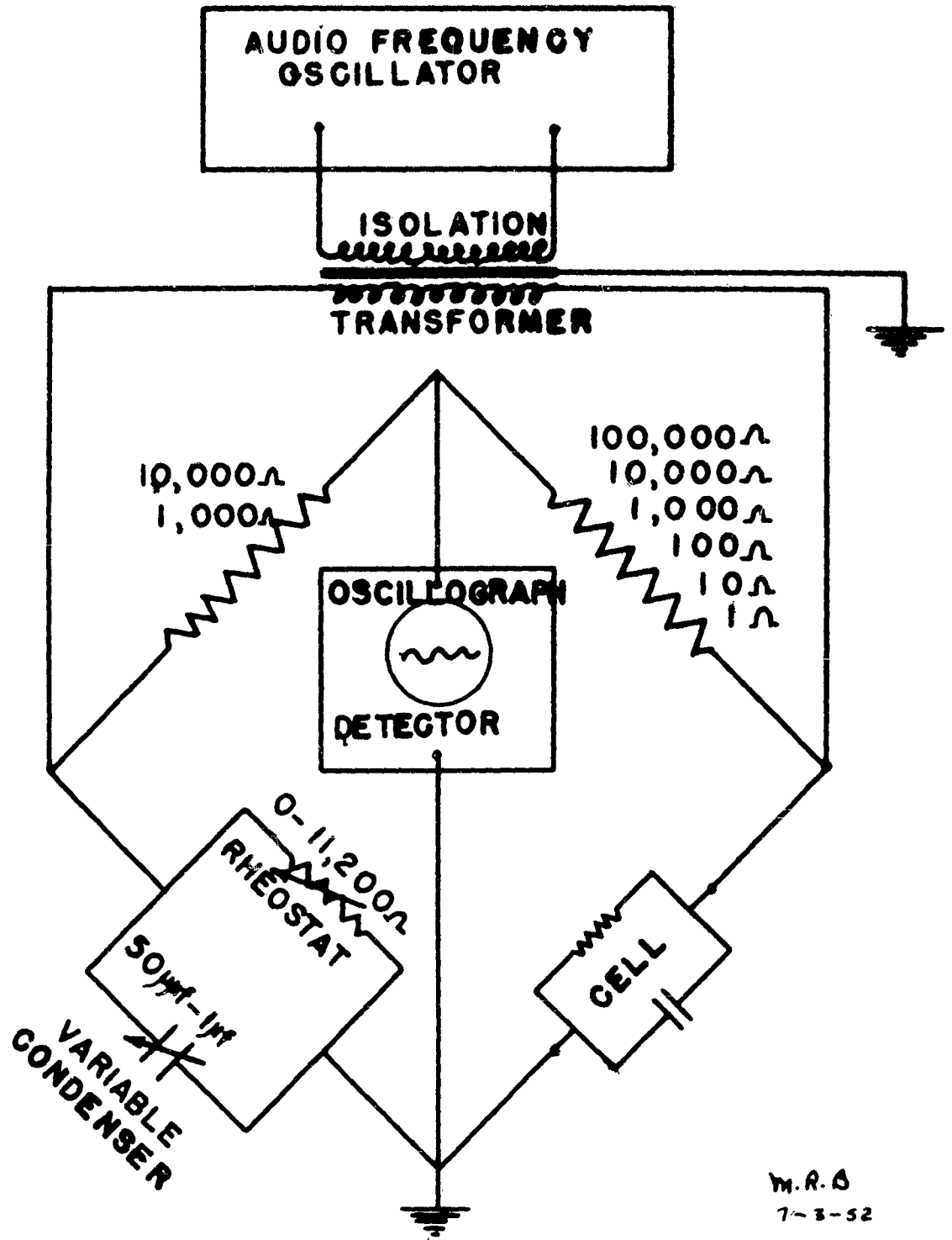


Fig. 4. Circuit for Impedance Measurements on Films.

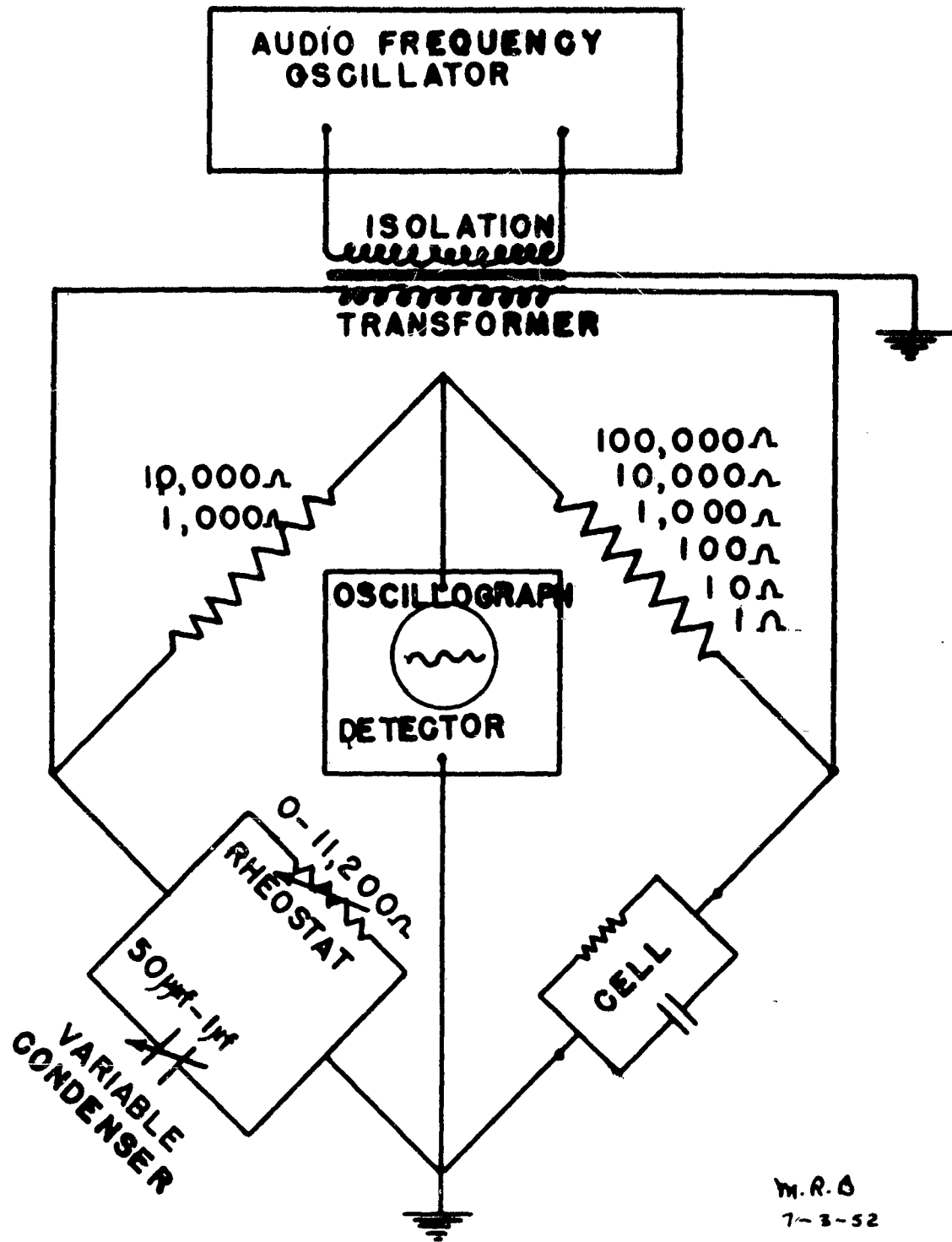
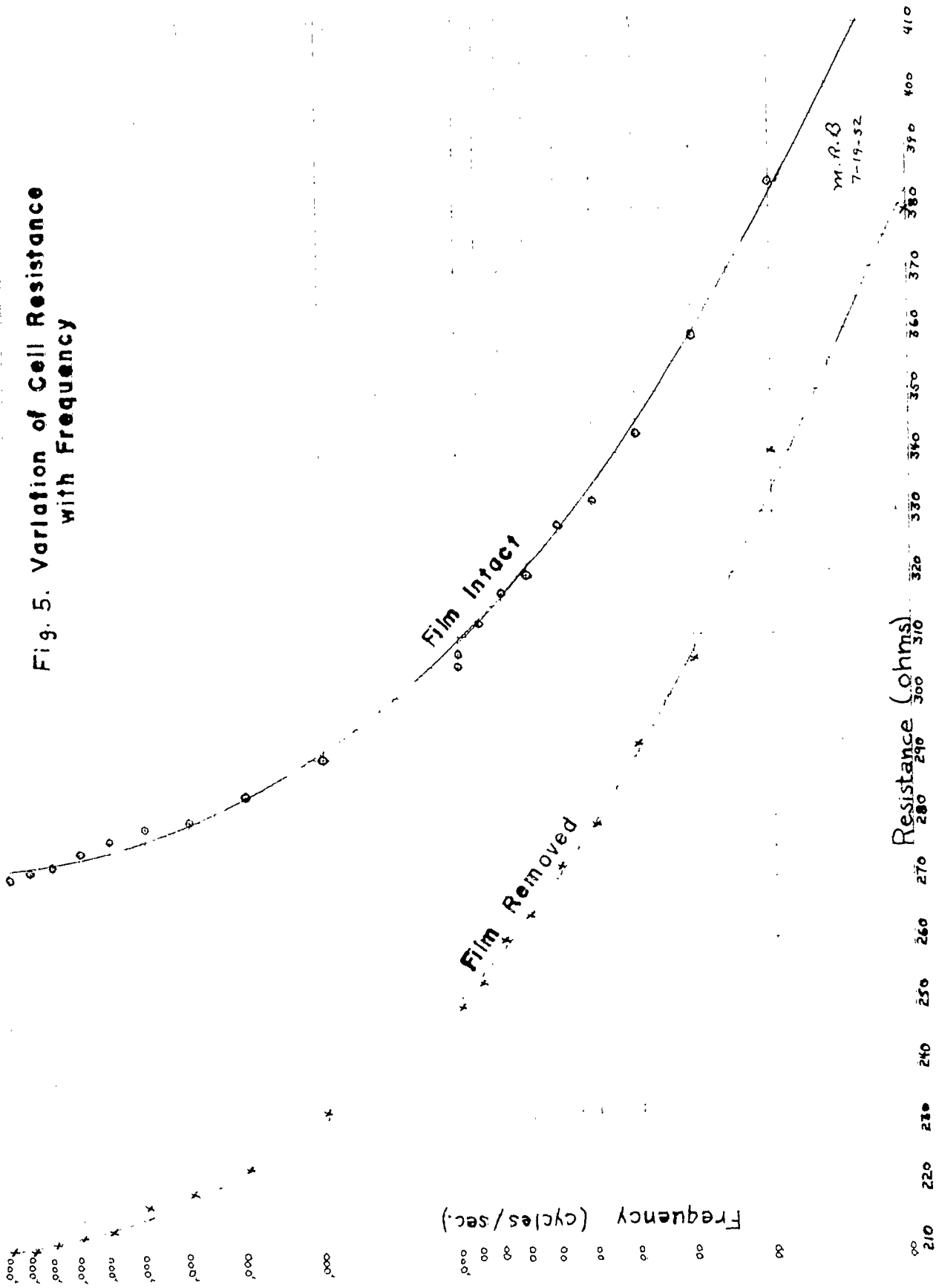


Fig. 4. Circuit for Impedance Measurements on Films.

Fig. 5. Variation of Cell Resistance with Frequency



25

24

23

22

21

20

19

18

17

16

15

Film Resistivity (ohm-cm<sup>2</sup>)

7 μ Film from Pure Magnesium X  
3-4 μ Film from Pure Magnesium A

12 μ Film from Pure Magnesium (Mean Curve) ②  
10 μ Film from ES-1 Alloy (Mean Curve) ①

Time (Hours)

0

1

2

3

4

5

6

7

8

9

10

11

12

13

14

15

16

17

18

19

20

21

22

23

24

25

26

27

28

29

30

31

32

33

34

35

36

37

38

17

17

②

①

①

□

④

②

③

⑤

③

②

②

②

②

②

③

②

②

③

②

②

③

②

②

③

②

②

③

②

②

③

②

②

③

②

②

③

②

②

③

②

②

③

②

②

③

②

②

③

②

②

③

②

②

③

②

②

③

②

②

③

②

②

③

②

②

③

②

②

③

②

②

③

②

②

③

②

②

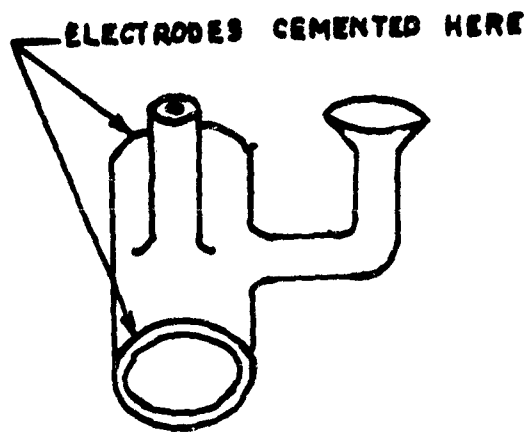


FIGURE 7  
CELL NO. 1

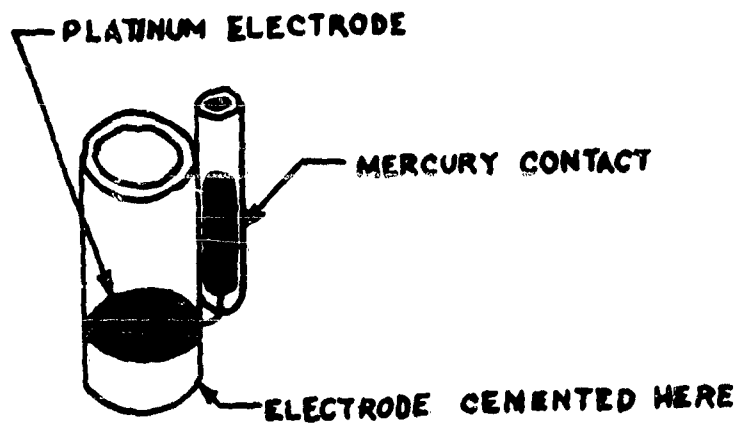


FIGURE 8  
CELL NO. 2



FIGURE 9. CELL NO. 3  
a = Magnesium electrode strip.  
b = Silver electrode.

FIGURE 10  
 ELECTRICAL CHARACTERISTICS OF DOW NO. 14  
 TREATED FS ELECTRODES IN CELL NO. 1

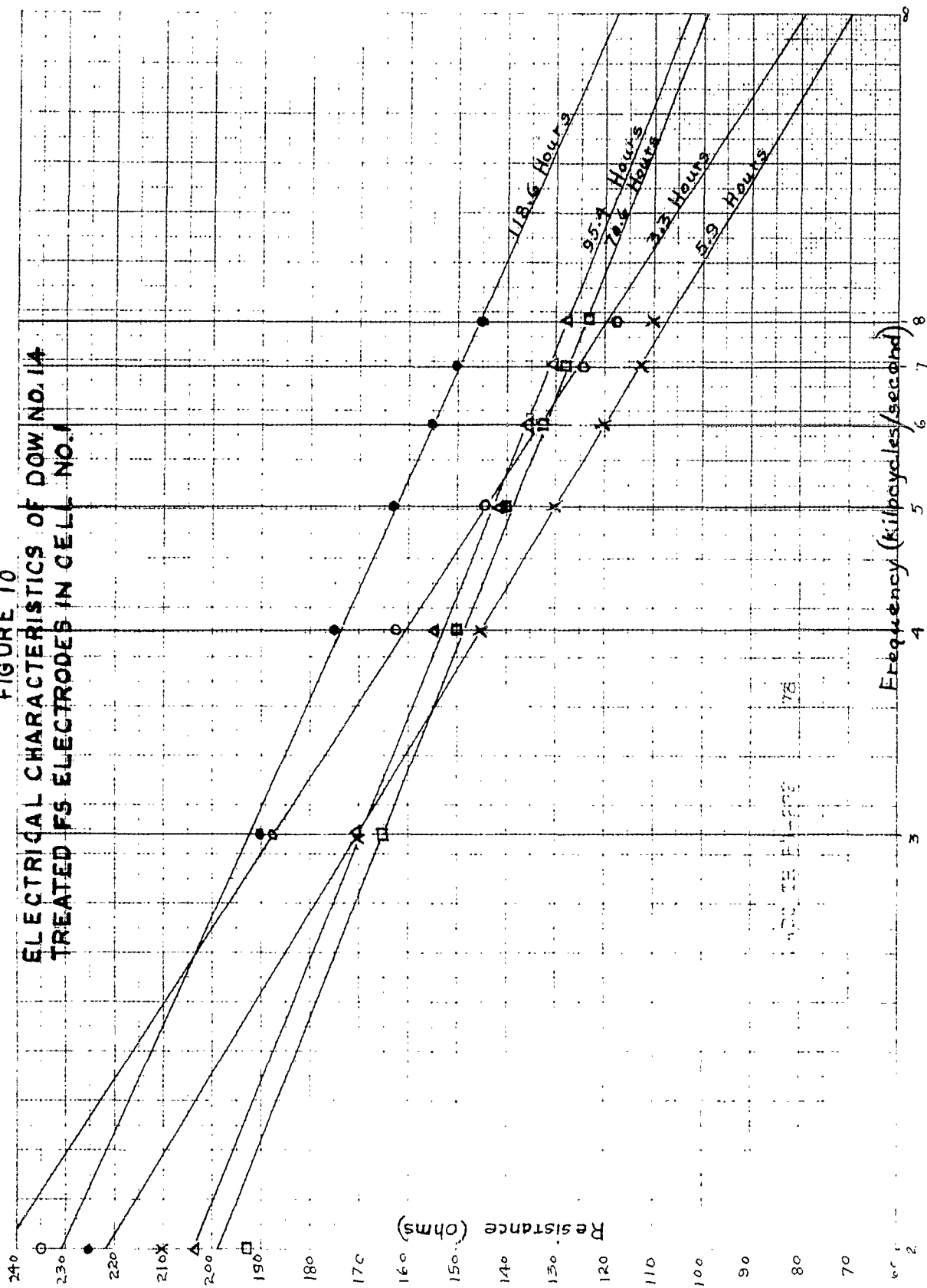
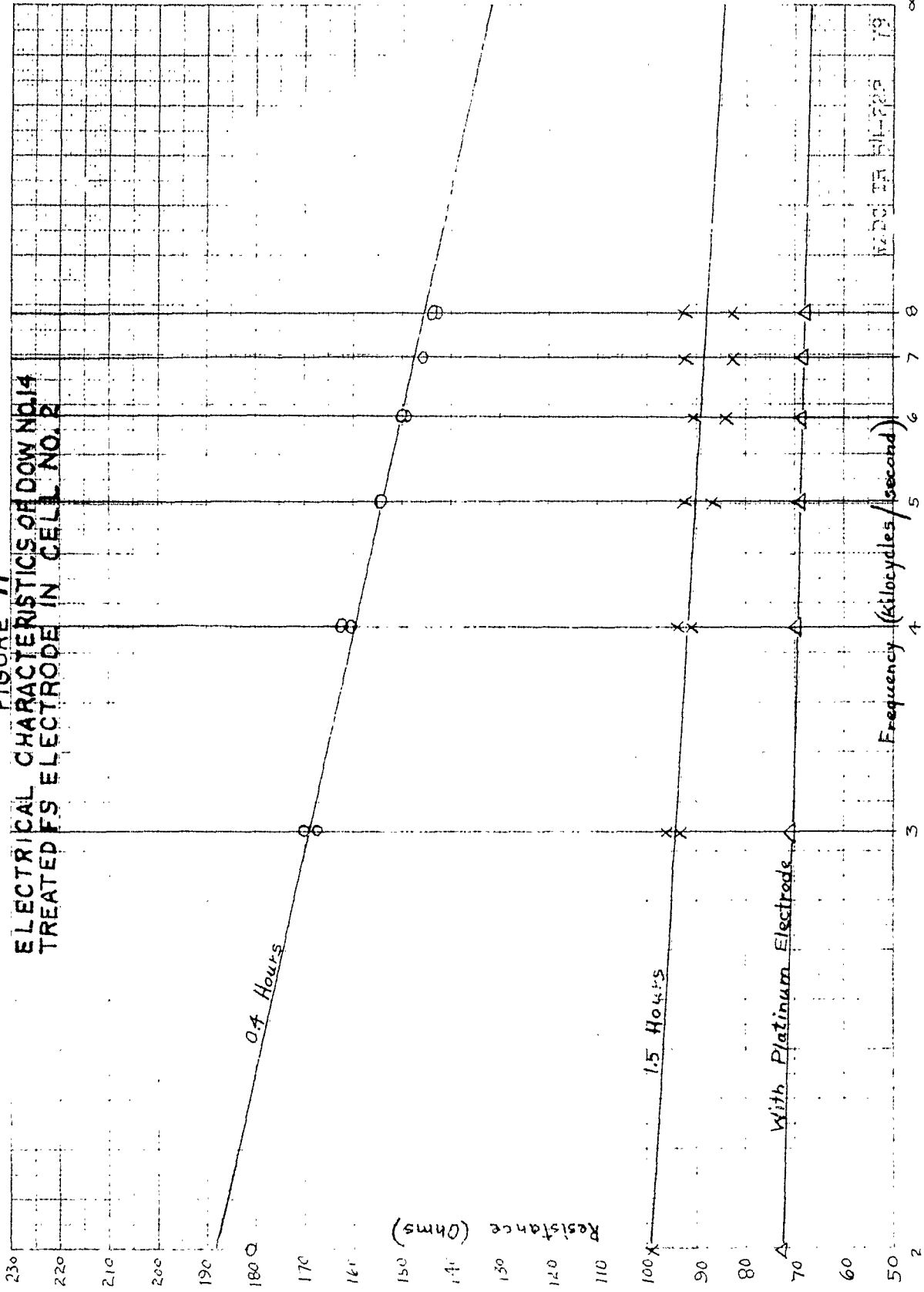
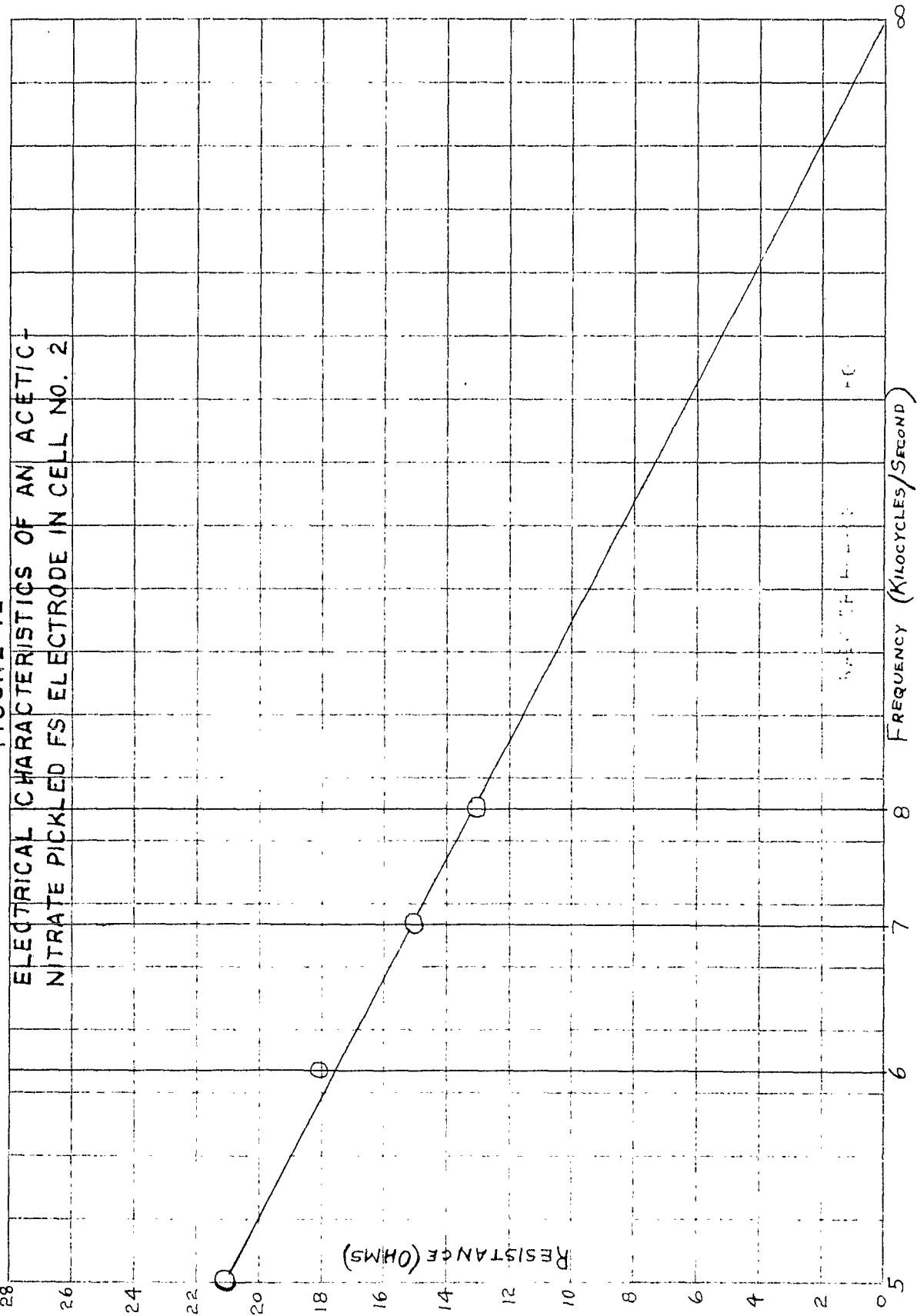


FIGURE 11  
ELECTRICAL CHARACTERISTICS OF DOW NO. 14  
TREATED FS ELECTRODE IN CELL NO. 2



W200 EA 511-225 79

FIGURE 12



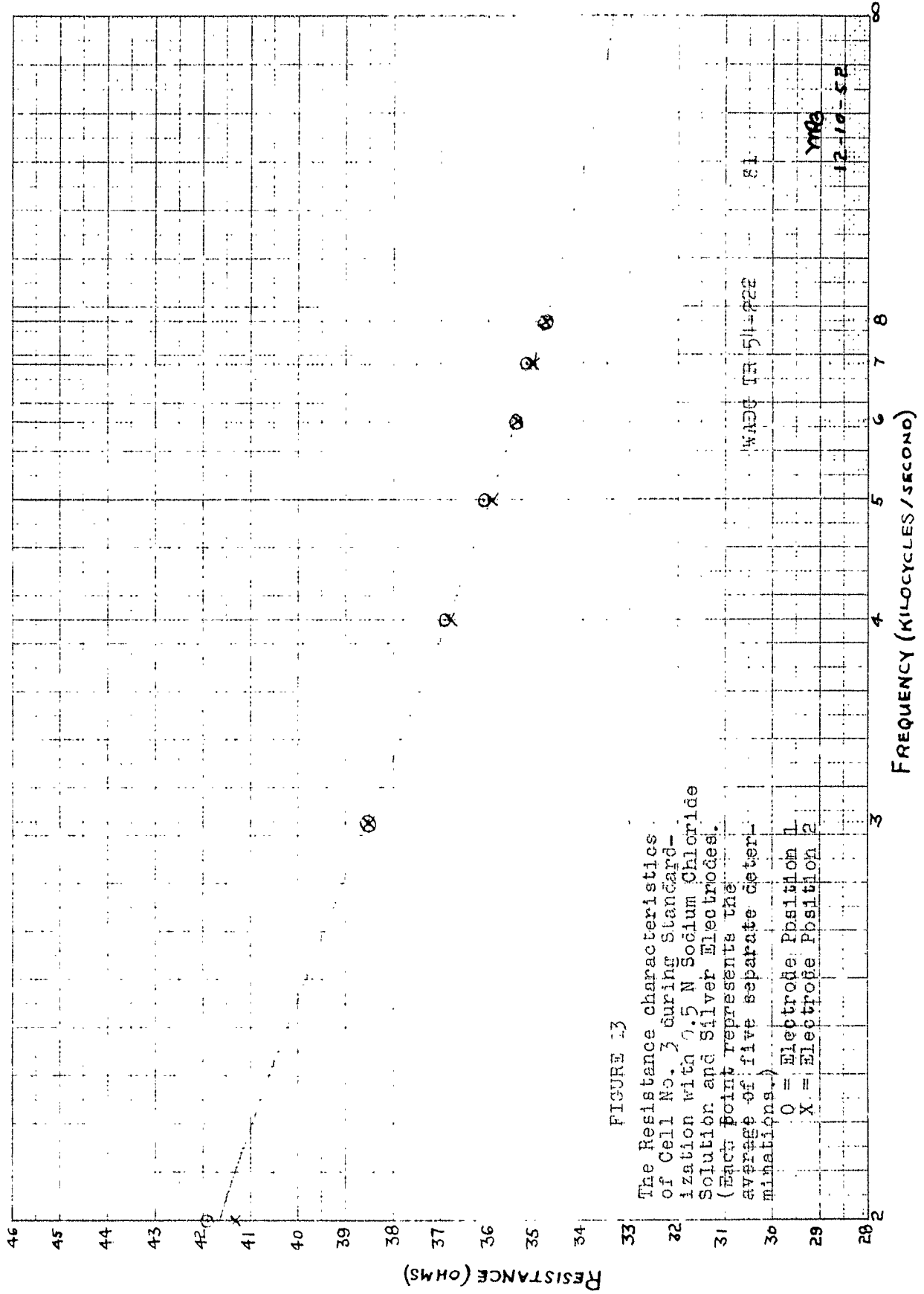


FIGURE 13

The Resistance characteristics of Cell No. 3 during Standardization with 0.5 N Sodium Chloride Solution and Silver Electrodes. (Each point represents the average of five separate determinations.)

- O = Electrode Position 1
- X = Electrode Position 2

WADD TR 511-222

81

YMB

12-10-52

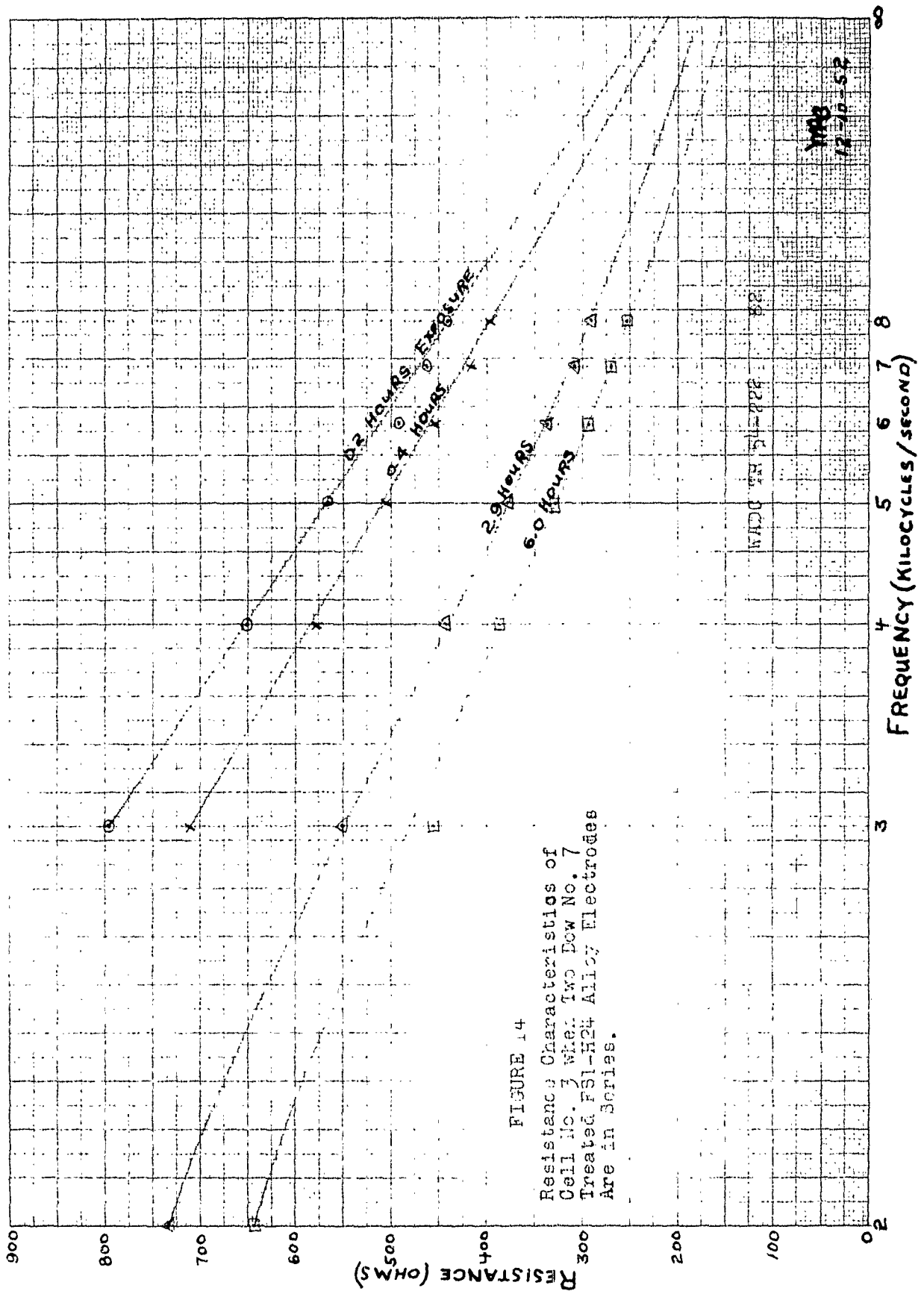


FIGURE 14  
 Resistance Characteristics of  
 Cell No. 3 when Two Dow No. 7  
 Treated FSL-H24 Alloy Electrodes  
 Are in Series.

W.D.C. TR 51722

17-10-52

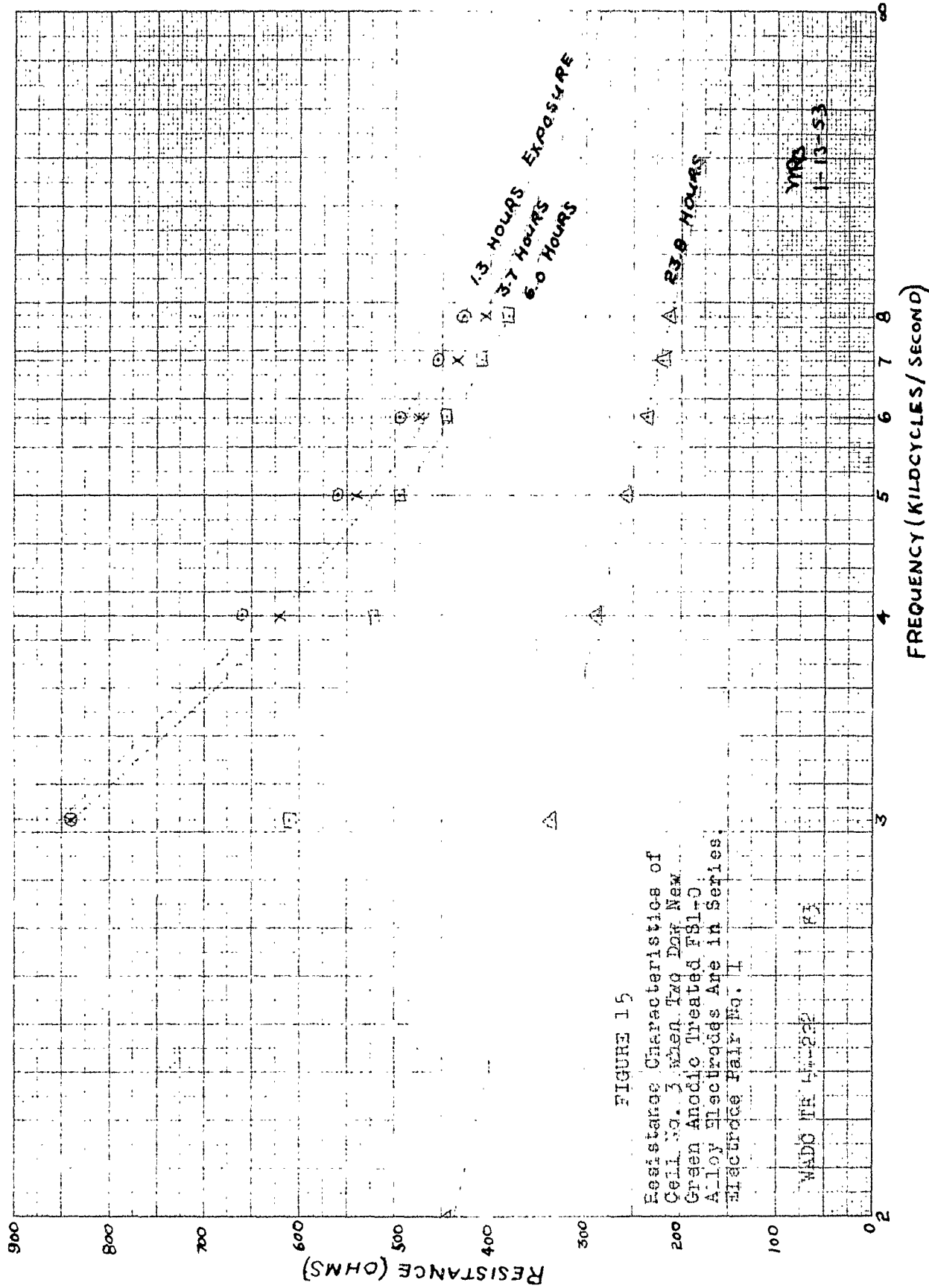
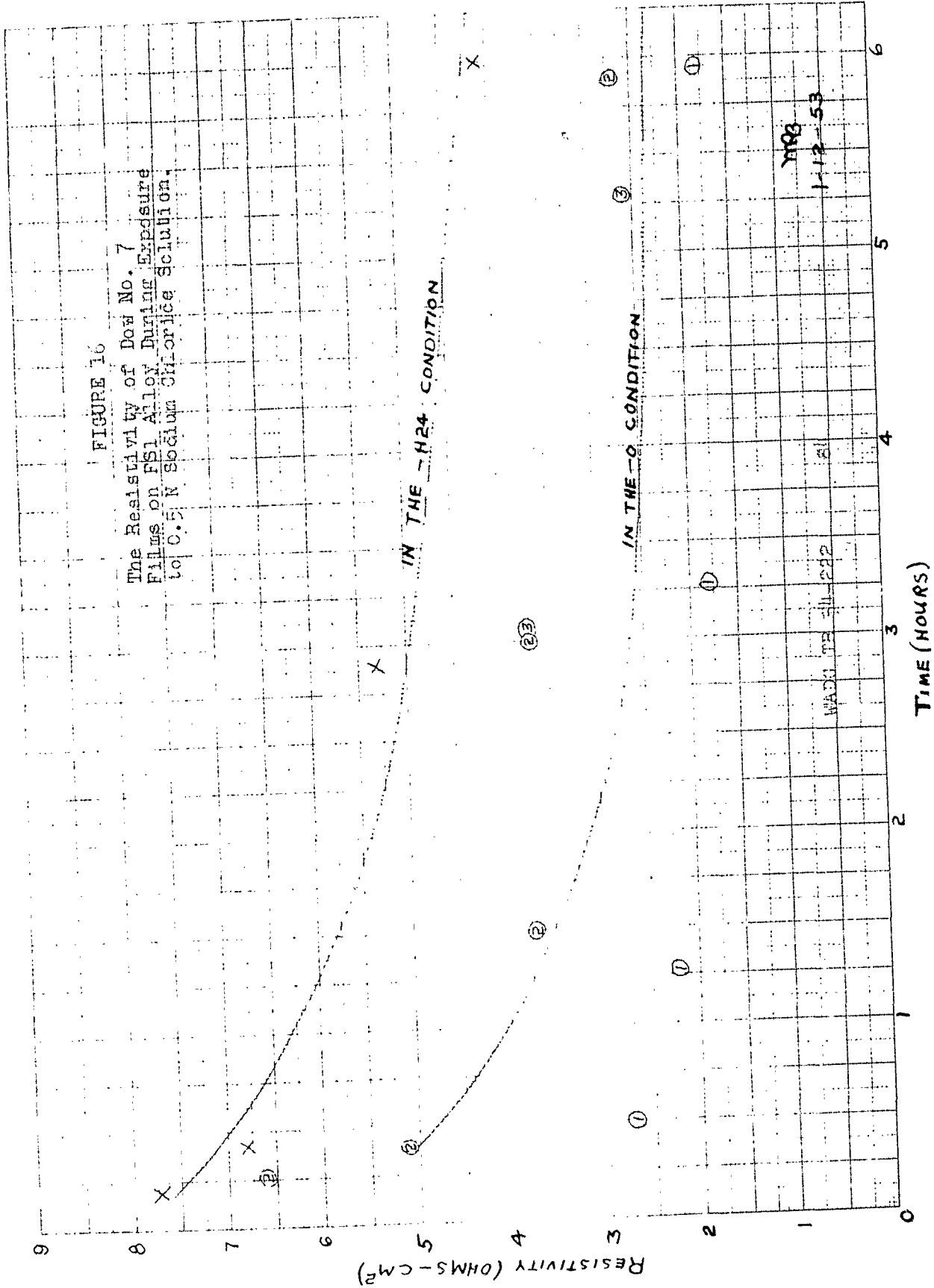


FIGURE 15  
 Resistance Characteristics of  
 Cell No. 3 when 170 Dcr New  
 Green Anodic Treated F81-C  
 Alloy Electrodes Are in Series  
 Electrode Pair No. 1

FIGURE 16

The Resistivity of Dow No. 7  
Films on FSI Alloy During Exposure  
to 0.5 N Sodium Chloride Solution



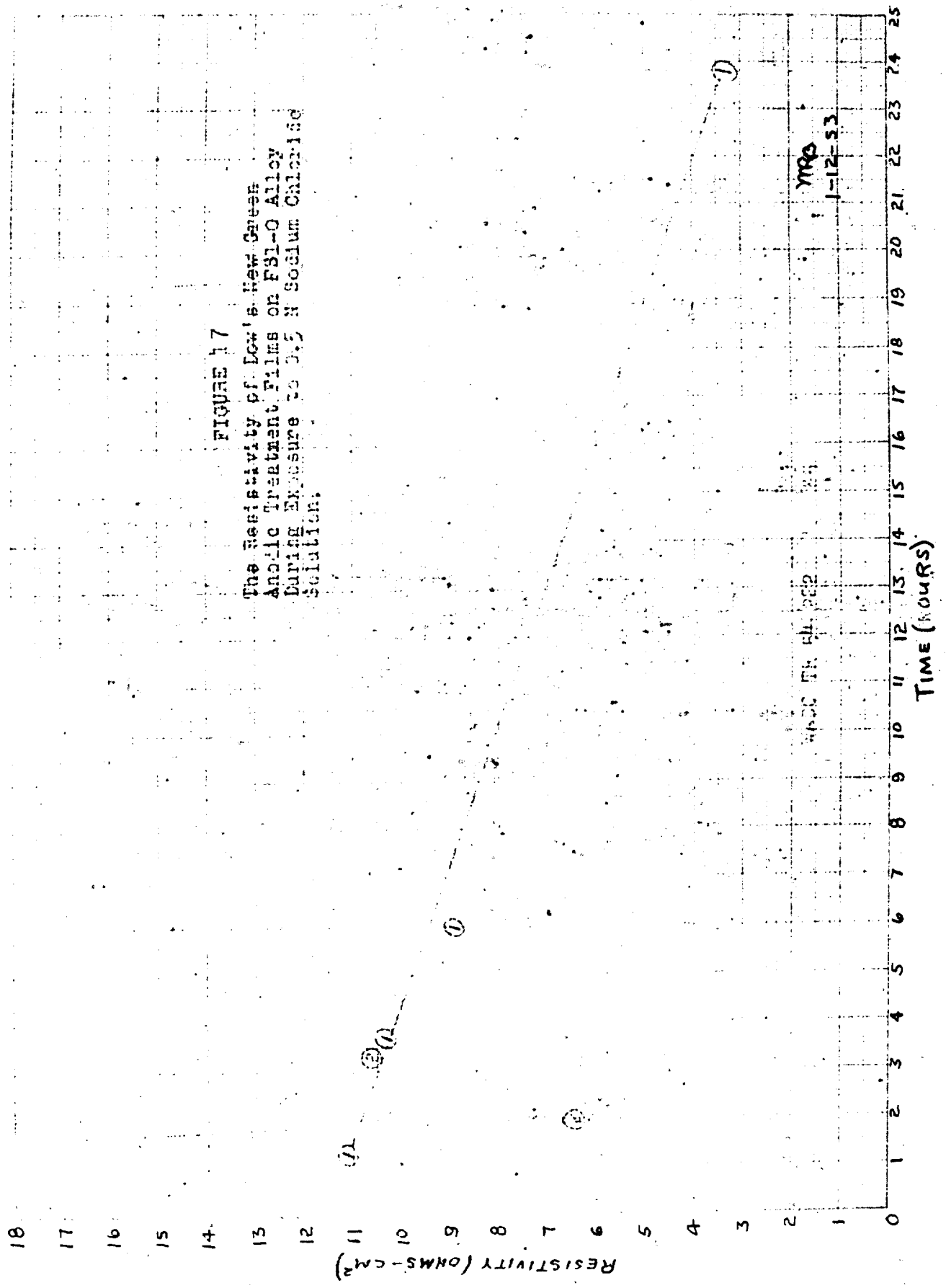
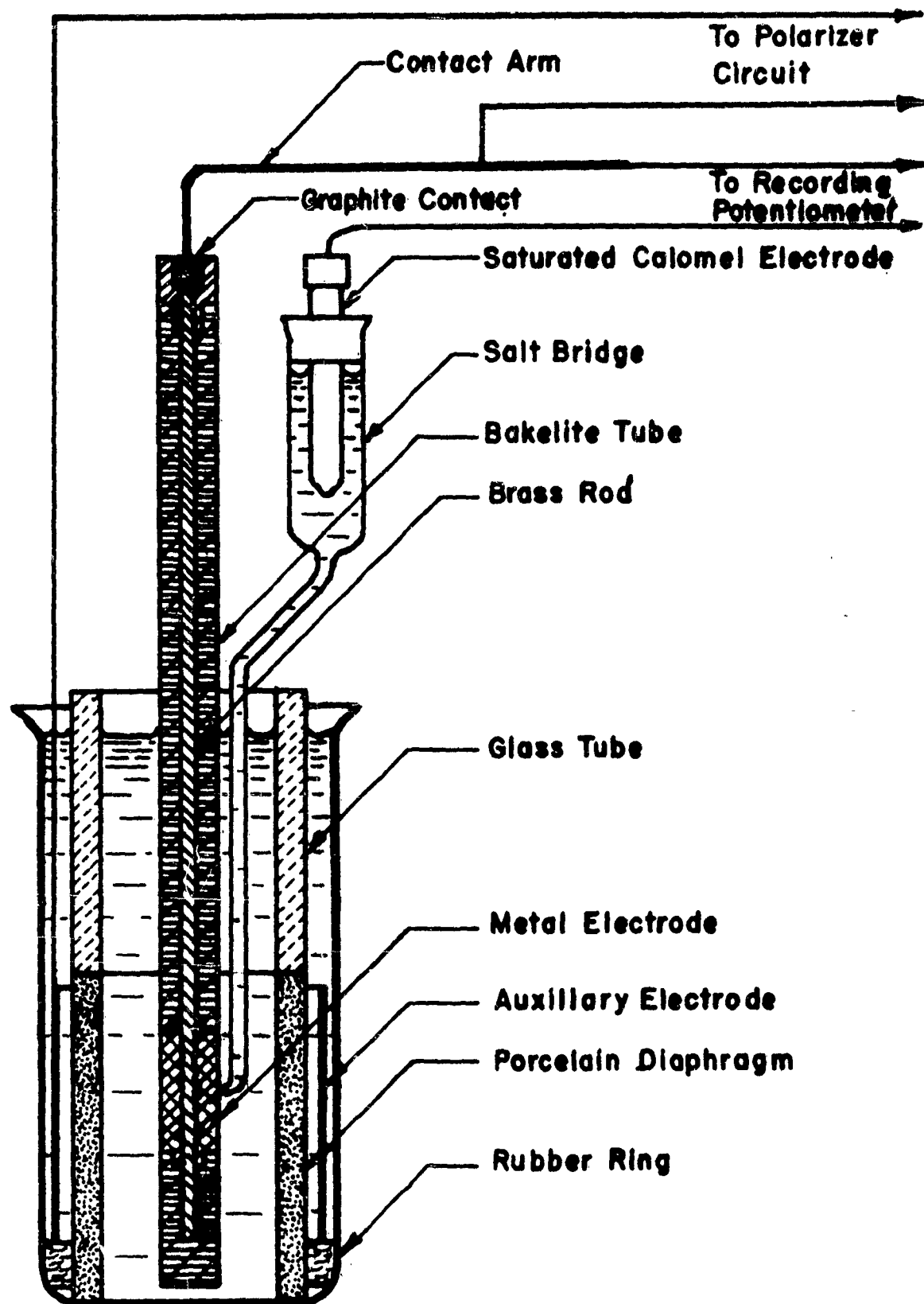


FIGURE 17  
 The Resistivity of Low-Resistance  
 Anodic Treatment Films on FSL-O Alloy  
 During Exposure to 0.5 N Sodium Chloride  
 Solution.





**Figure 19 CELL FOR POLARIZATION STUDIES**

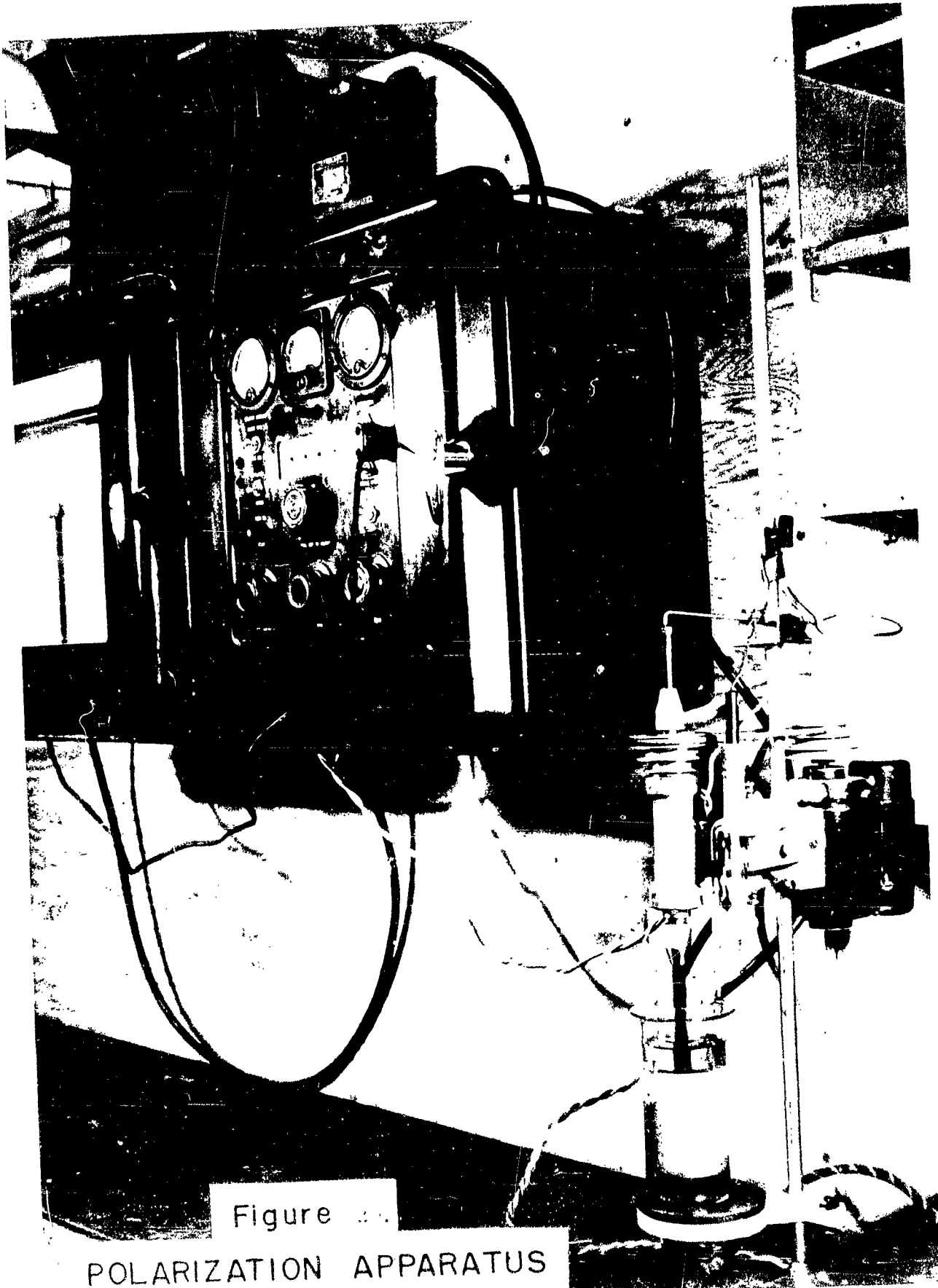


Figure 10.

POLARIZATION APPARATUS

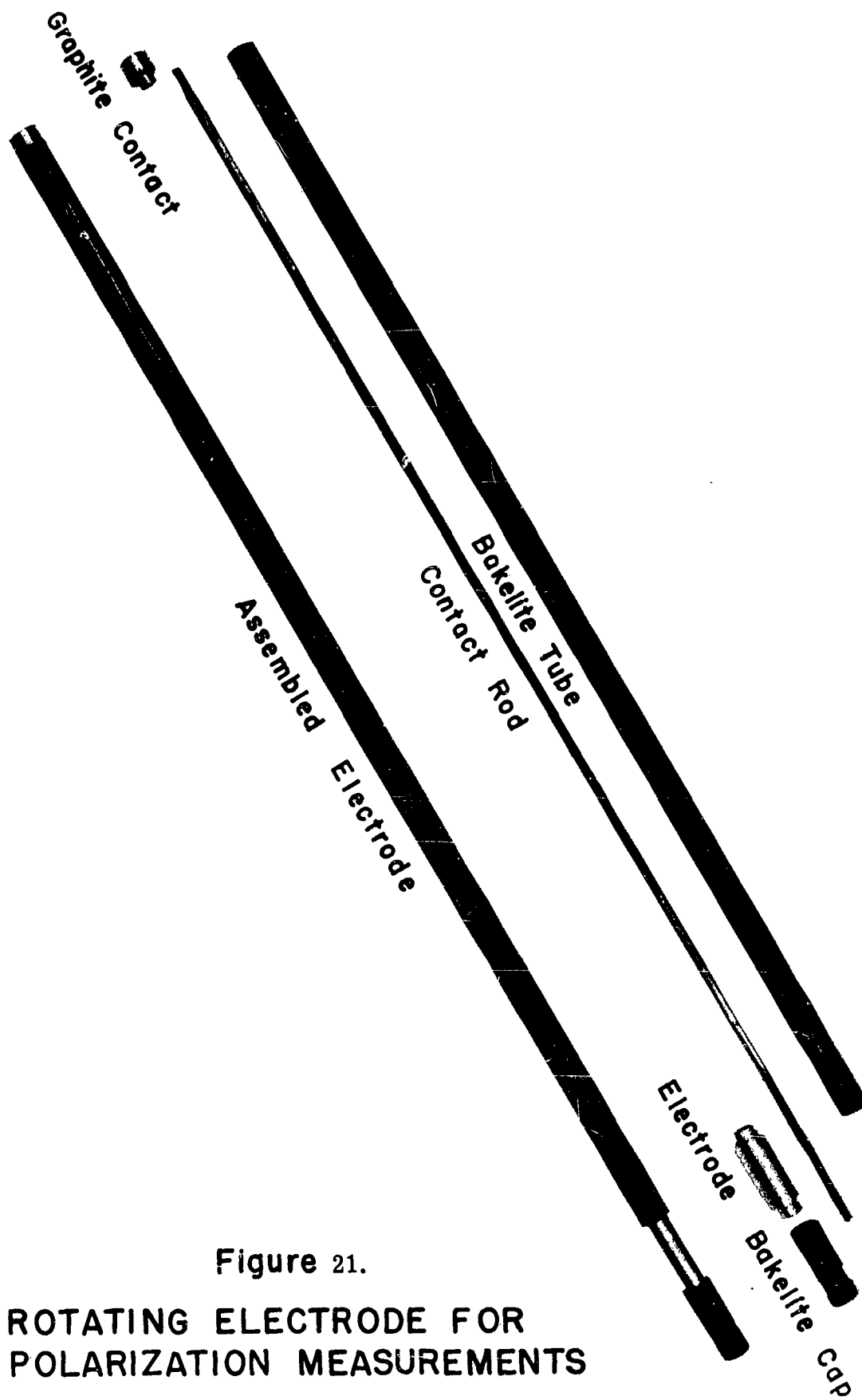
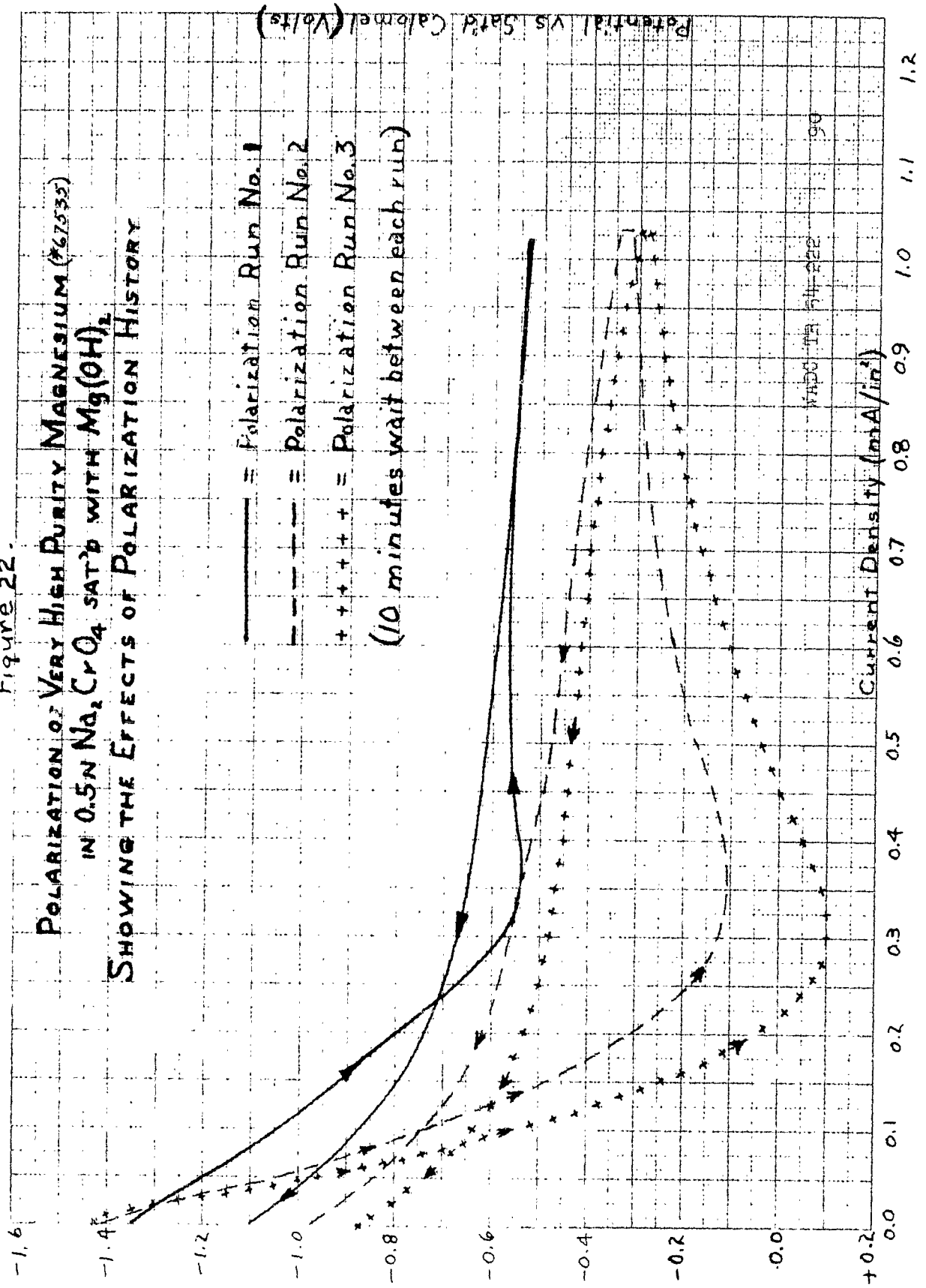


Figure 21.  
ROTATING ELECTRODE FOR  
POLARIZATION MEASUREMENTS

Figure 22.

POLARIZATION OF VERY HIGH PURITY MAGNESIUM (#67535)  
IN 0.5N Na<sub>2</sub>CrO<sub>4</sub> SAT'D WITH Mg(OH)<sub>2</sub>  
SHOWING THE EFFECTS OF POLARIZATION HISTORY



MAGNETA #44-222 90

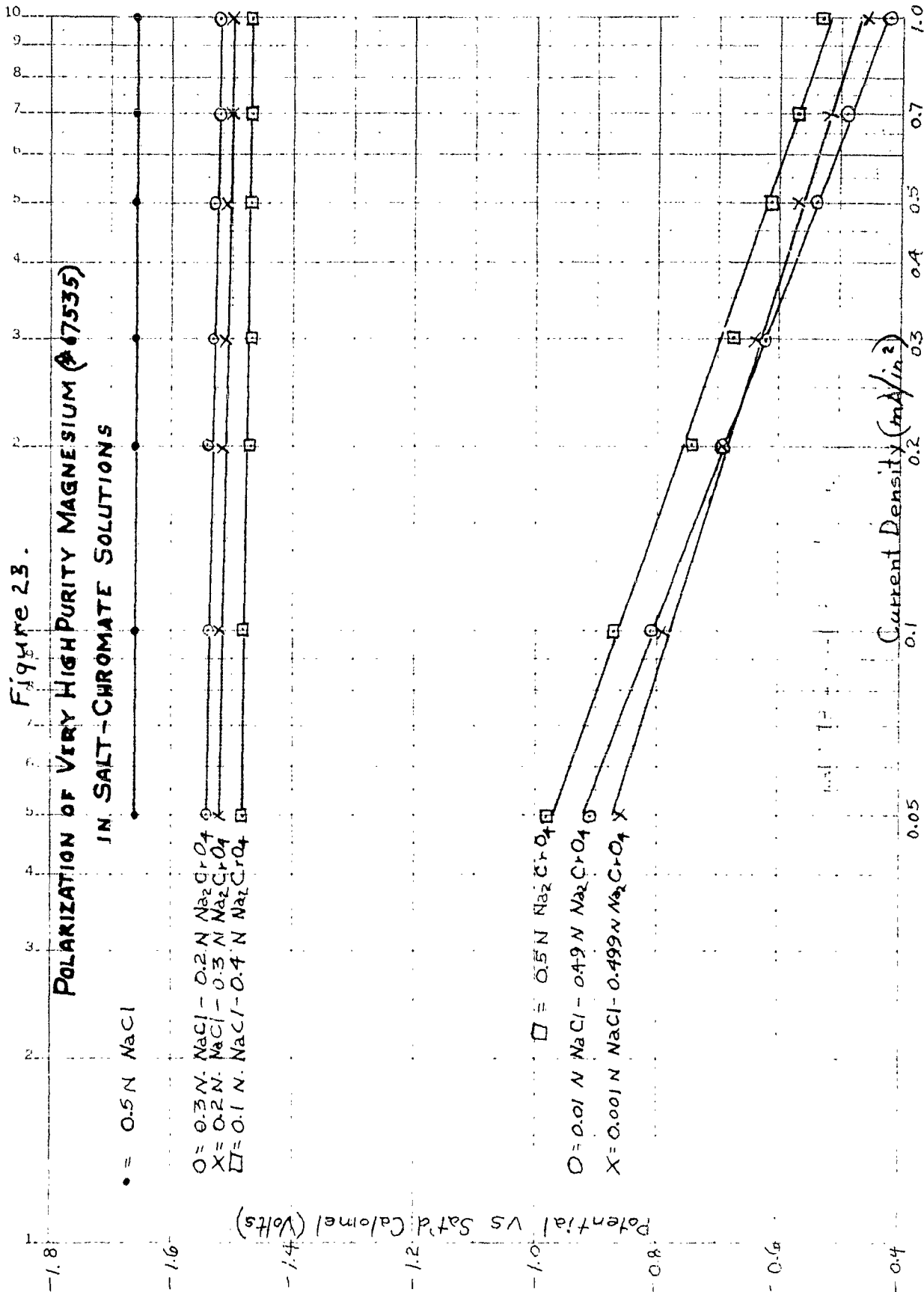
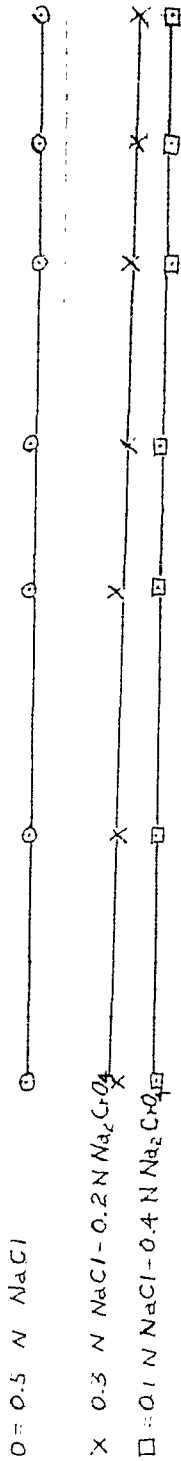


Figure 24.

POLARIZATION OF CELL MAGNESIUM (#70812)  
IN SALT-CHROMATE SOLUTIONS

-1.8



-1.6



-1.4

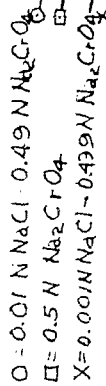


-1.2

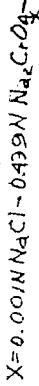
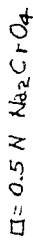
-1.0

Potential vs Sat'd Calomel (Volts)

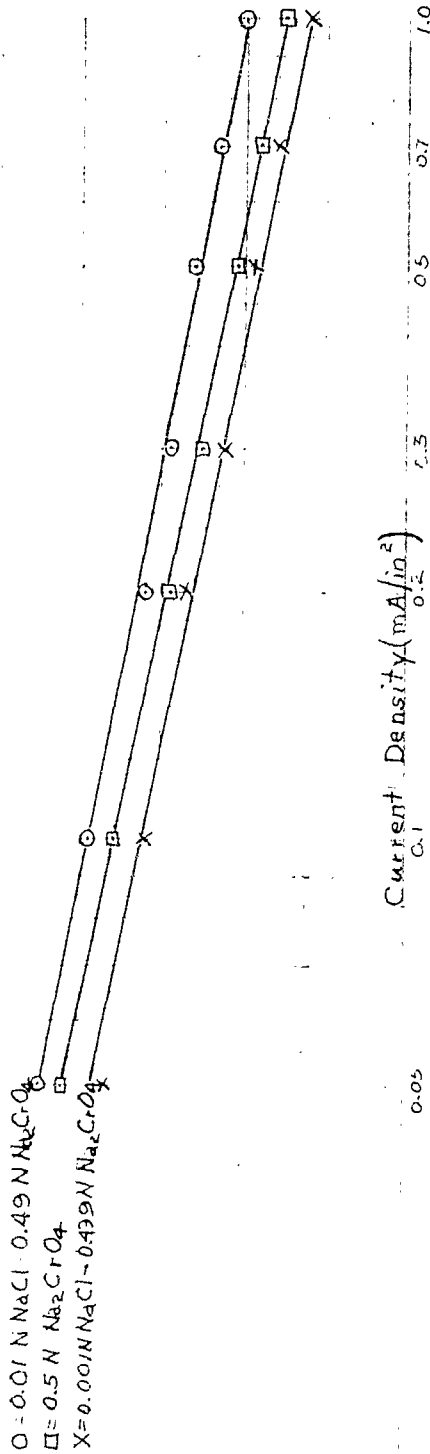
-0.8



-0.6



-0.4



Current Density (mA/in²)

0.05

0.1

0.5

0.7

1.0

Figure 25.  
POLARIZATION OF AZ10A ALLOY  
IN SALT-CHROMATE SOLUTIONS

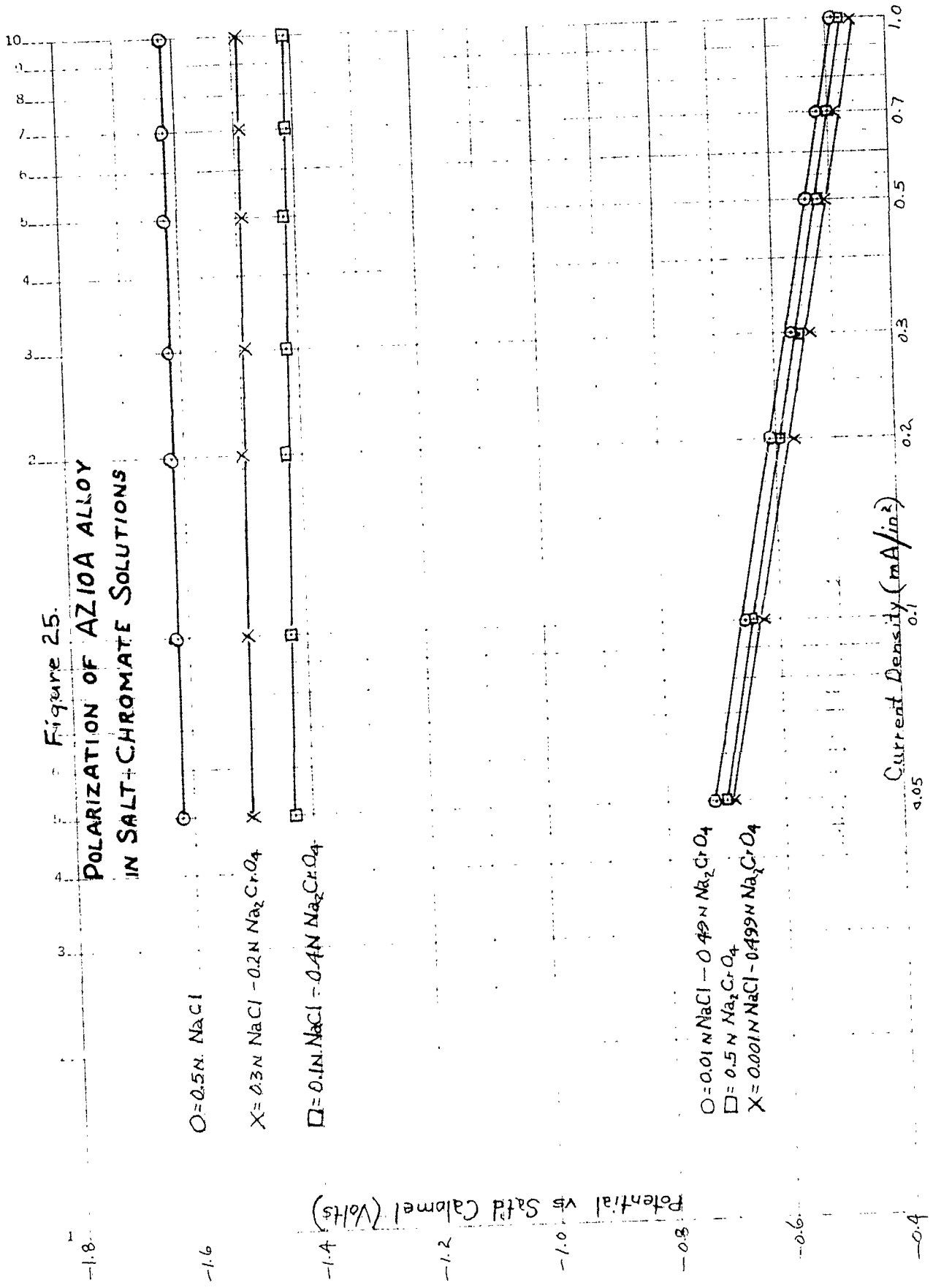


Figure 26  
 POLARIZATION OF AZ31A ALLOY  
 IN SALT-CHROMATE SOLUTIONS

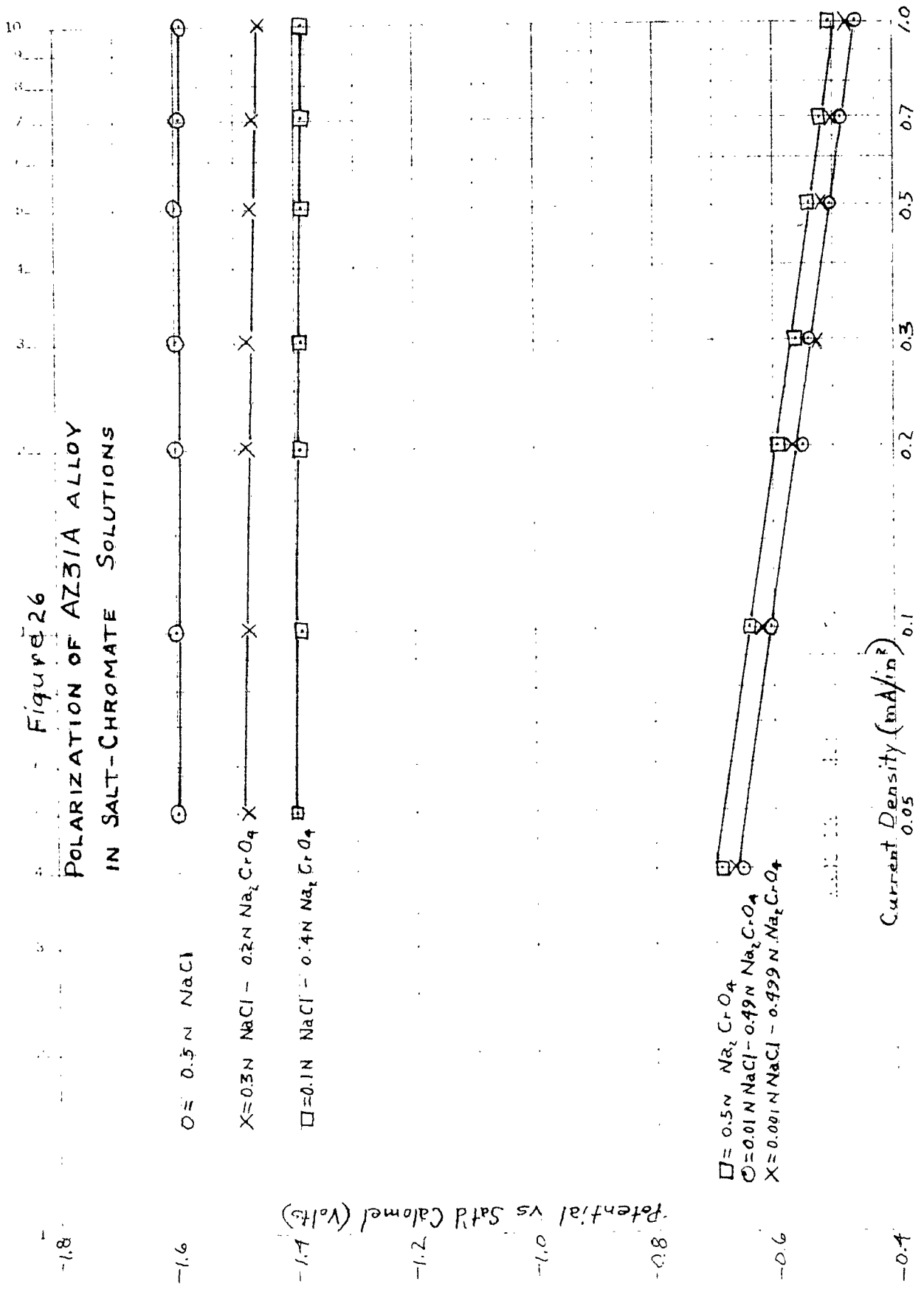


Figure 27.  
POLARIZATION OF AZ31B ALLOY  
IN SALT-CHROMATE SOLUTIONS

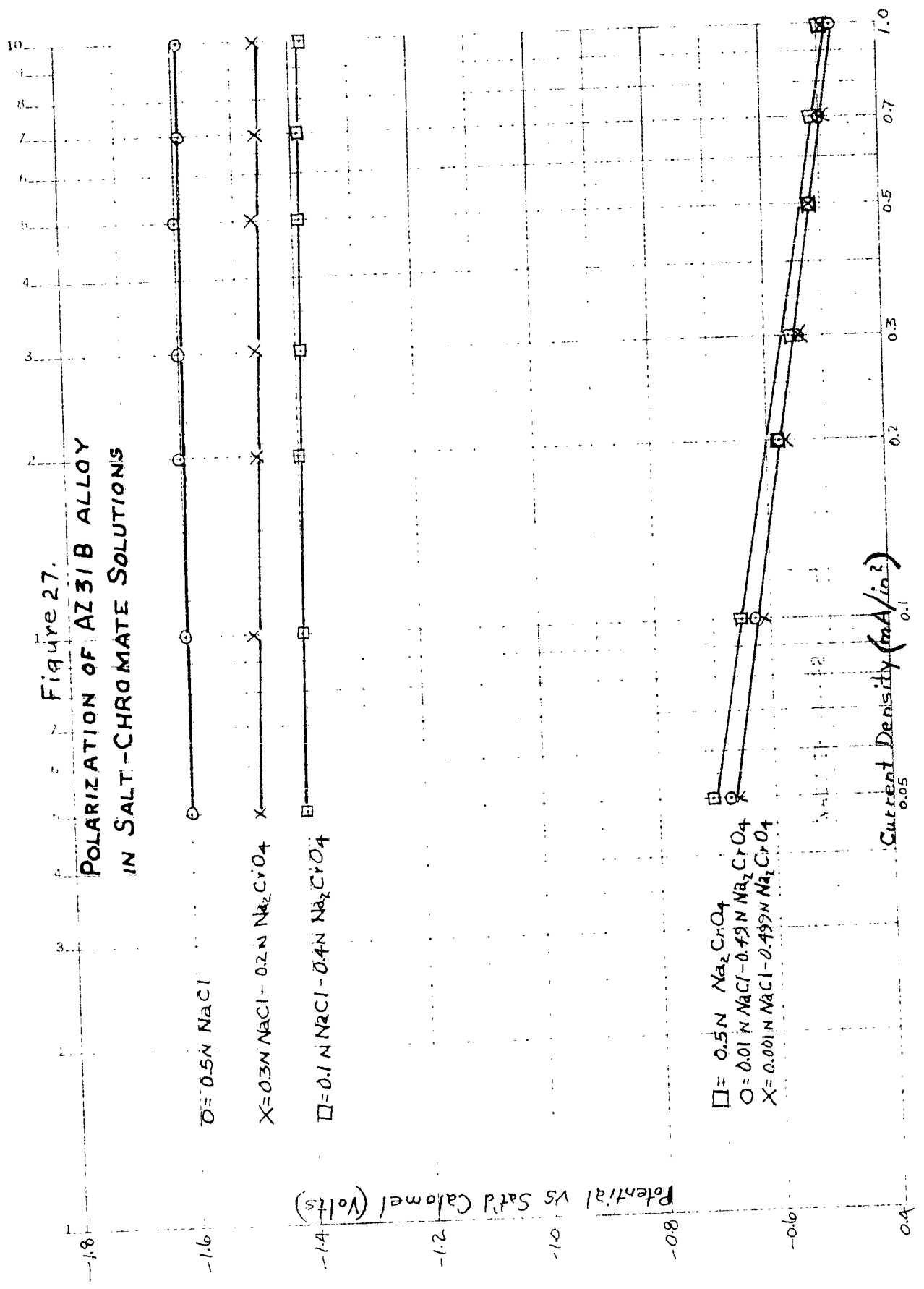


Figure 28.  
 POLARIZATION OF AZ63A ALLOY (X46732)  
 IN SALT-CHROMATE SOLUTIONS

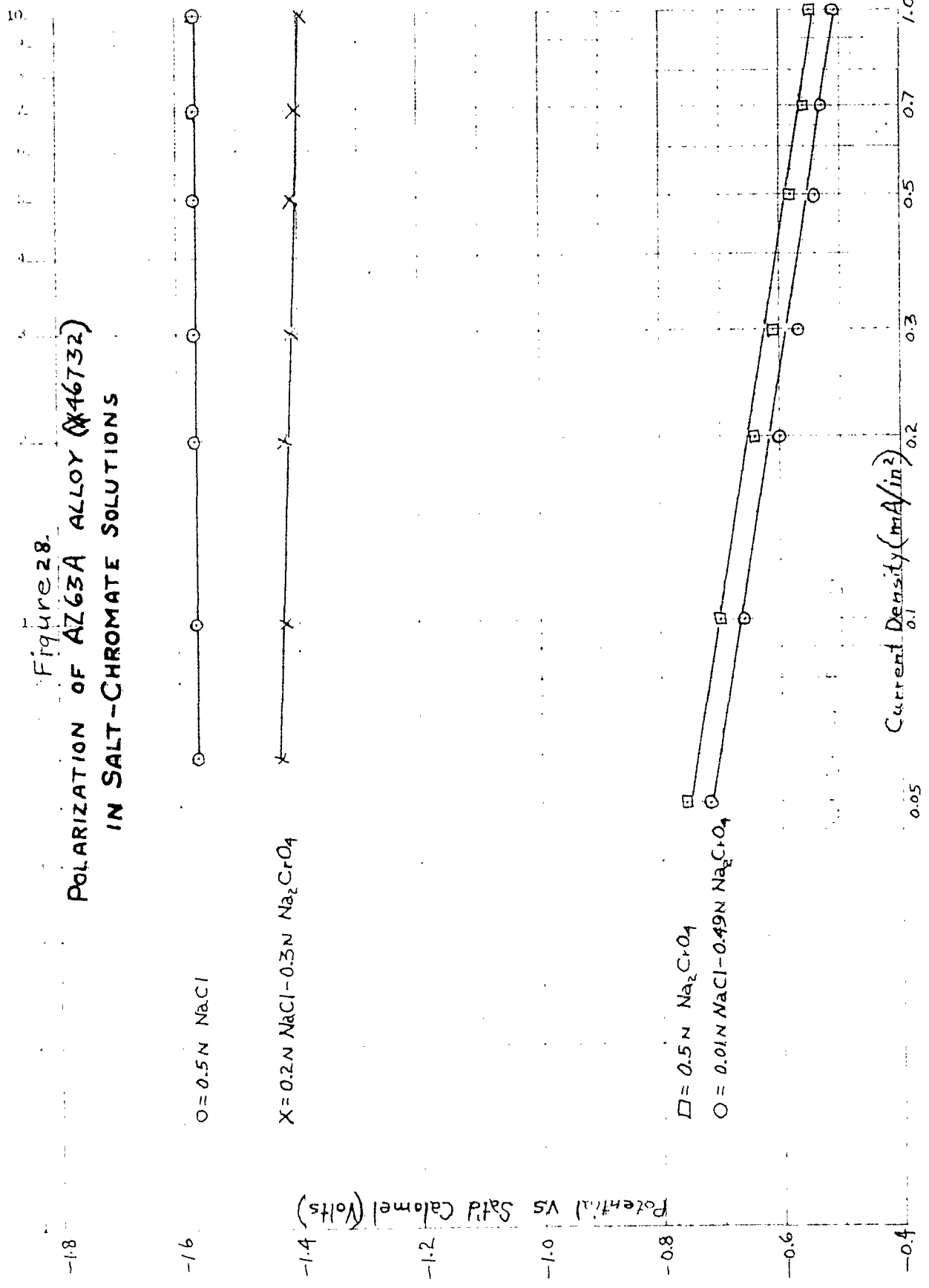


Figure 29.

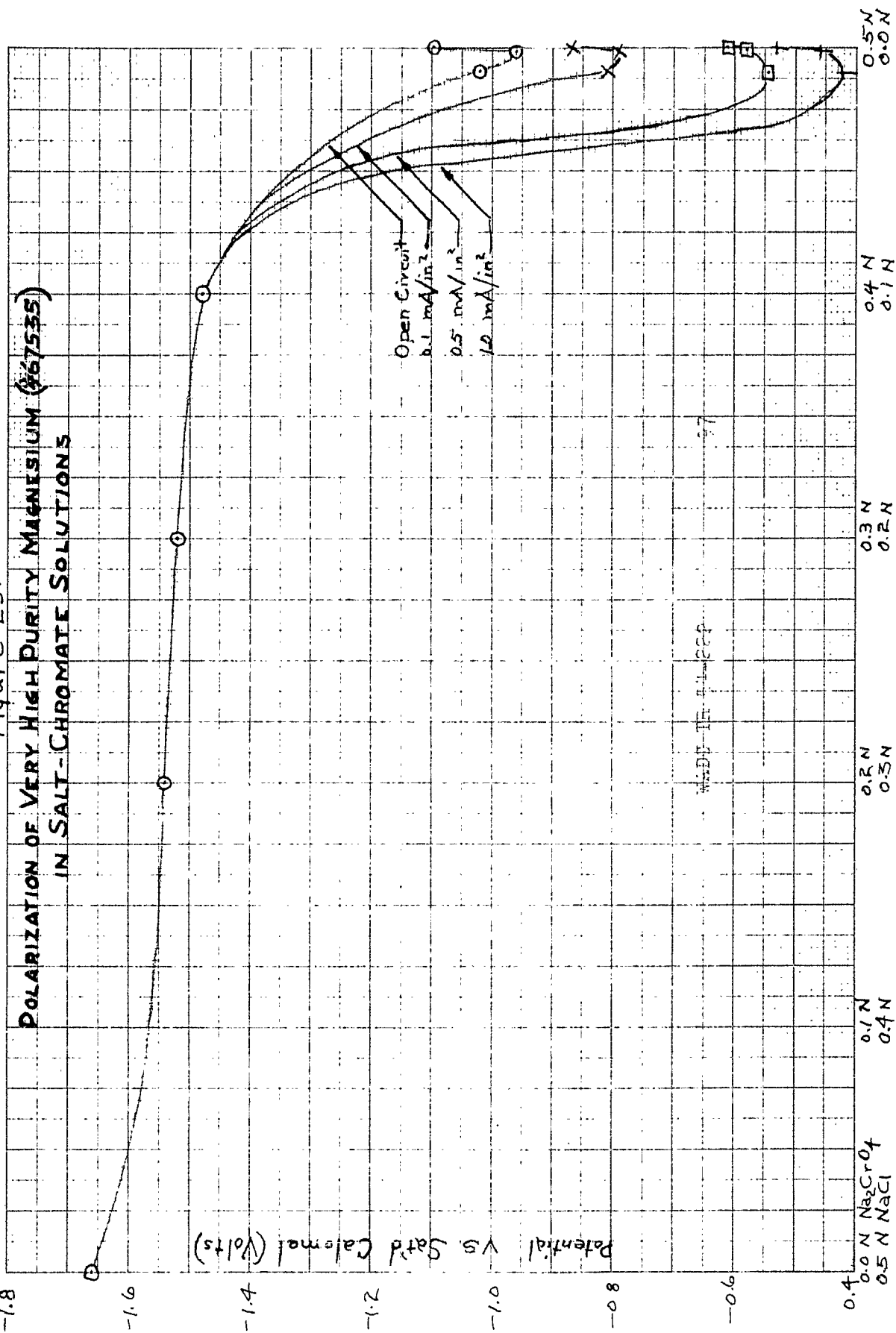


Figure 30.

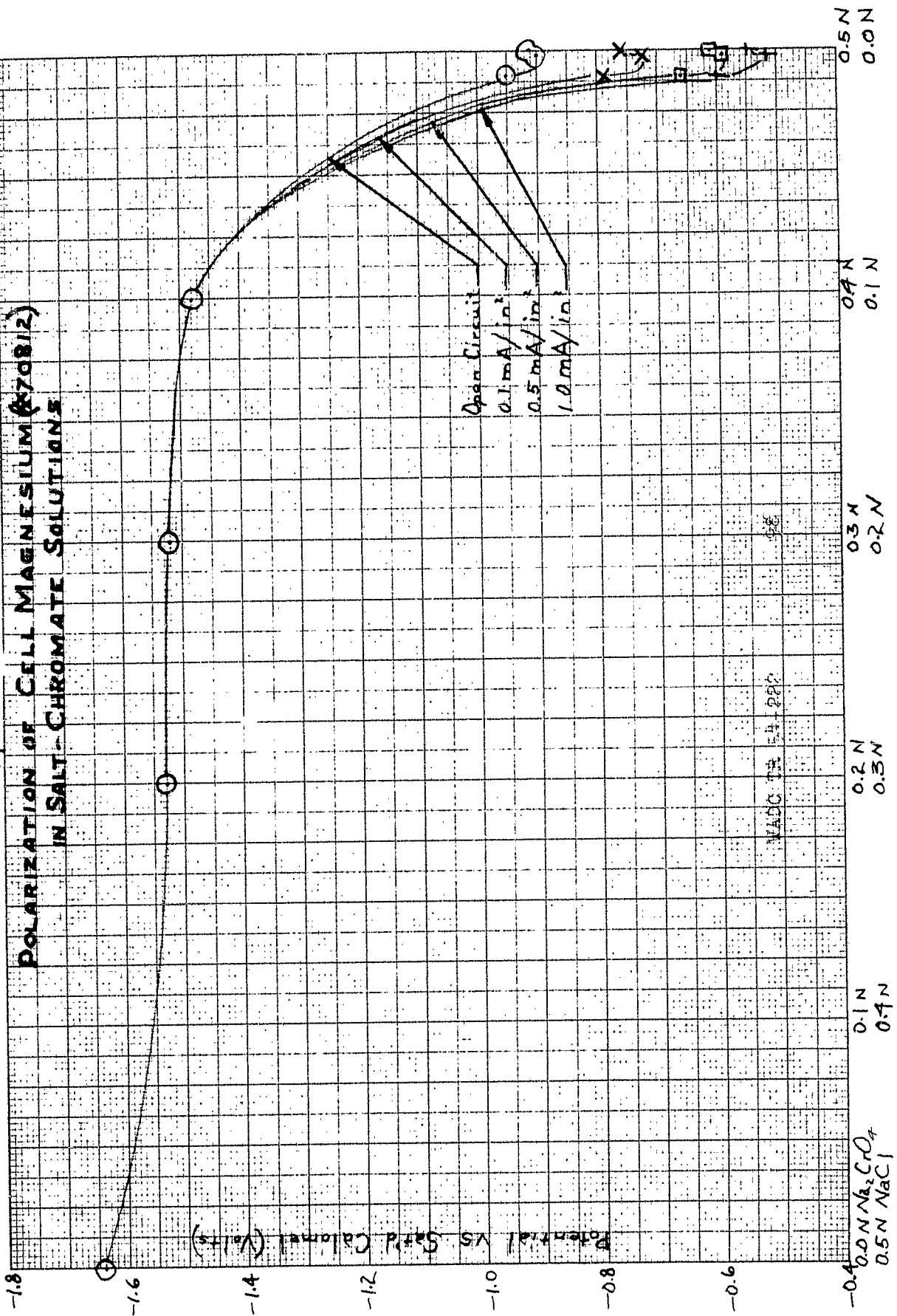


Figure 31.

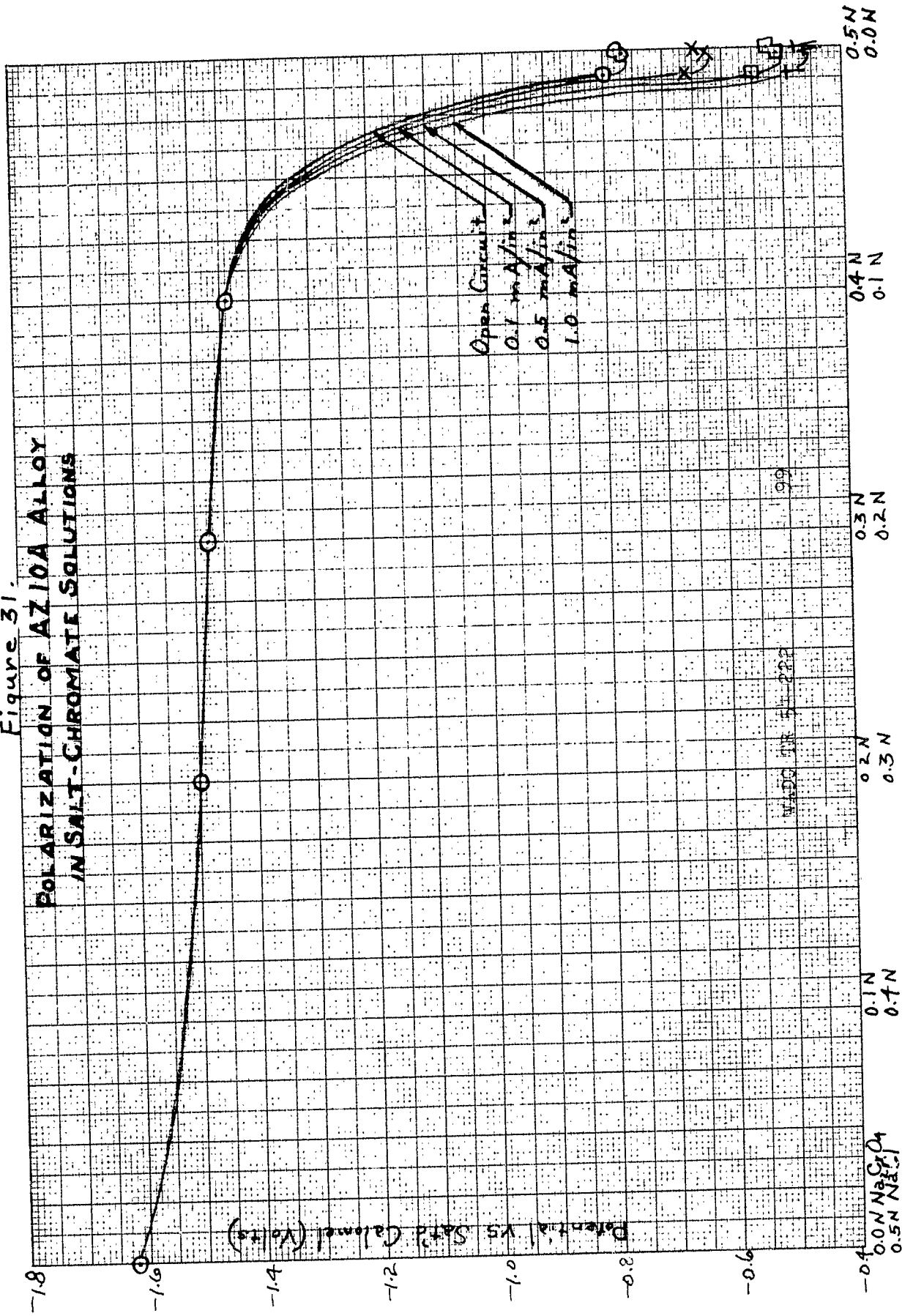


Figure 32.

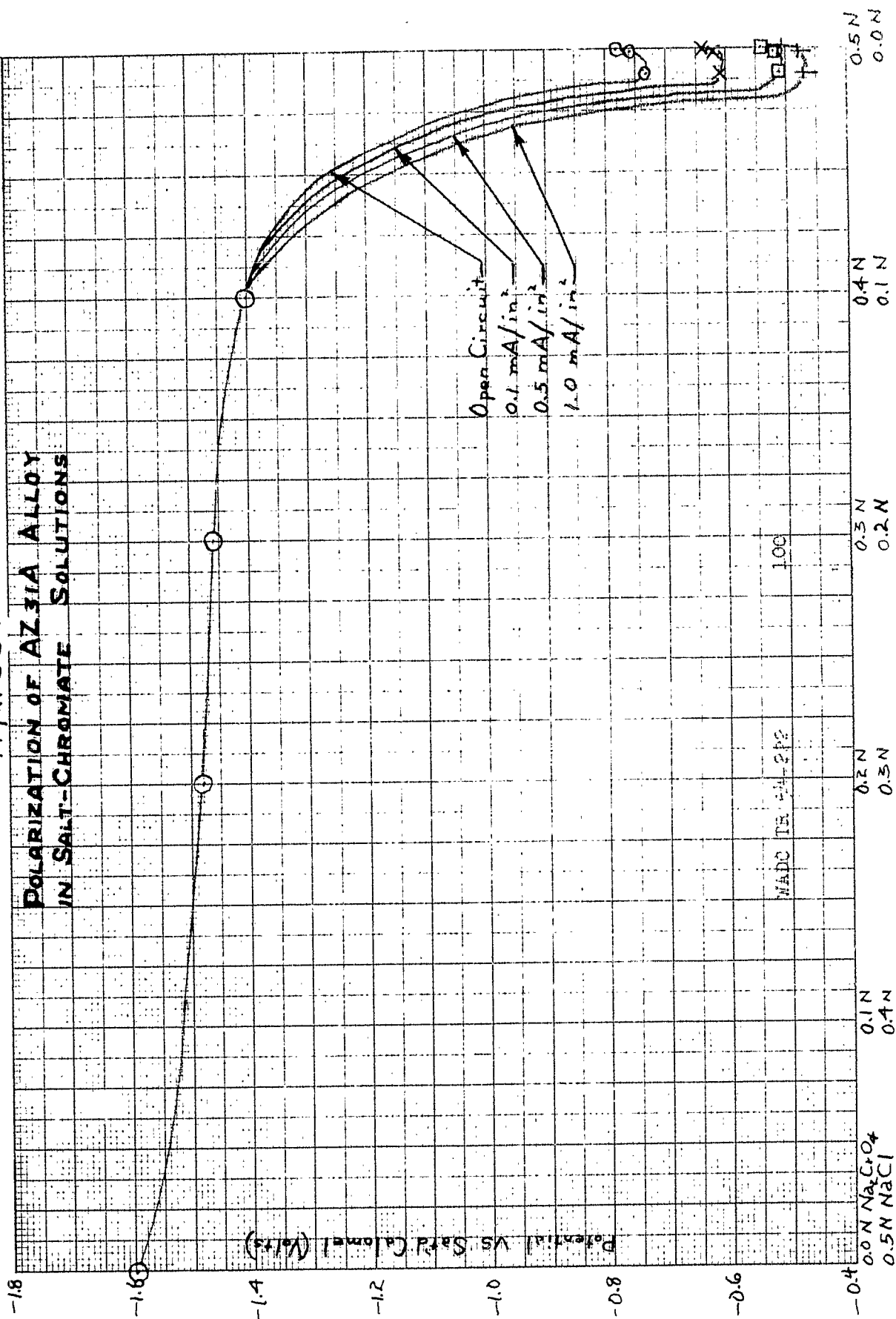


Figure 33.

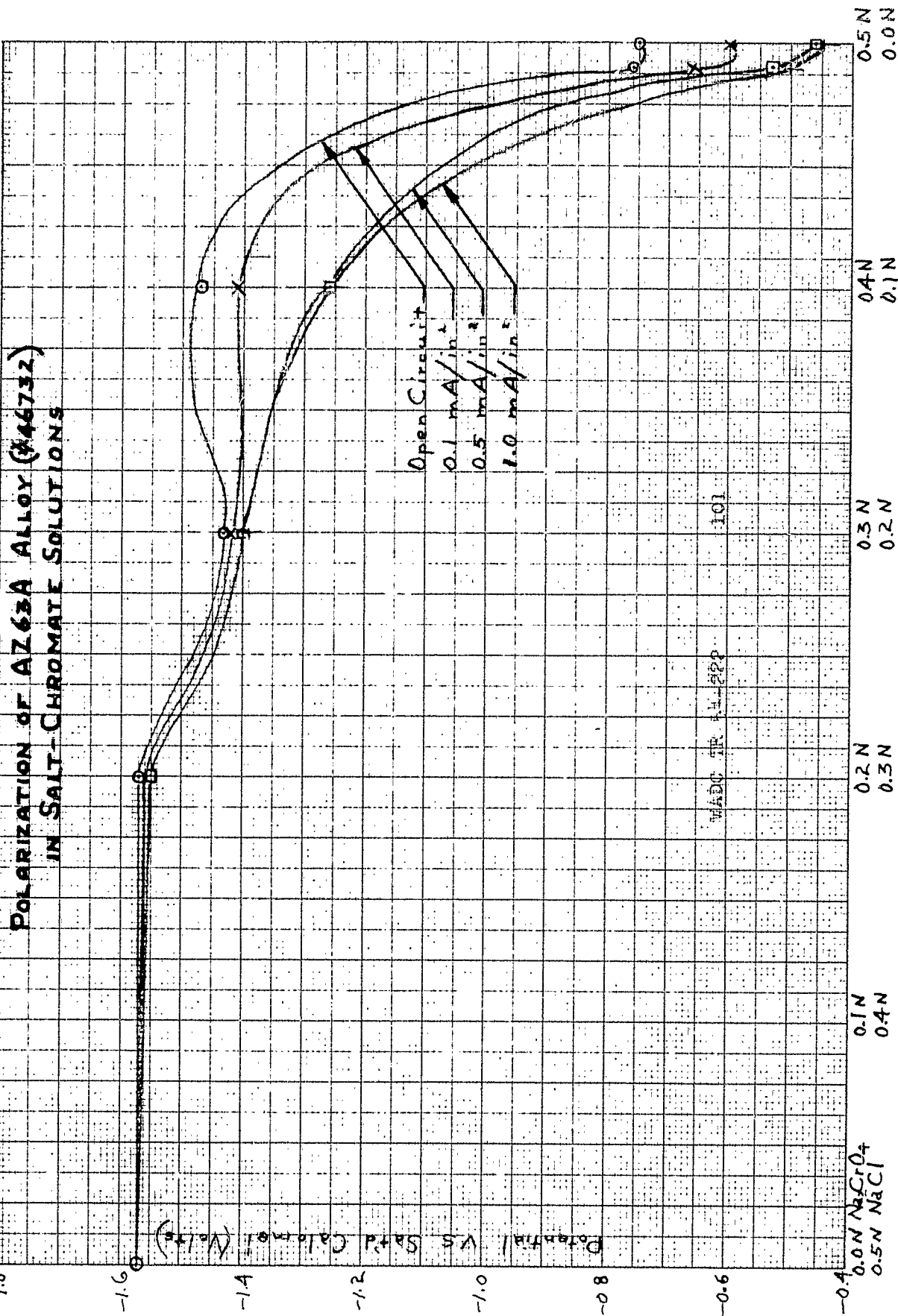
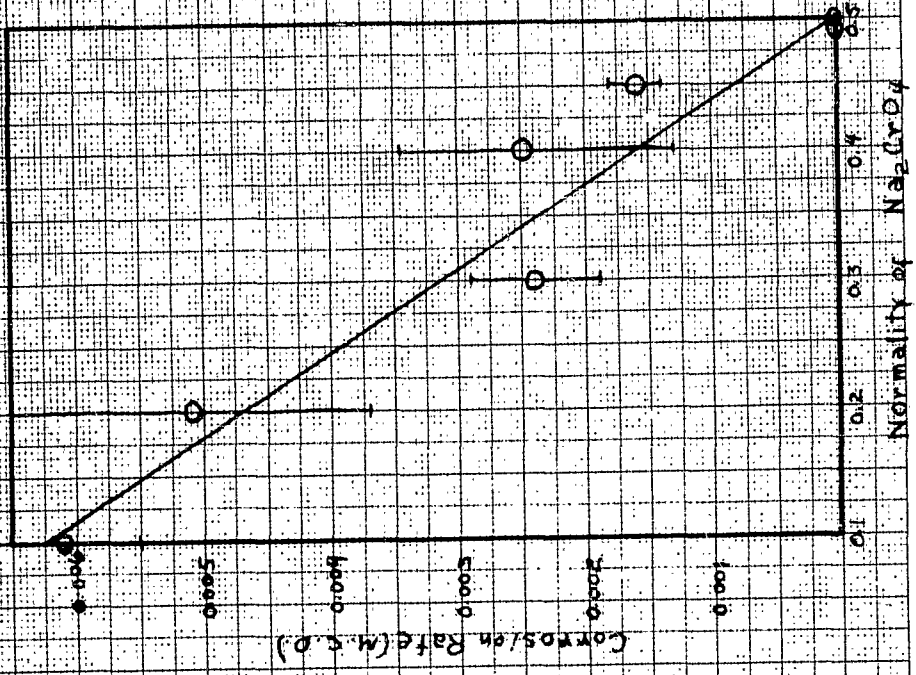
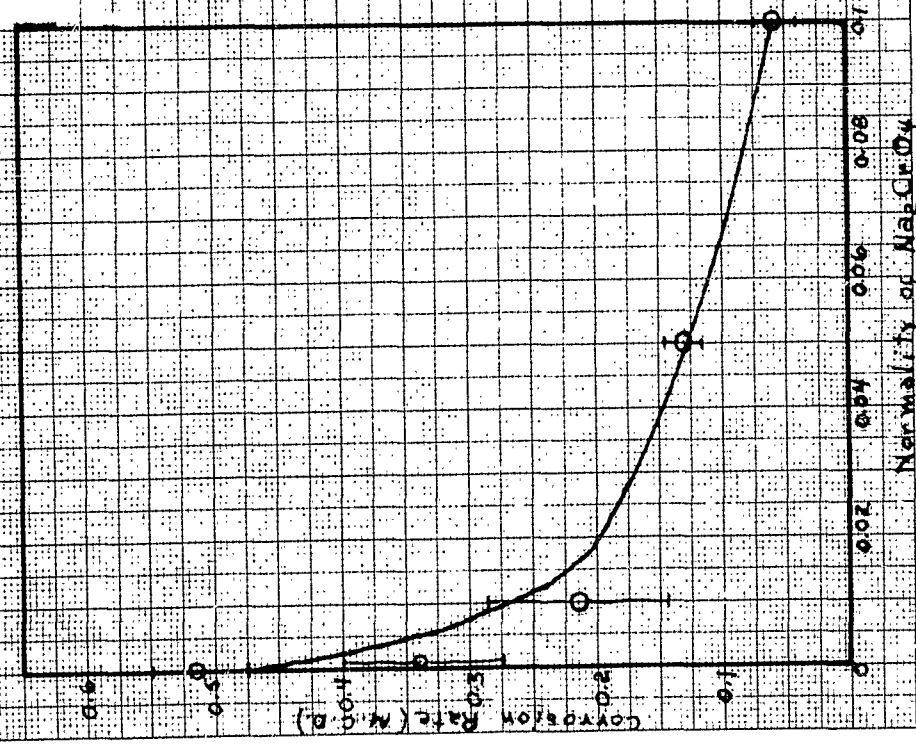


FIGURE 34

Corrosion Rate of AZ13A-0 Alloy Sheet in  
 Aqueous Sodium Chloride-Sodium Chromate Solutions  
 (All concentrations plus sodium chloride to make total normality 0.5 N.)



117

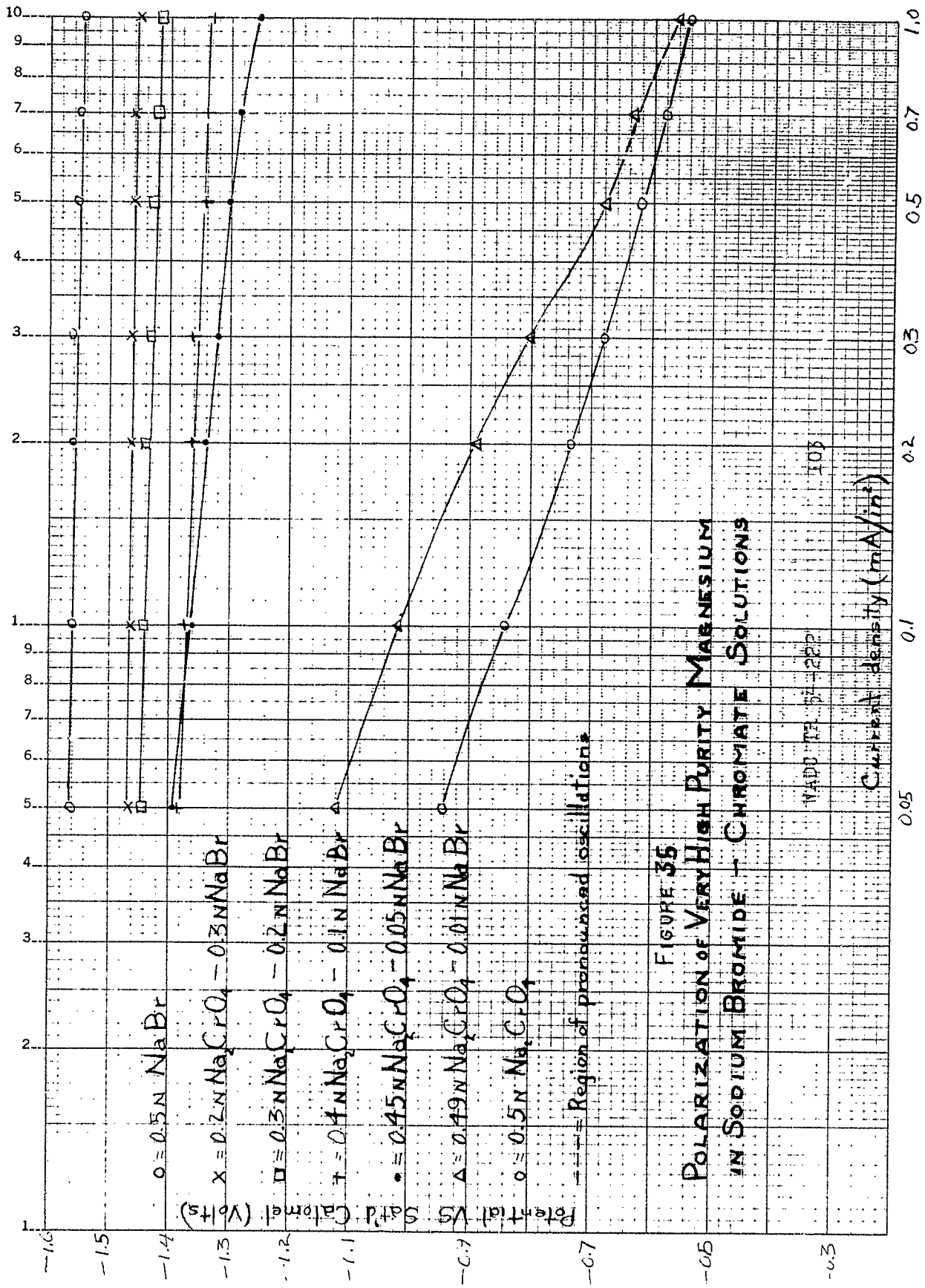
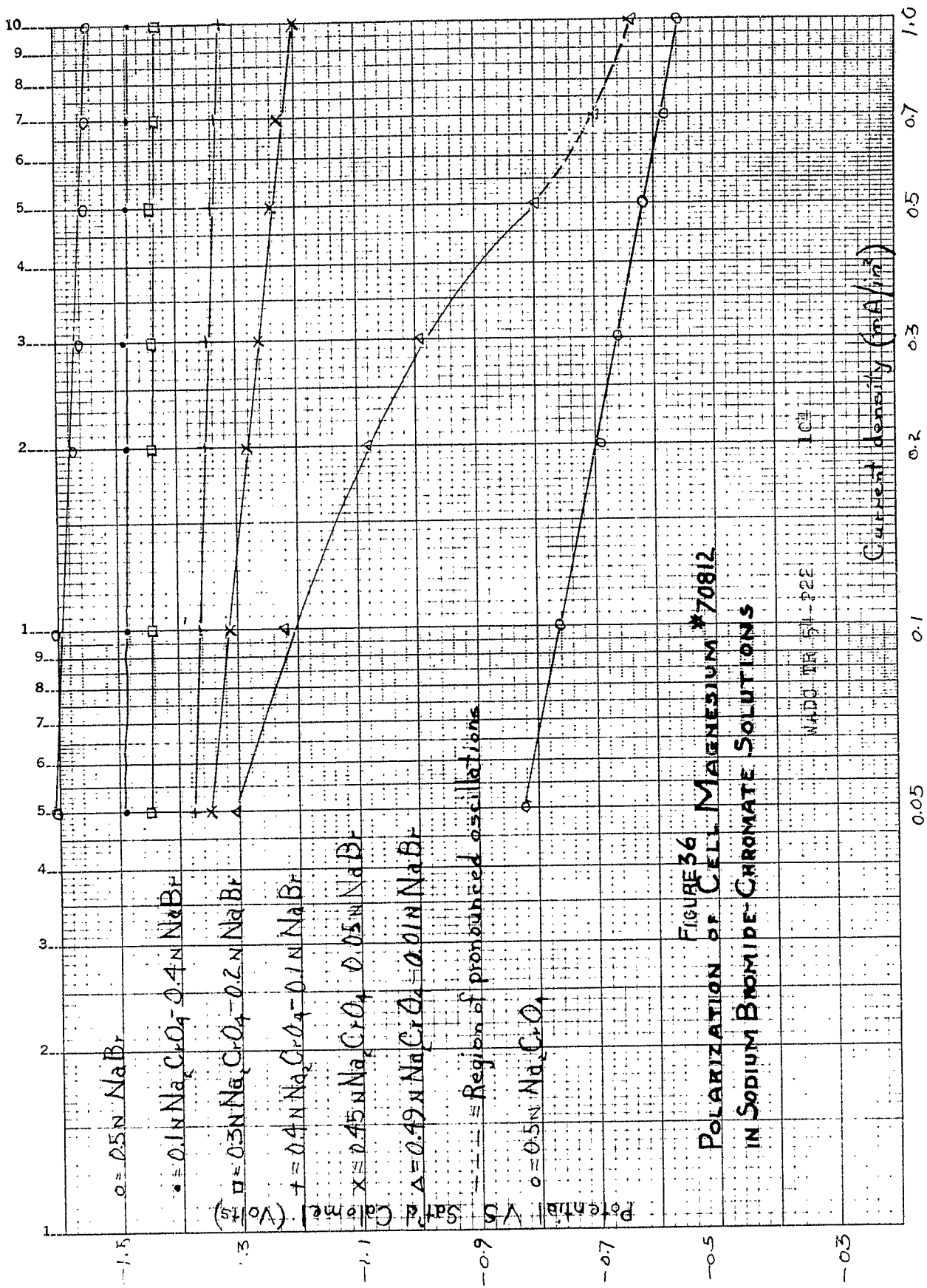
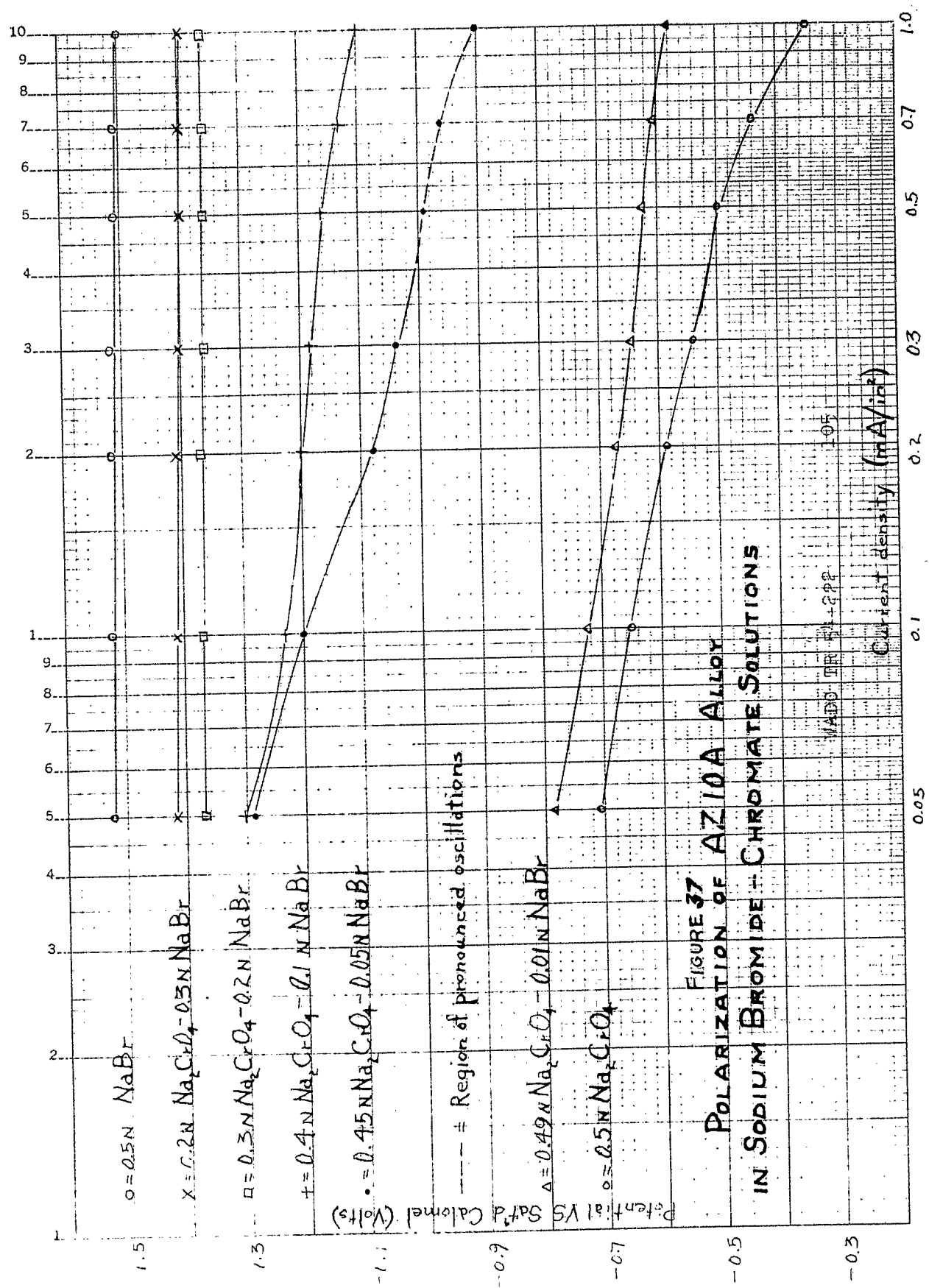


FIGURE 35  
 POLARIZATION OF VERY HIGH PURITY MAGNESIUM  
 IN SODIUM BROMIDE + CHROMATE SOLUTIONS





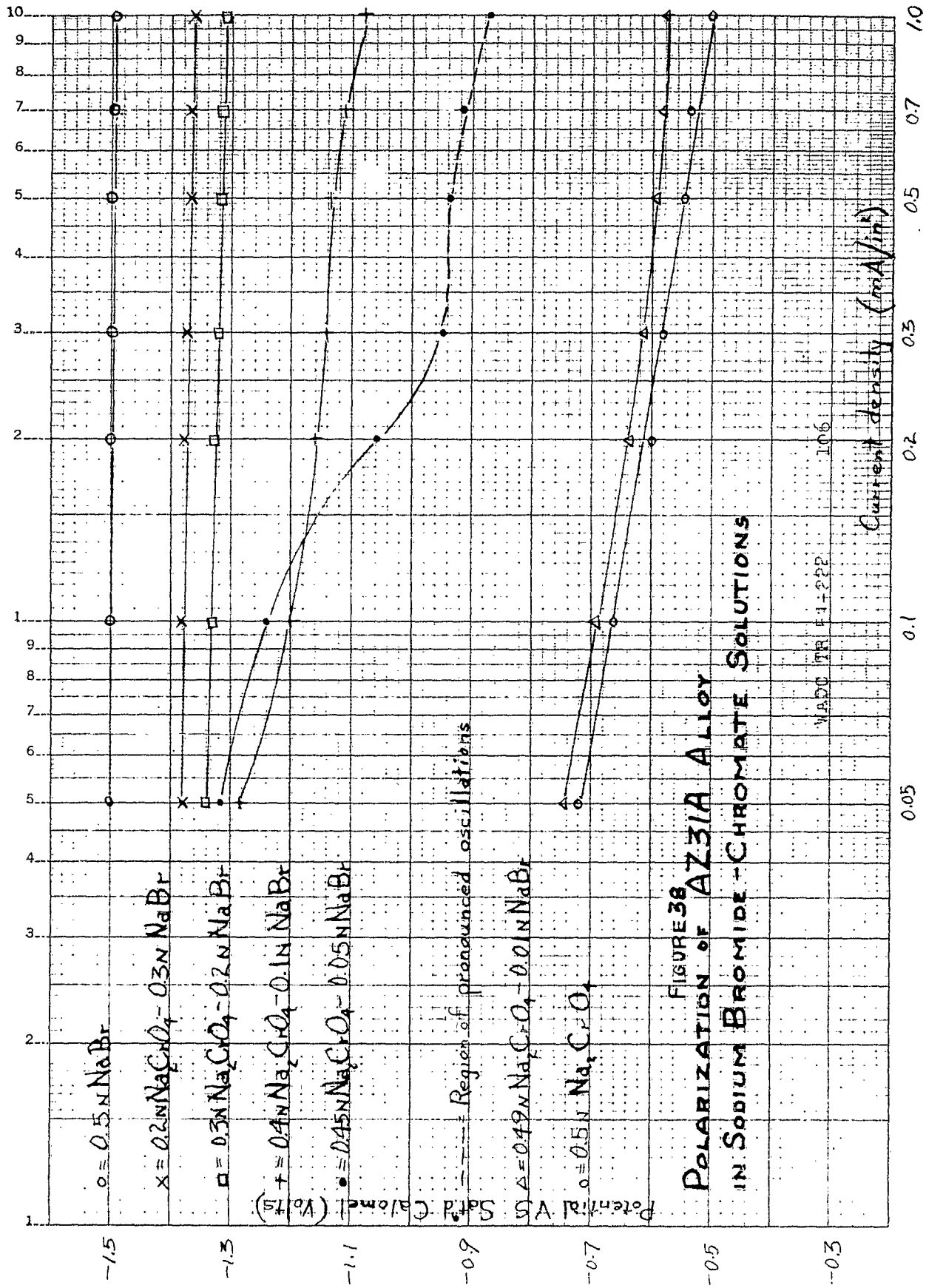
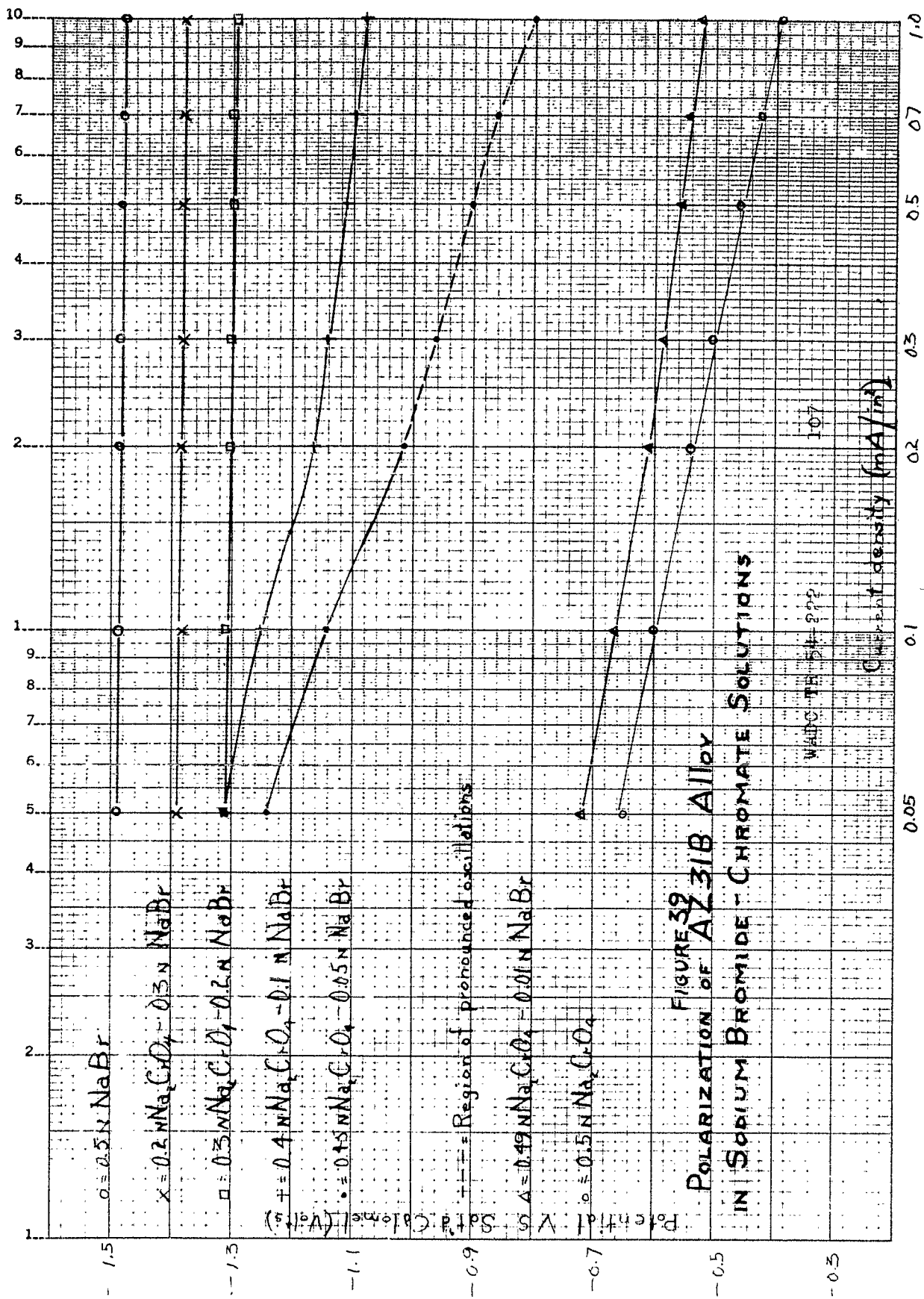


FIGURE 38  
POLARIZATION OF AZ31A ALLOY  
IN SODIUM BROMIDE - CHROMATE SOLUTIONS

WADD TR 41-222

106



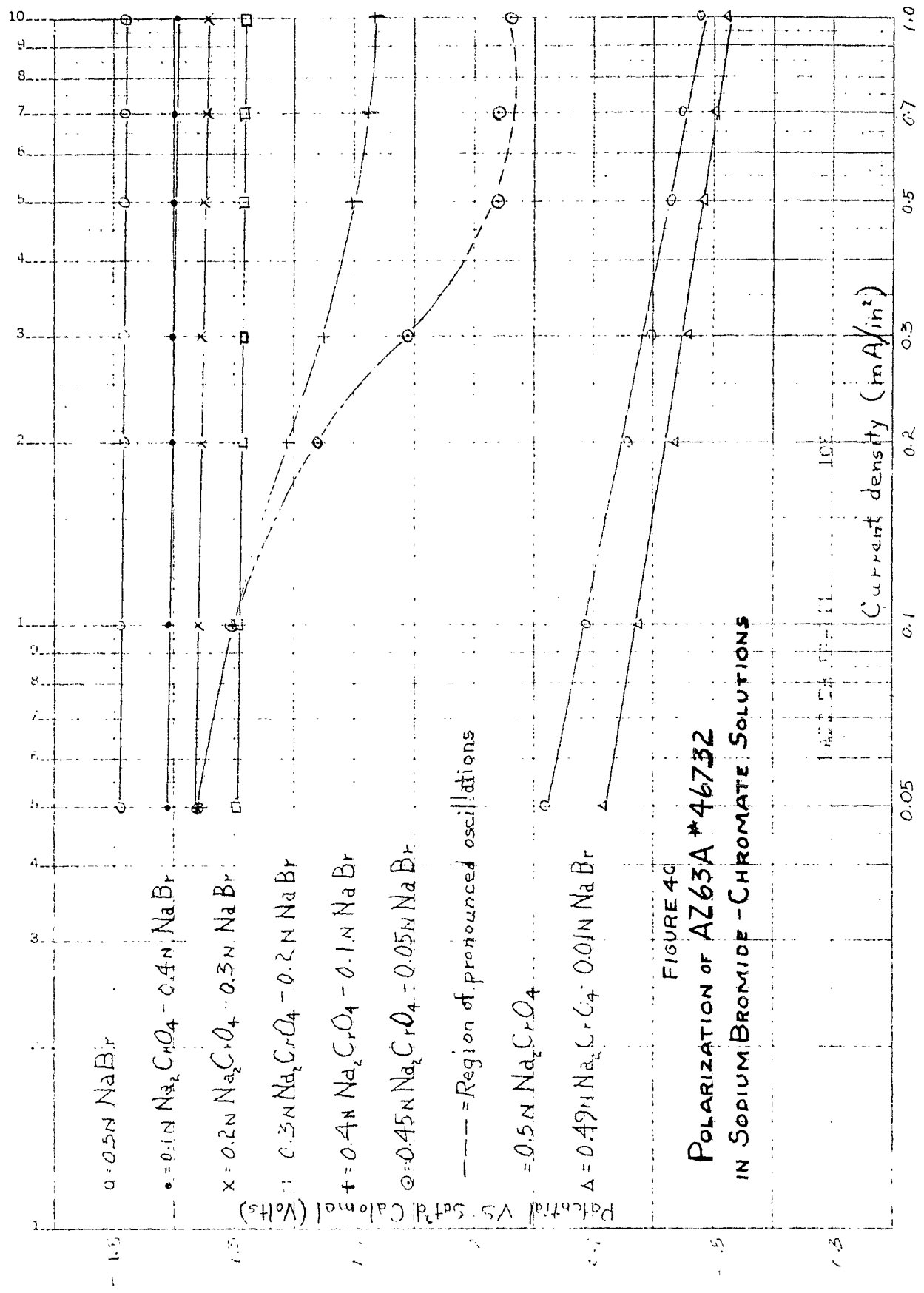


FIGURE 4C  
 POLARIZATION OF AZ63A #46732  
 IN SODIUM BROMIDE - CHROMATE SOLUTIONS

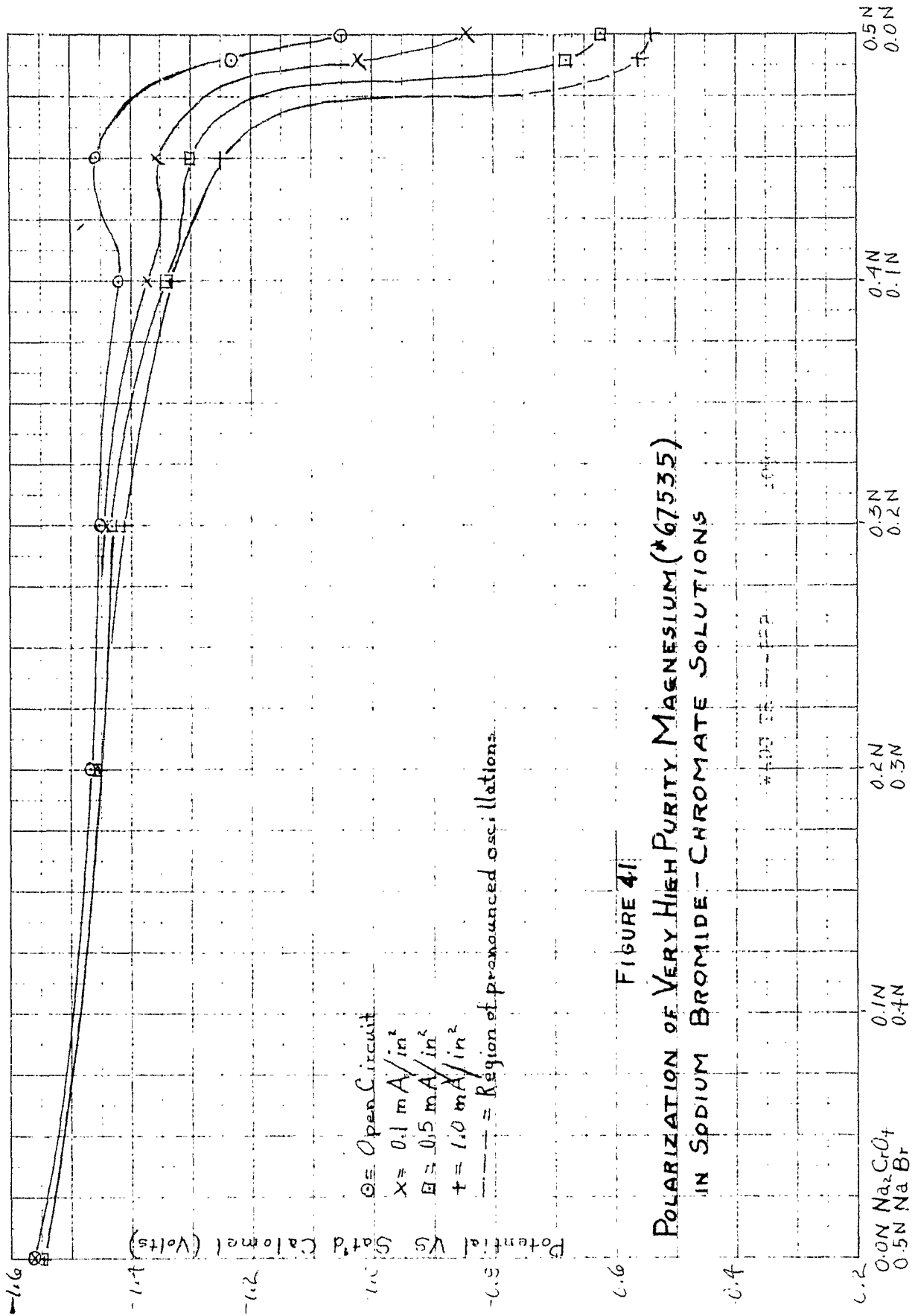


FIGURE 41

POLARIZATION OF VERY HIGH PURITY MAGNESIUM (\*67535) IN SODIUM BROMIDE-CHROMATE SOLUTIONS

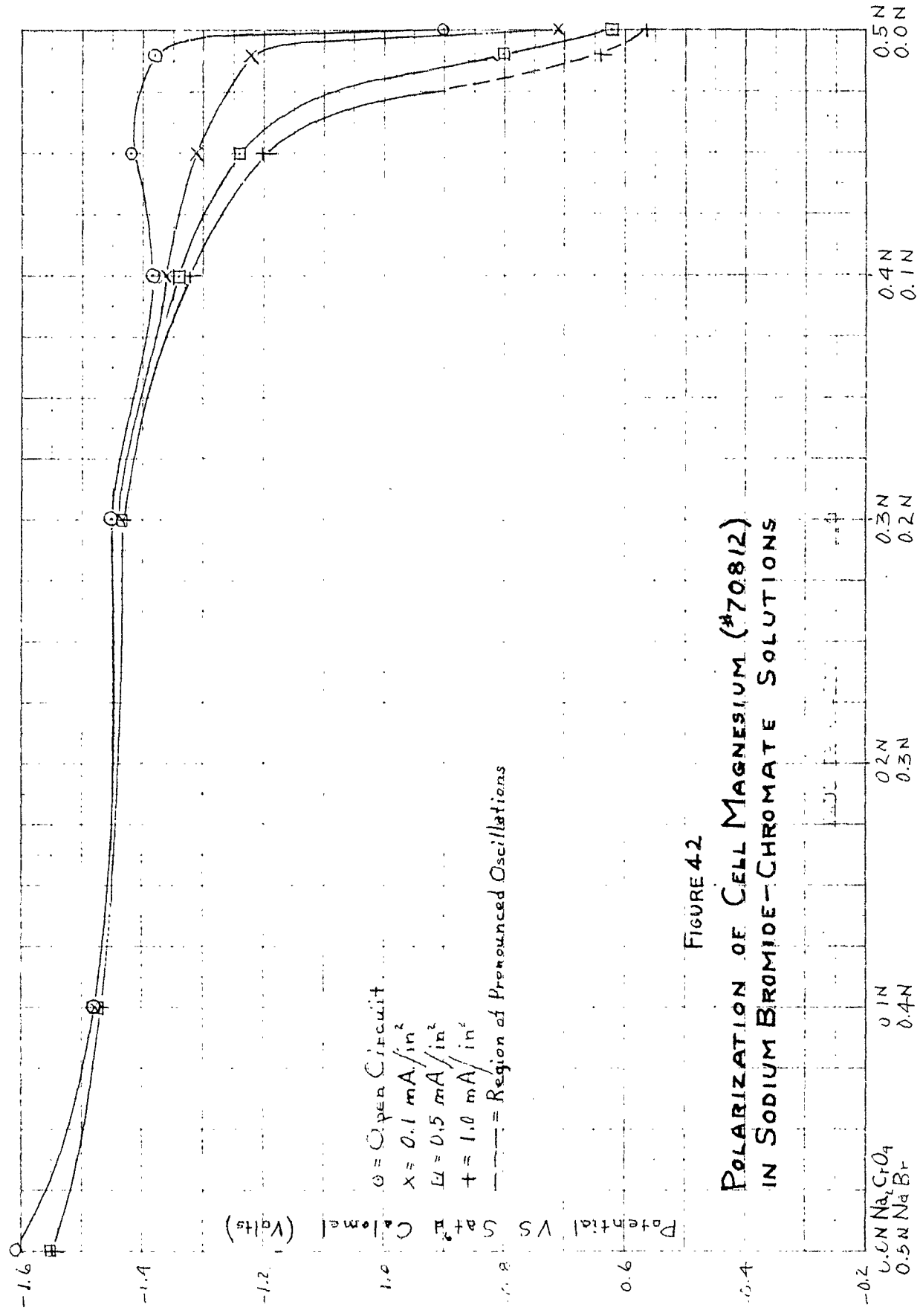


FIGURE 42  
 POLARIZATION OF CELL MAGNESIUM (#70812)  
 IN SODIUM BROMIDE-CHROMATE SOLUTIONS

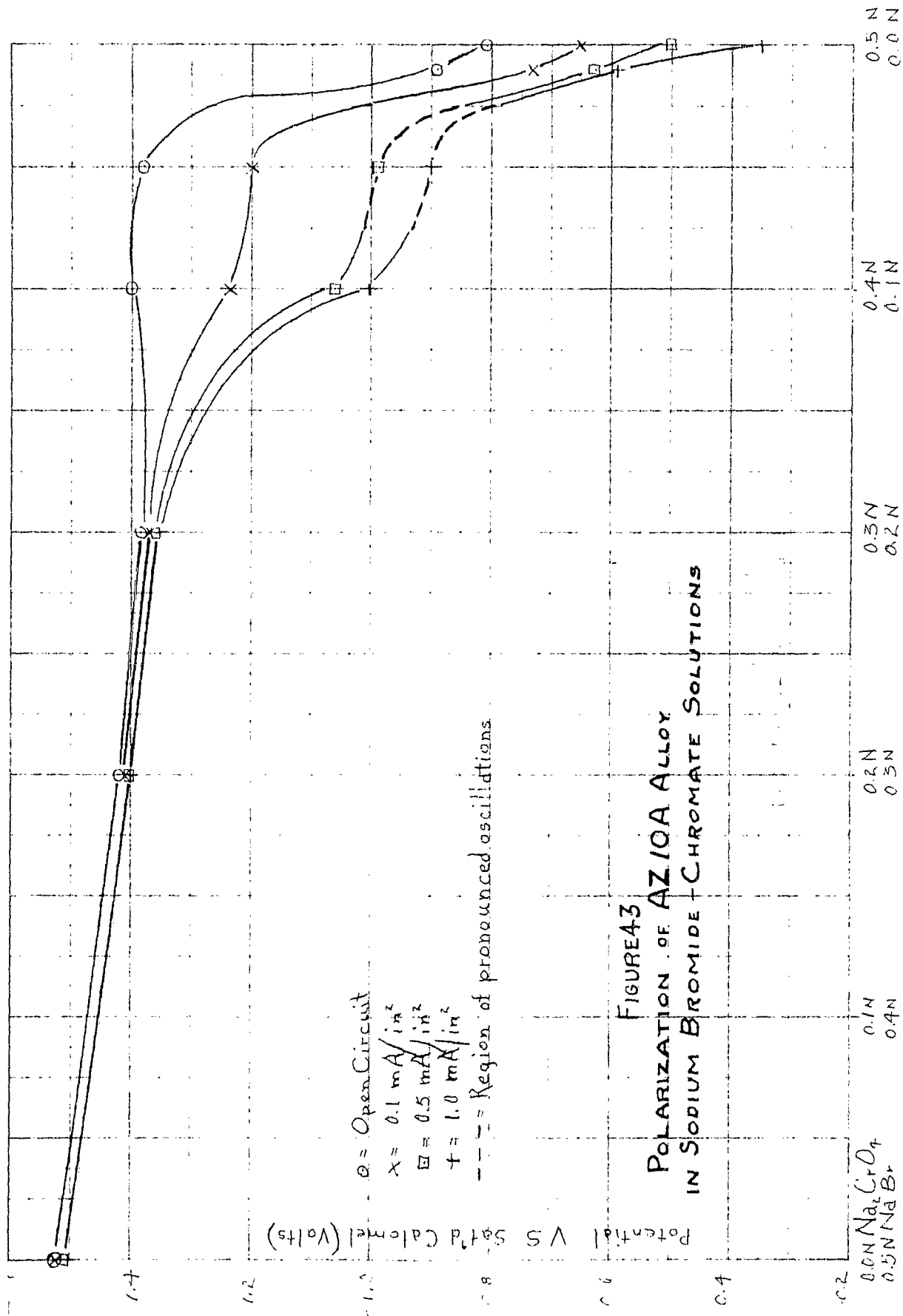
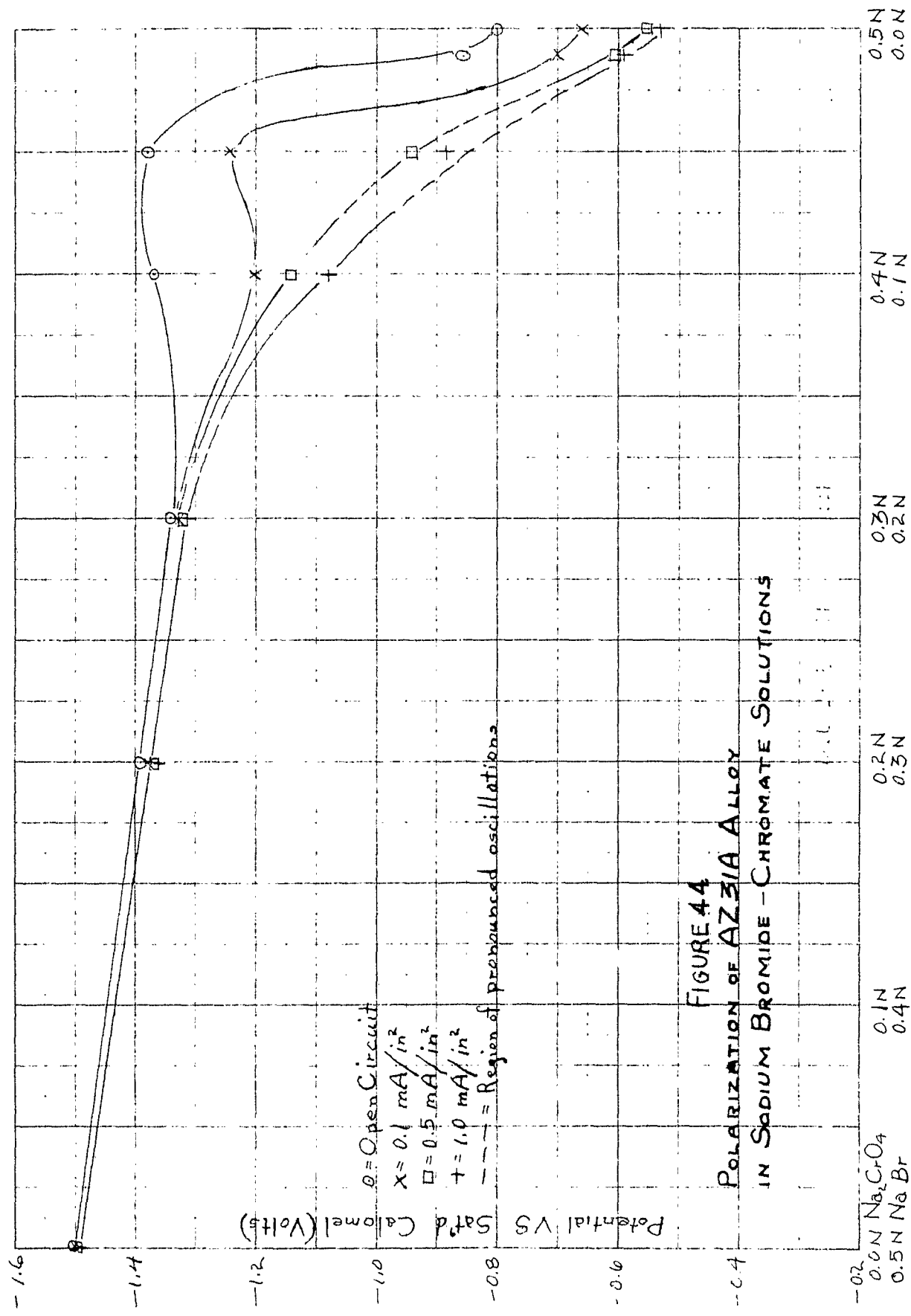


FIGURE 43  
 POLARIZATION OF AZ10A ALLOY  
 IN SODIUM BROMIDE + CHROMATE SOLUTIONS



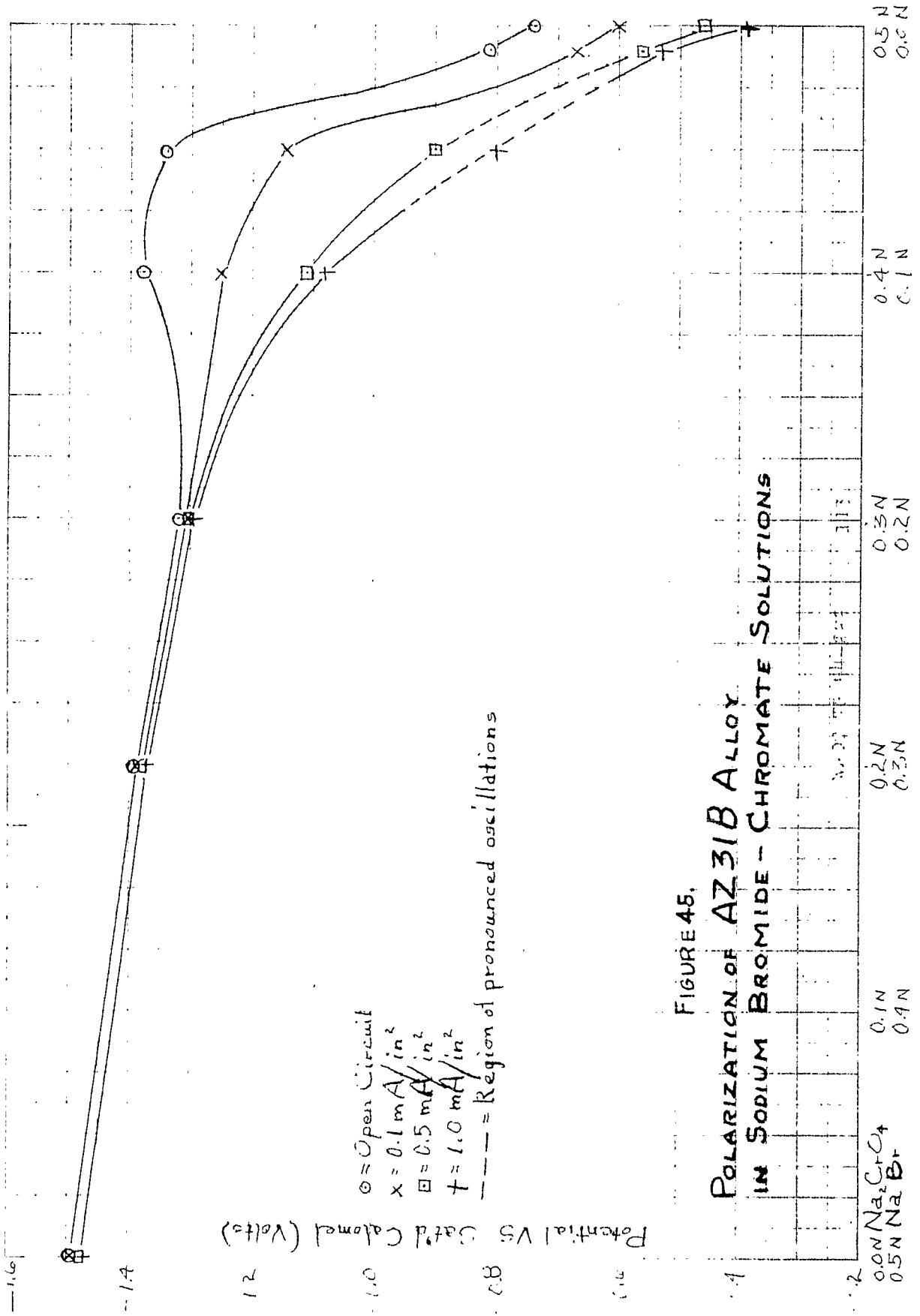


FIGURE 45.  
 POLARIZATION OF AZ31B ALLOY  
 IN SODIUM BROMIDE - CHROMATE SOLUTIONS

○ = Open Circuit  
 x = 0.1 mA/in<sup>2</sup>  
 □ = 0.5 mA/in<sup>2</sup>  
 + = 1.0 mA/in<sup>2</sup>  
 --- = Region of pronounced oscillations

Potential VS. Cath'd Current (Volts)

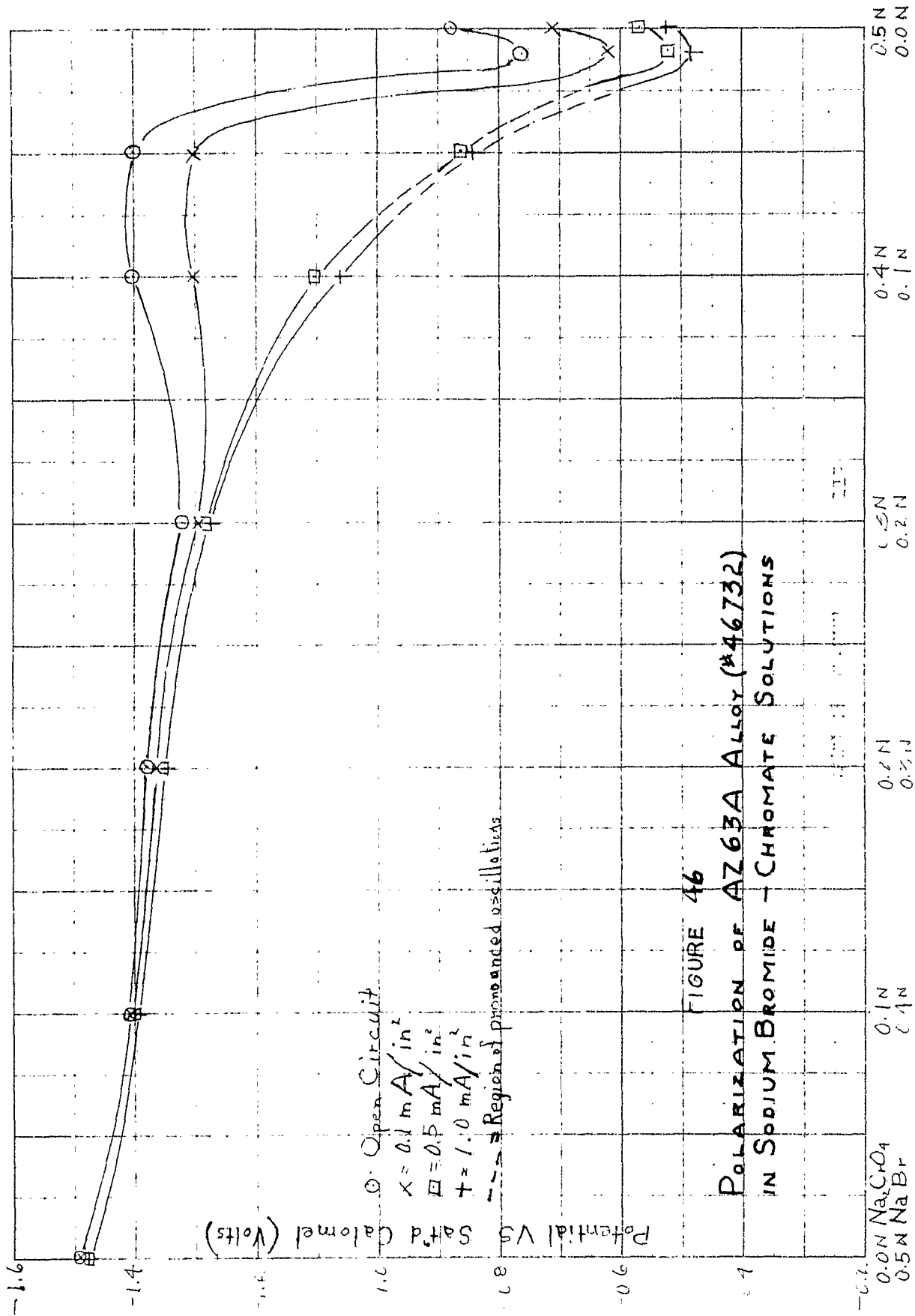
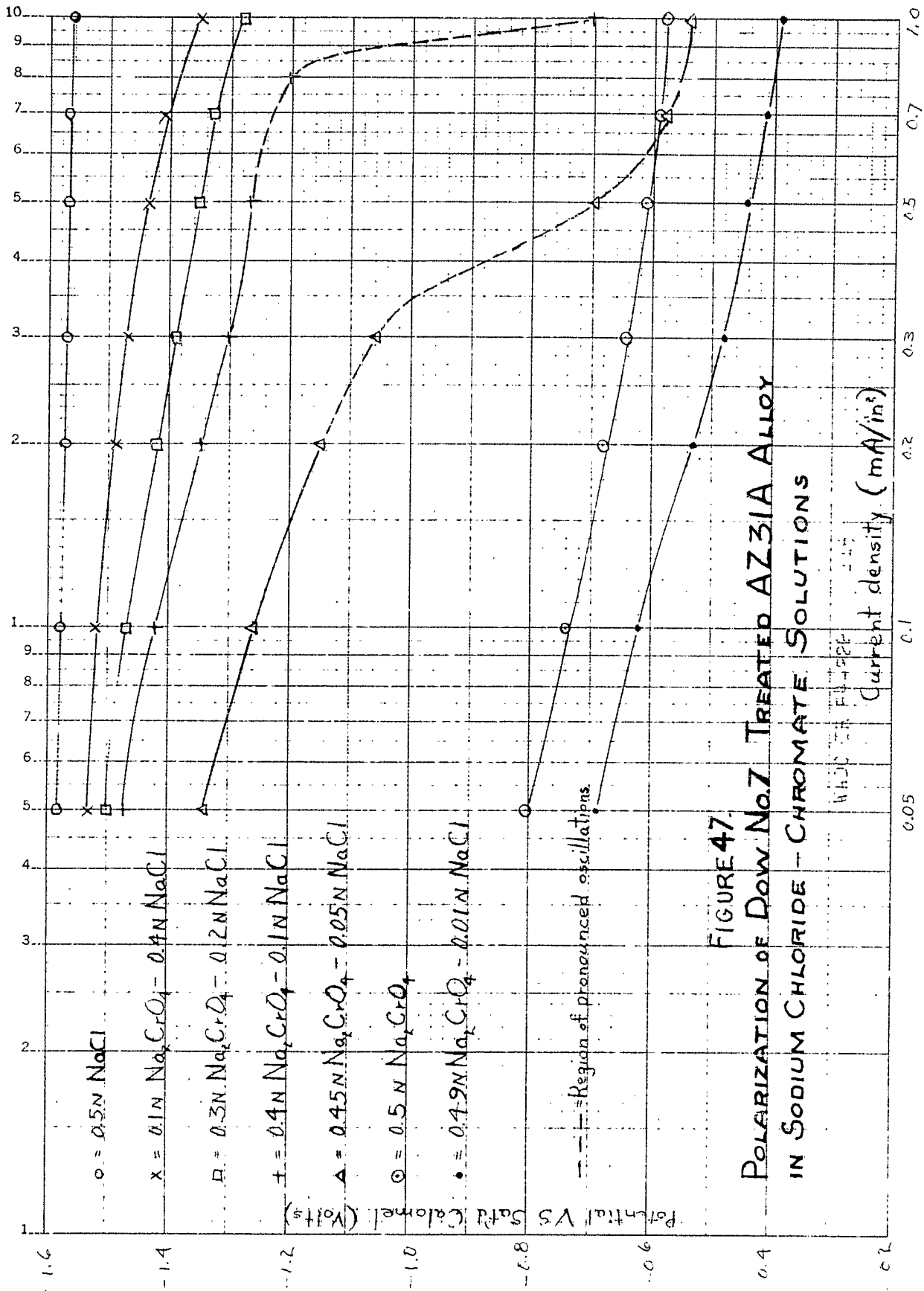


FIGURE 46  
 POLARIZATION OF AZ63A ALLOY (#46732)  
 IN SODIUM BROMIDE - CHROMATE SOLUTIONS



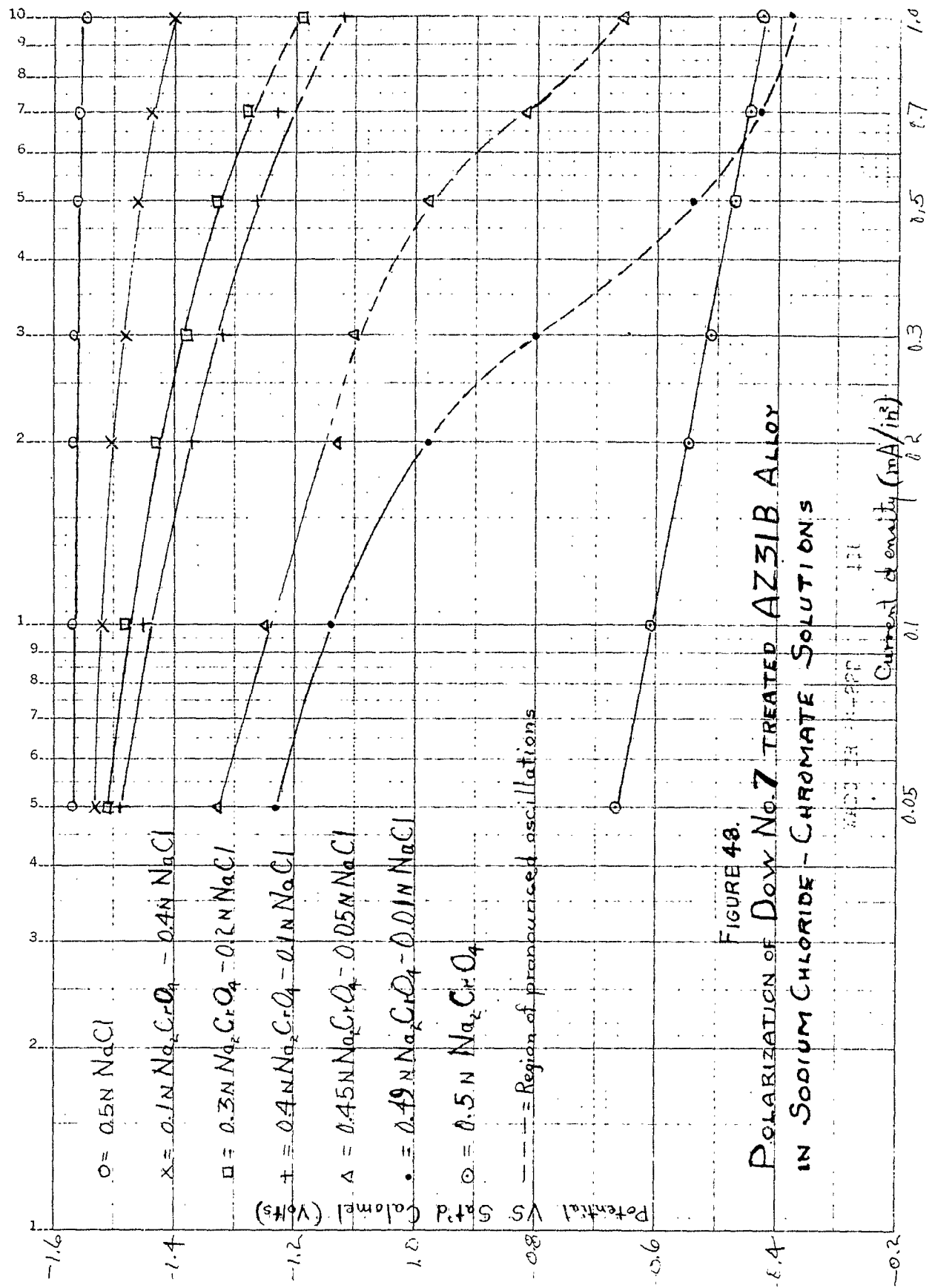


FIGURE 48.  
 POLARIZATION OF DOW NO. 7 TREATED AZ31B ALLOY  
 IN SODIUM CHLORIDE - CHROMATE SOLUTIONS

MADE IN U.S.A.



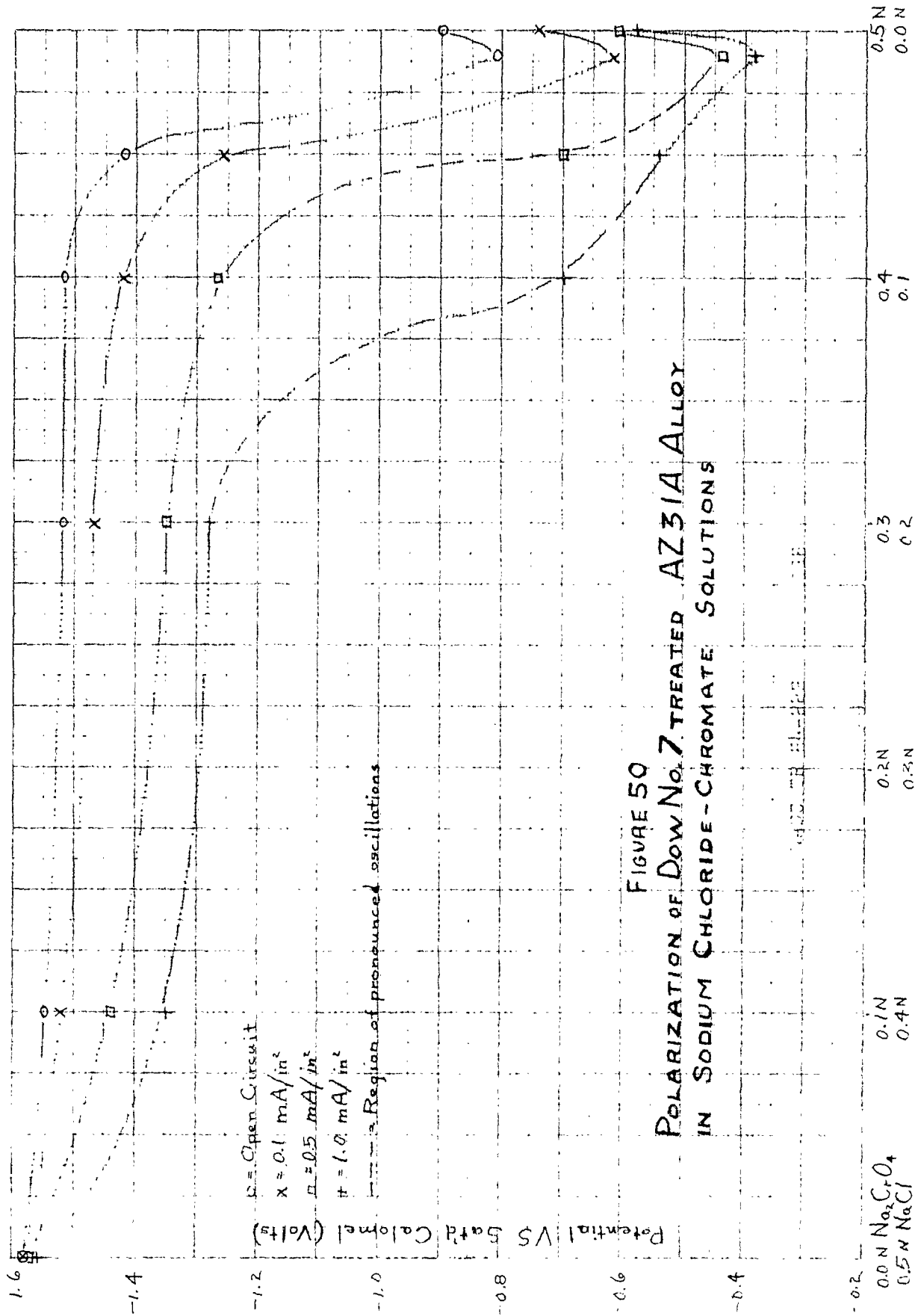


FIGURE 50  
 POLARIZATION OF DOW No. 7 TREATED AZ31A ALLOY  
 IN SODIUM CHLORIDE-CHROMATE SOLUTIONS

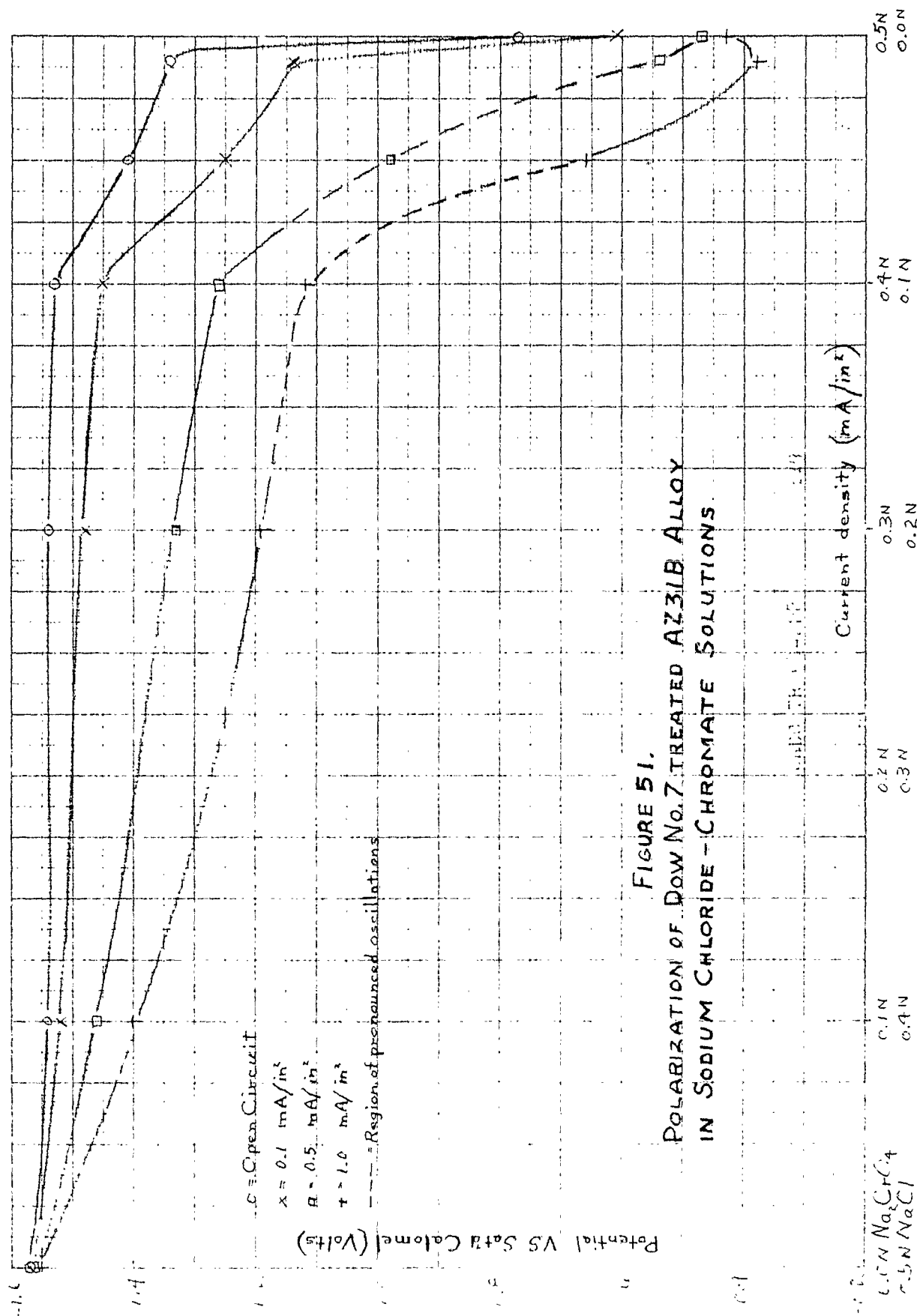


FIGURE 51.  
 POLARIZATION OF DOW NO. 7 TREATED AZ31B ALLOY  
 IN SODIUM CHLORIDE - CHROMATE SOLUTIONS.

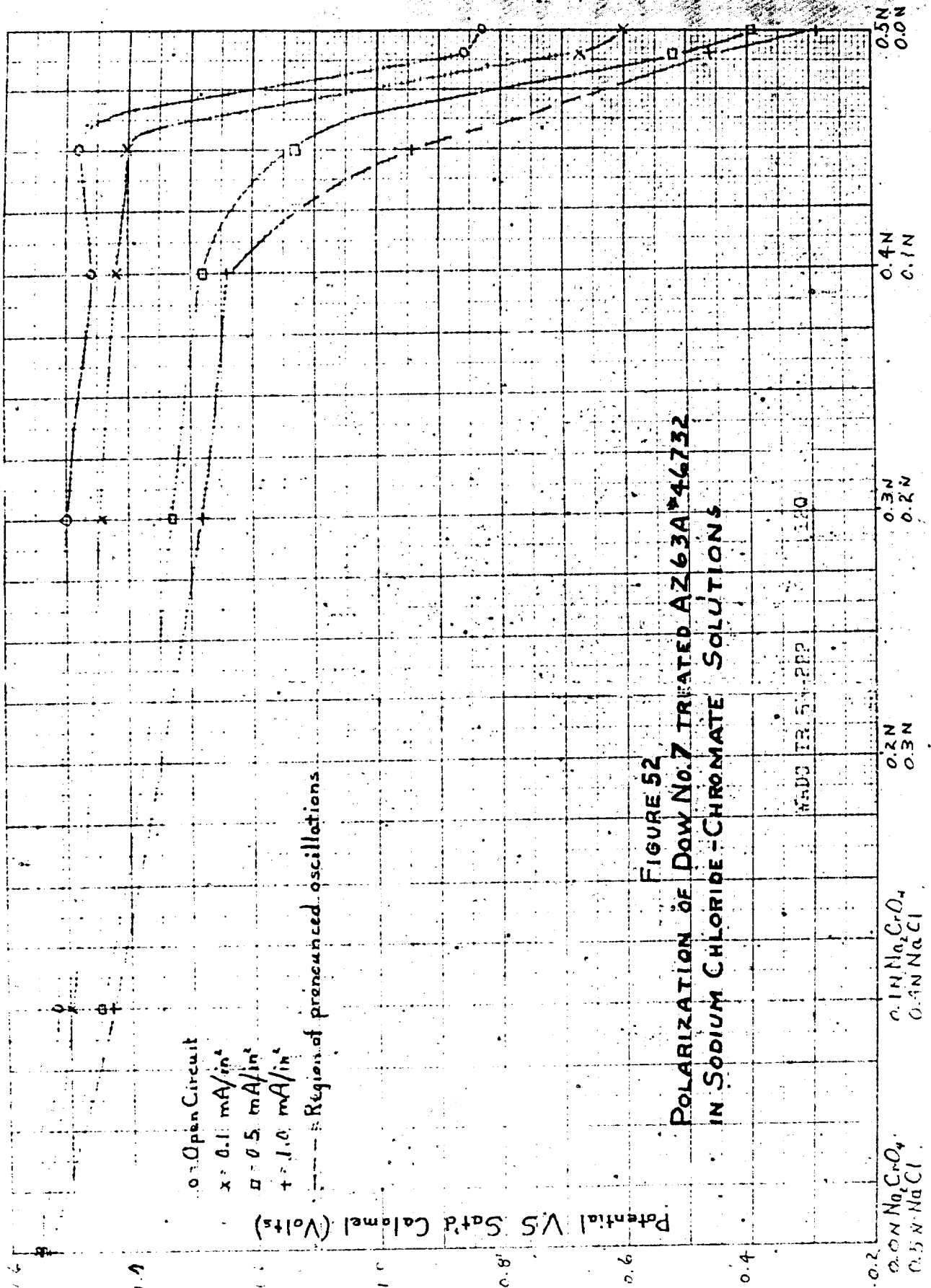


FIGURE 52  
POLARIZATION OF DOW NO. 7 TREATED AZ 63A 46732  
IN SODIUM CHLORIDE-CHROMATE SOLUTIONS

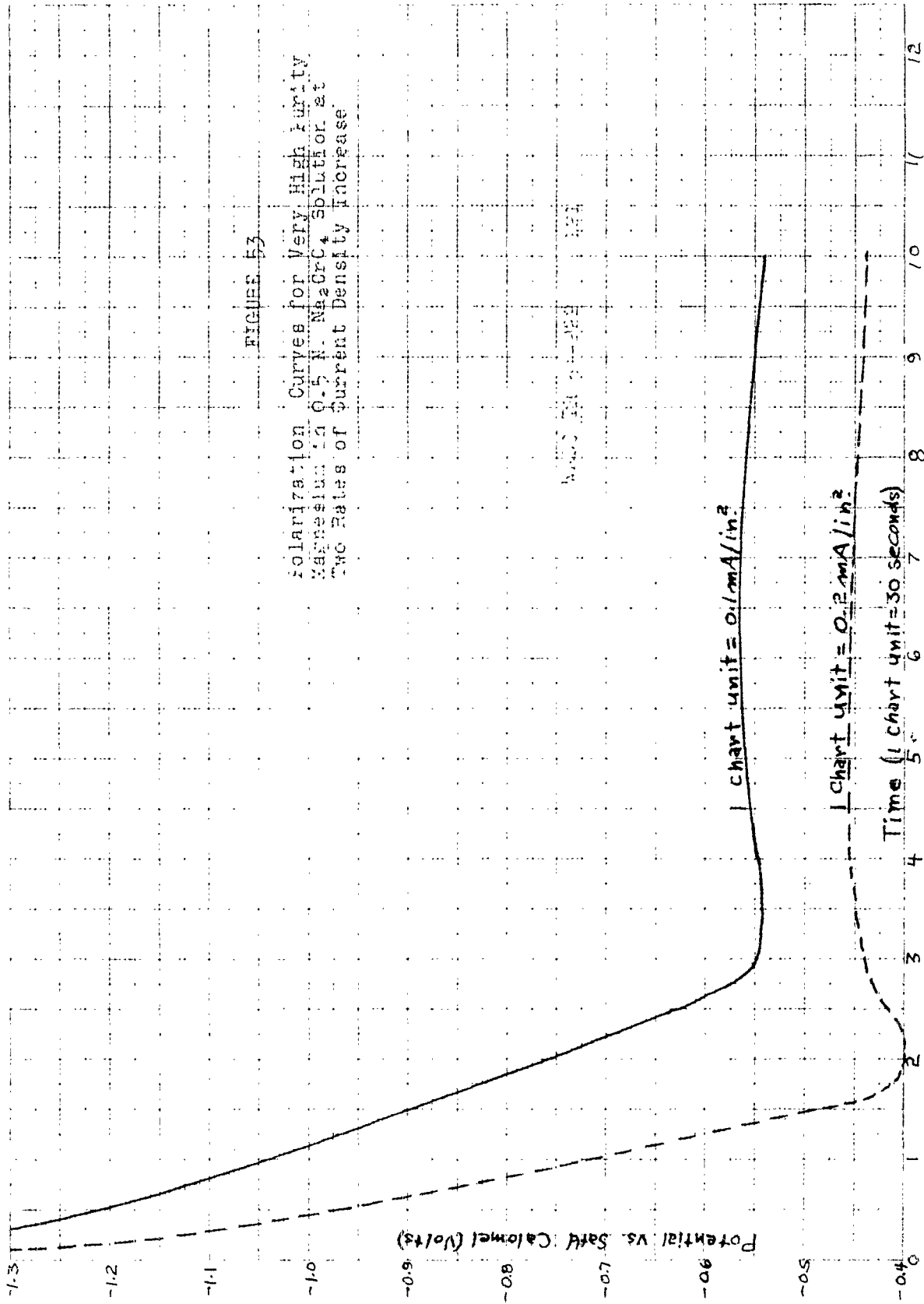


FIGURE 53

Polarization Curves for Very High Purity Magnesium in 0.5 N. Na<sub>2</sub>Cr<sub>2</sub>O<sub>7</sub> solution at two Rates of current Density Increase

WAS IN 1954

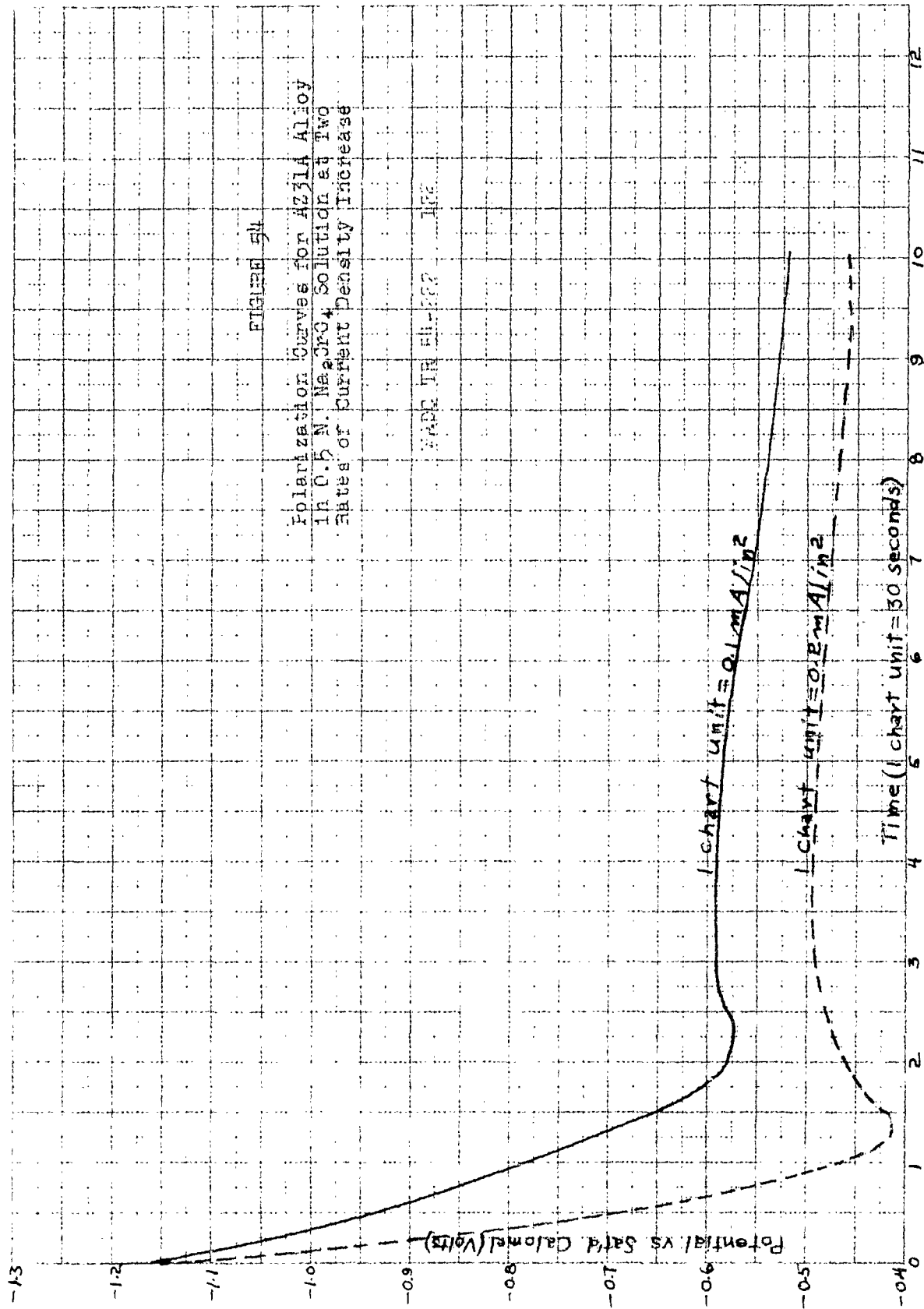


FIGURE 54

Polarization Curves for AZ31A Alloy  
 in 0.5 N. Na<sub>2</sub>CrO<sub>4</sub> Solution at Two  
 Rates of Current Density Increase

MADE IN U.S.A. IFA

1 chart unit = 0.1 mA/in<sup>2</sup>

1 chart unit = 0.2 mA/in<sup>2</sup>

Time (1 chart unit = 30 seconds)

Potential vs Sat'd. Calomel (Volts)

FIGURE 55



Metal

Phase 1 of coating  
Phase 2 of coating  
Supporting resin

Profile View at 1025X of Dow No. 14 Anodic  
Treatment on FSL-O Alloy  
Sheet (No. 31321, Glycol Etchant, Bright Light plus Green Filter)

FIGURE 56



Metal

Phase 1 of coating  
Phase 2 of coating

Supporting Resin

Profile View at 1025X of Above Treatment that  
has Been Interrupted at 85 volts.  
(No. 31322, Glycol Etchant, Bright Light plus Green Filter)

note: It would appear that Phase 2 is much harder than Phase 1. Also  
notice the bubbles in Phase 2 and the uneven distribution of  
both phases.

Profile Views of Dow No. 17 A.C. Anodic Treatment Films.

(All views 500X, sensitive tint, green filter.)



Fig. 57a. 90 Volt Coating. (Neg. No. 32807)



Fig. 57b. 85 Volt Coating. (Neg. No. 32807)



Fig. 57c. 80 Volt Coating. (Neg. No. 32808)



Fig. 57d. 75 Volt Coating. (Neg. No. 32808)



Fig. 57e. 70 Volt Coating. (Neg. No. 32809)

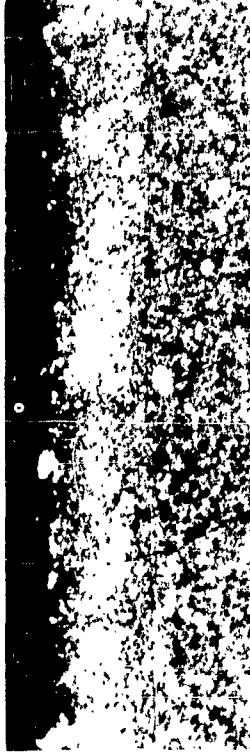


Fig. 57f. 65 Volt Coating. (Neg. No. 32810)

Profile Views of Dow D.C. Anodic Treatment Films.  
(All views 500X, sensitive tint, green filter.)

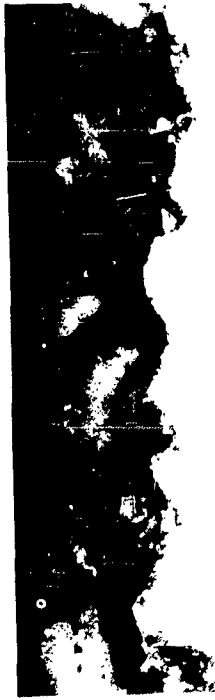


Fig. 58a 95 Volt Coating. (Neg. No. 32774)



Fig. 58b 90 Volt Coating. (Neg. No. 32774)



Fig. 58c 85 Volt Coating. (Neg. No. 32775)



Fig. 58d 80 Volt Coating. (Neg. No. 32775)



Fig. 58e 75 Volt Coating. (Neg. No. 32776)



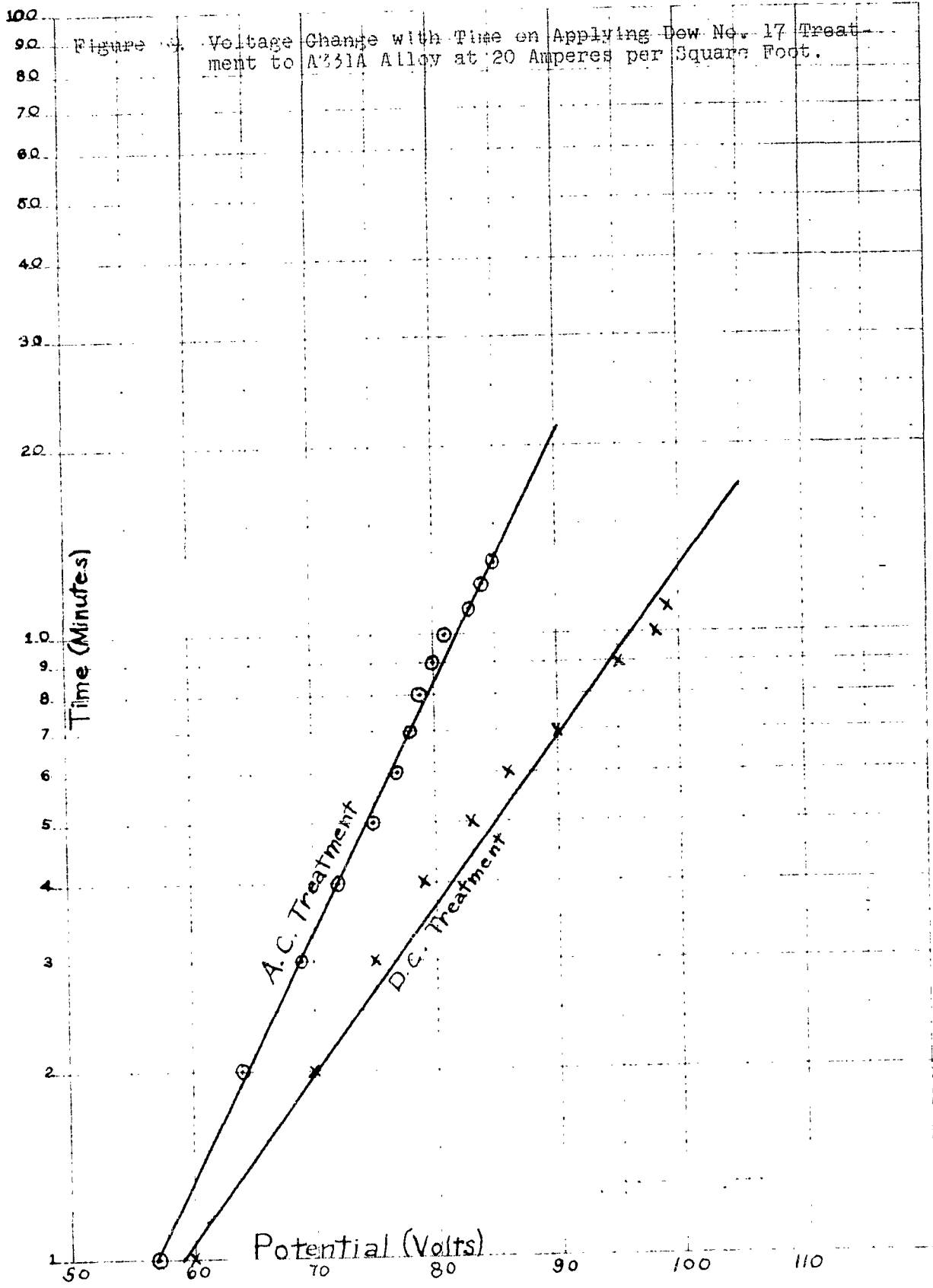
Fig. 58f 70 Volt Coating. (Neg. No. 32776)

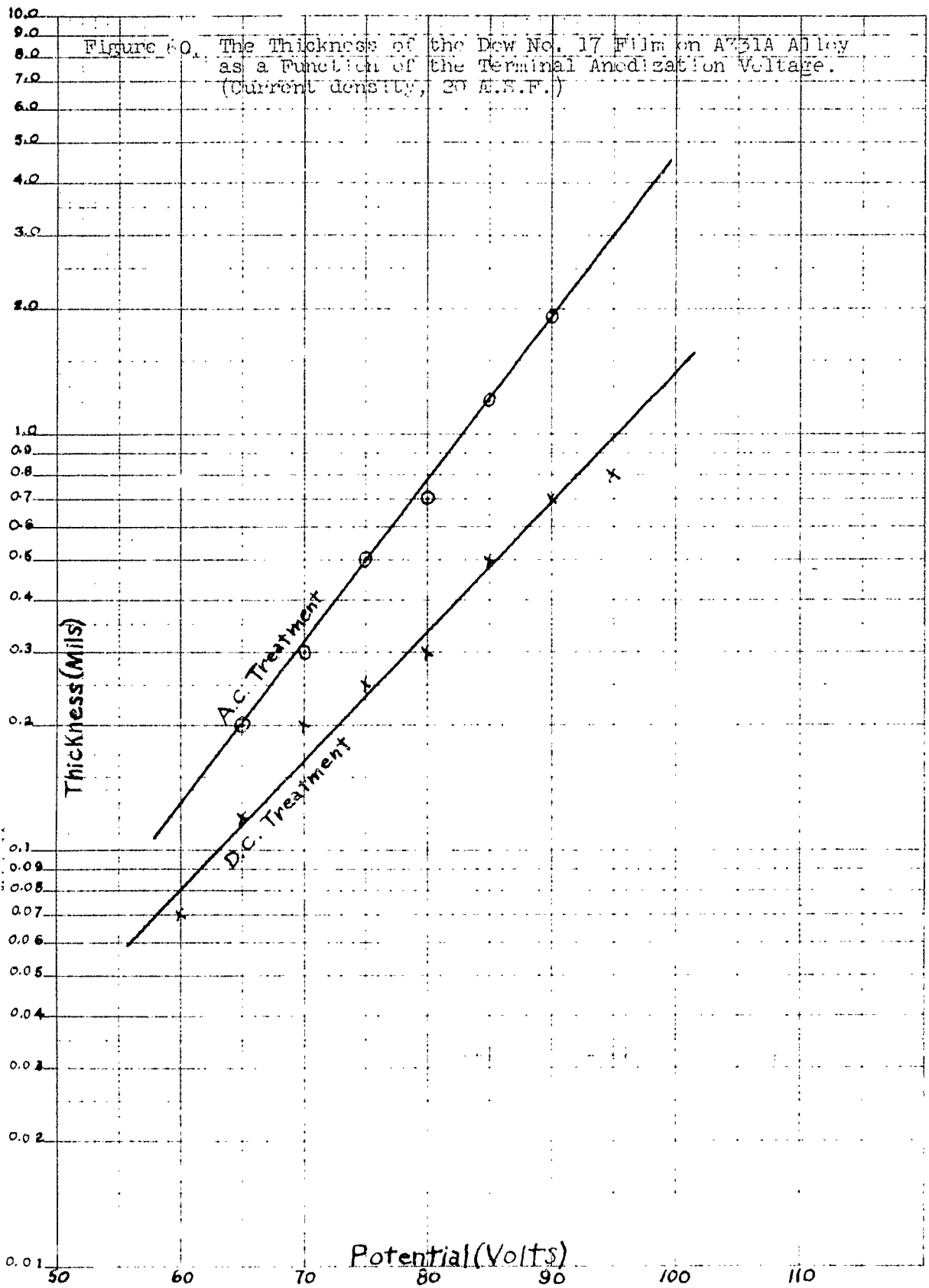


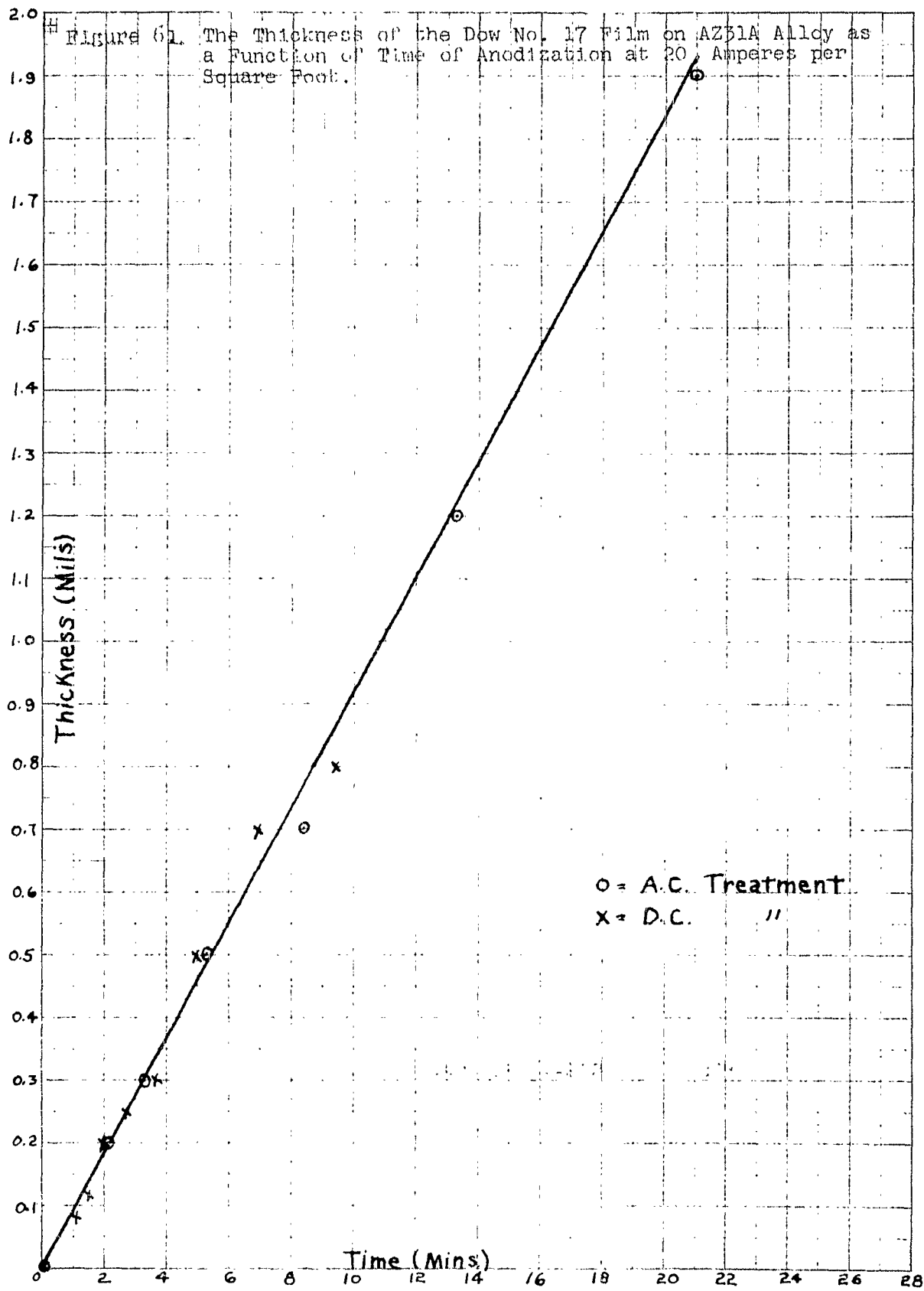
Fig. 58g 65 Volt Coating. (Neg. No. 32777)



Fig. 58h 60 Volt Coating. (Neg. No. 32777)







Profile Views of the H.A.E. Treatment Film.



Figure 62  
Neg. 31976.

500 X  
Oblique Light.

Note the physical resemblance to the  
Dow No. 17 Treatment Film. (Figure  
12 in Third Quarterly Report.)

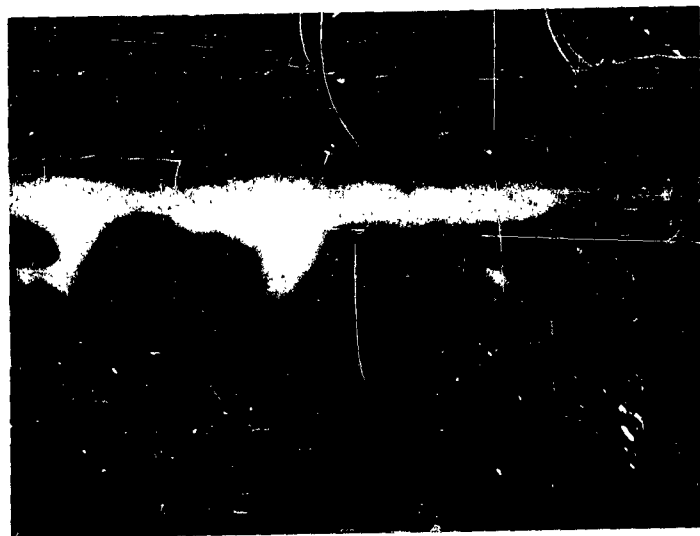
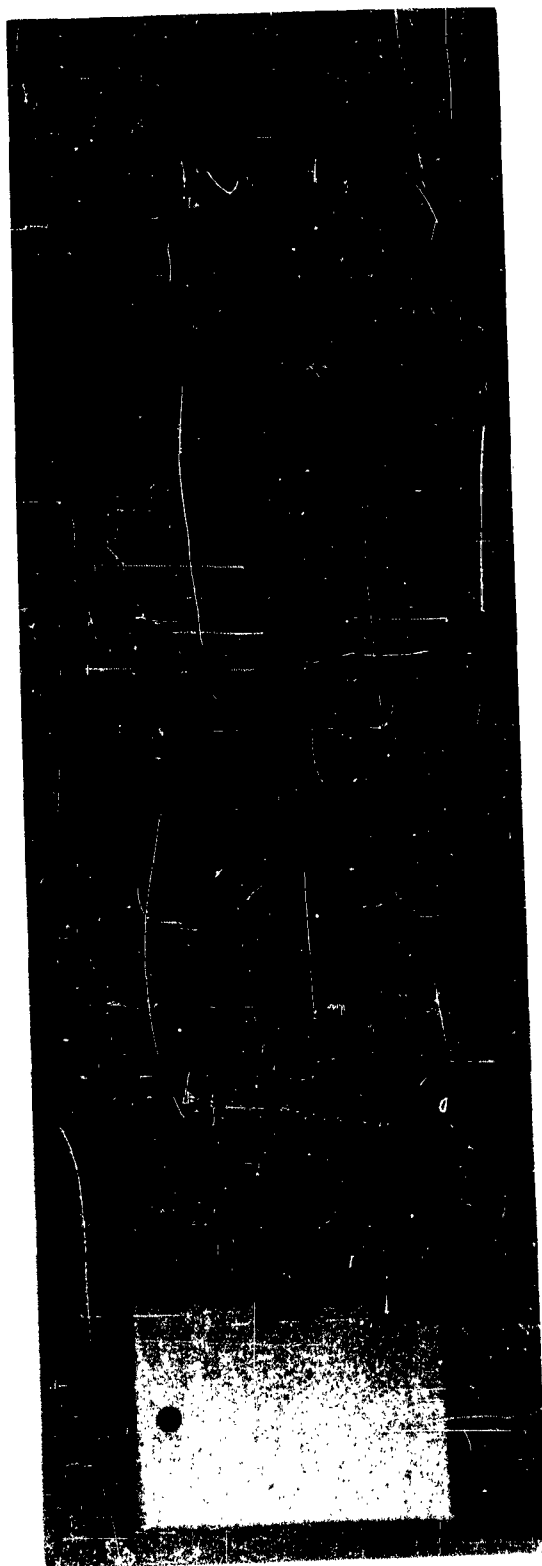


Figure 63  
Neg. 31977-2.

500 X  
Polarized Light.

Figure 64. Fading of Dow No. 7 Treatment Films on Exposure to  
3 Per Cent Sodium Chloride Solution.

Exposure in Hours



0

1/4

1

3

15

24

Profile Views of Dow No. 7 Treatment Films After Exposure to 3 Per Cent Sodium Chloride Solution. (All Views 2000 X, Sensitive Tint, Green Filter.)

	<u>Time of Exposure</u> (Hours)	<u>Approx. Thickness</u> (Microns)
	0	1.5
Fig. 65a Neg. 32072		
	1/4	1.5
Fig. 65b Neg. 32073		
	1	1.3
Fig. 65c Neg. 32074		
	3	1.2
Fig. 65d Neg. 32075		
	15	0.9
Fig. 65e Neg. 32076		

Top Surface Views of Dow No. 7 Treatment Films After Exposure to 3 Per Cent Sodium Chloride Solution. (All Views 500X, Polarized Light, Green Filter.)



Fig. 66a 1/4 Hour Exposure  
(Neg. 32045)



Fig. 66b 1 Hour Exposure  
(Neg. 32047)

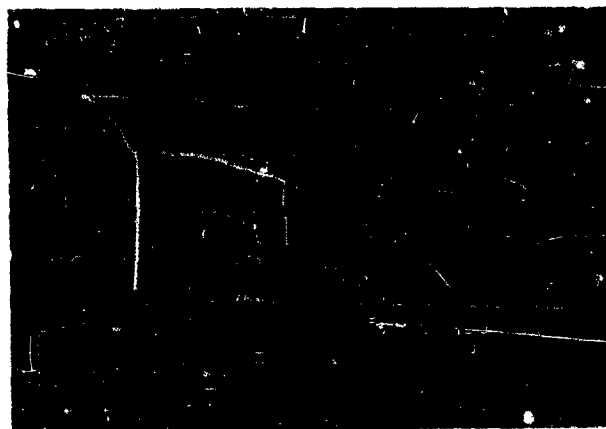


Fig. 66c 3 Hours Exposure  
(Neg. 32049)

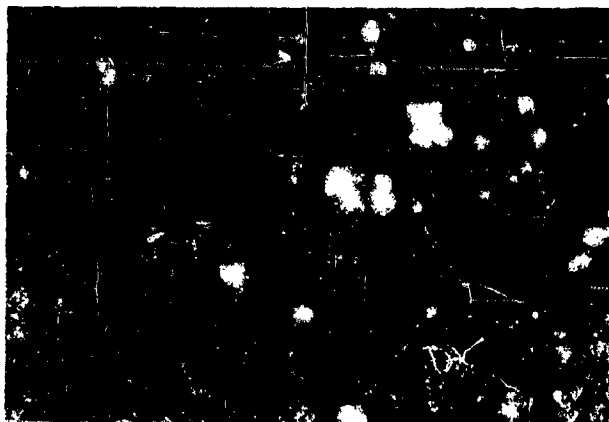


Fig. 66d 15 Hours Exposure  
(Neg. 32051)

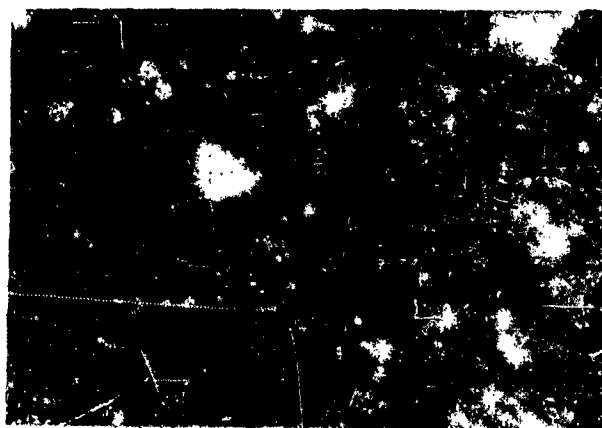


Fig. 66e 24 Hours Exposure  
(Neg. 32053)

Top Surface View of a Dow No. 7 Treatment Film that Was Exposed Indoors for One Month and then Exposed to Distilled Water for 15 Hours.

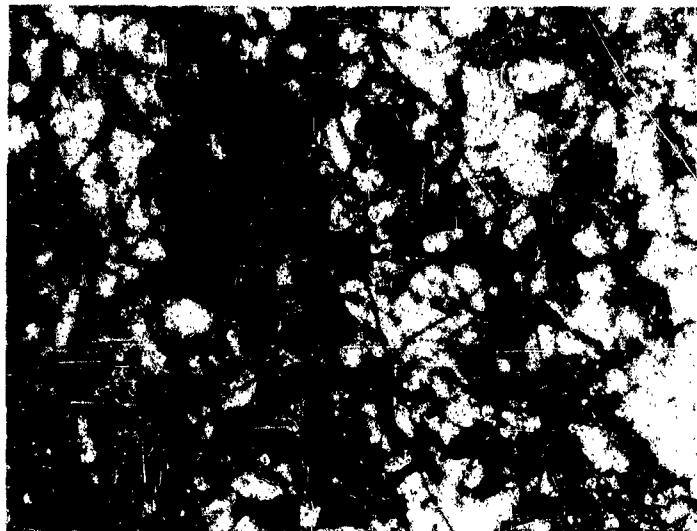


Fig. 67a Neg. 32225. 500X, Oblique Light, Green Filter.

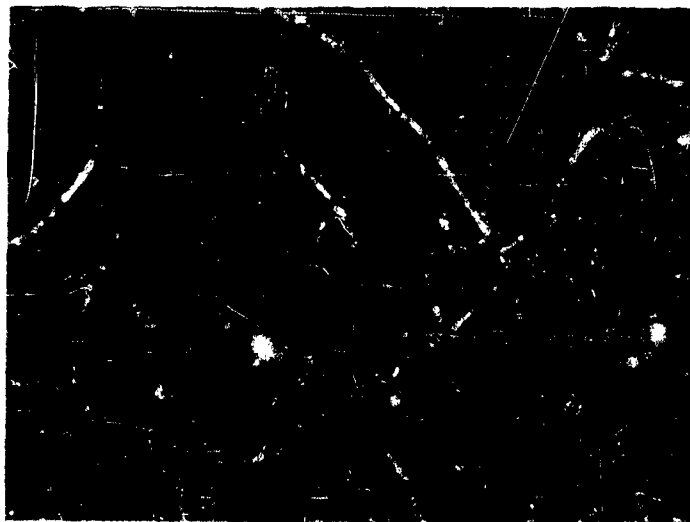


Fig. 67b Neg. 32226. 500X, Polarized Light, Green Filter.

Profile Views of Dow No. 7 Treatment Films Showing Manganese  
Precipitate Protruding into or Through the Film.



Figure 68a            2000X  
Neg. 32146    Bright Light

The precipitate is  
slightly below the film's  
outer surface.

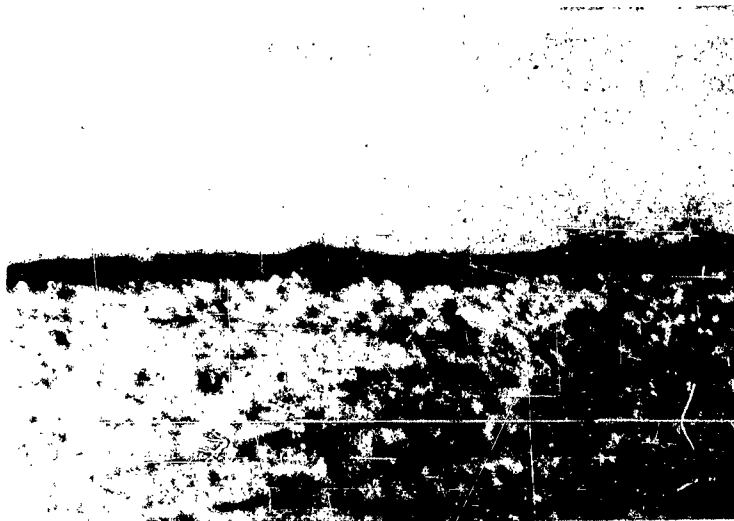


Figure 68b            2000X  
Neg. 32151    Sensitive Tint

The precipitate is flush  
with the film's outer sur-  
face.



Figure 68c            2000X  
Neg. 32148    Sensitive Tint

The precipitate is pro-  
truding through the film's  
outer surface.

Top Surface Views of No. 7 Treatment Films Showing the Effect of Heating. (All views 1000X, oblique light, green filter.)



Fig. 69a One Week at 25C.  
(Neg. 32117)

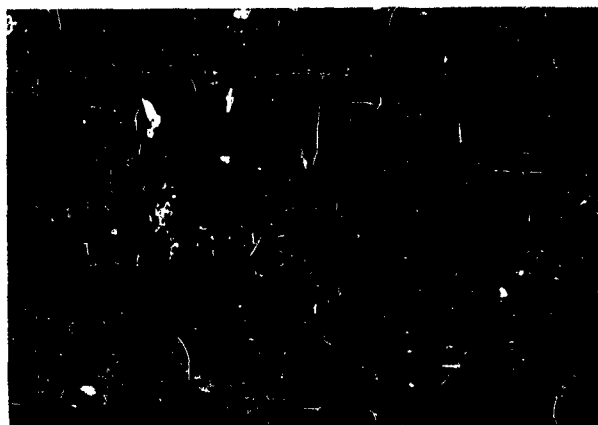


Fig. 69b 68 Minutes at 125C.  
(Neg. 32113)

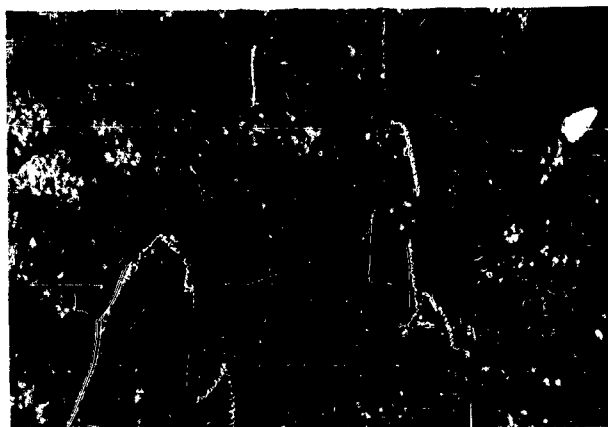


Fig. 69c 60 Minutes at 156C.  
(Neg. 32112)



Fig. 69d 64 Minutes at 185C.  
(Neg. 32114)



Fig. 69e 60 Minutes at 205C.  
(Neg. 32115)



Fig. 69f 64 Minutes at 232C.  
(Neg. 32116)

Profile Views of No. 7 Treatment Films Showing The Effect of Heating.  
(All views 200X, sensitive tint, green filter.)



Fig. 70a One Week at 25C.  
(Neg. 32681).

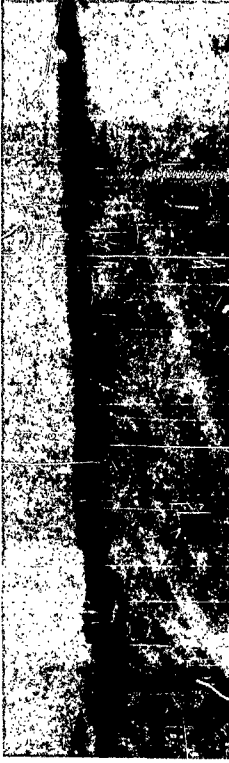


Fig. 70d 64 Minutes at 185C.  
(Neg. 32678).



Fig. 70b 68 Minutes at 125C.  
(Neg. 32677).



Fig. 70e 60 Minutes at 205C.  
(Neg. 32679).

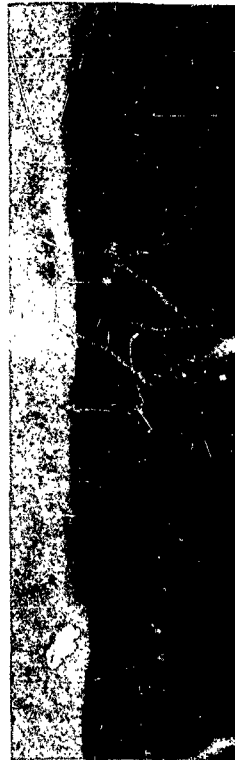


Fig. 70c 60 Minutes at 156C.  
(Neg. 32676).



Fig. 70f 64 Minutes at 232C.  
(Neg. 32680).

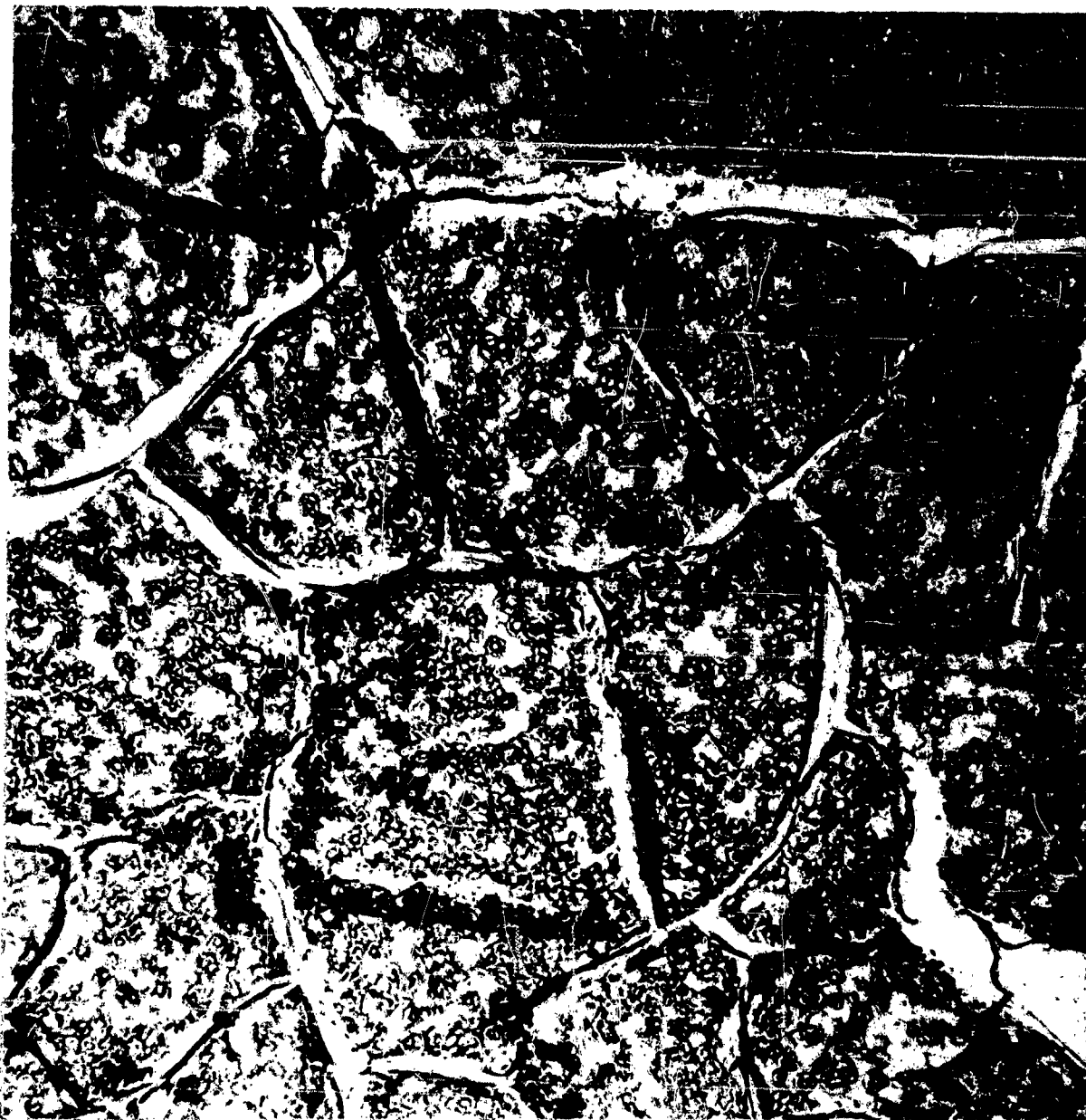


Figure 71

Neg. No. M-1359d

5,800 X

Electronmicrograph of the External Surface of a Dow No. 7 Treatment Film. (Hot molded polystyrene negative - SiO positive replica technique). Note the cracks and craters caused by dehydration of the film in the negative replica process.

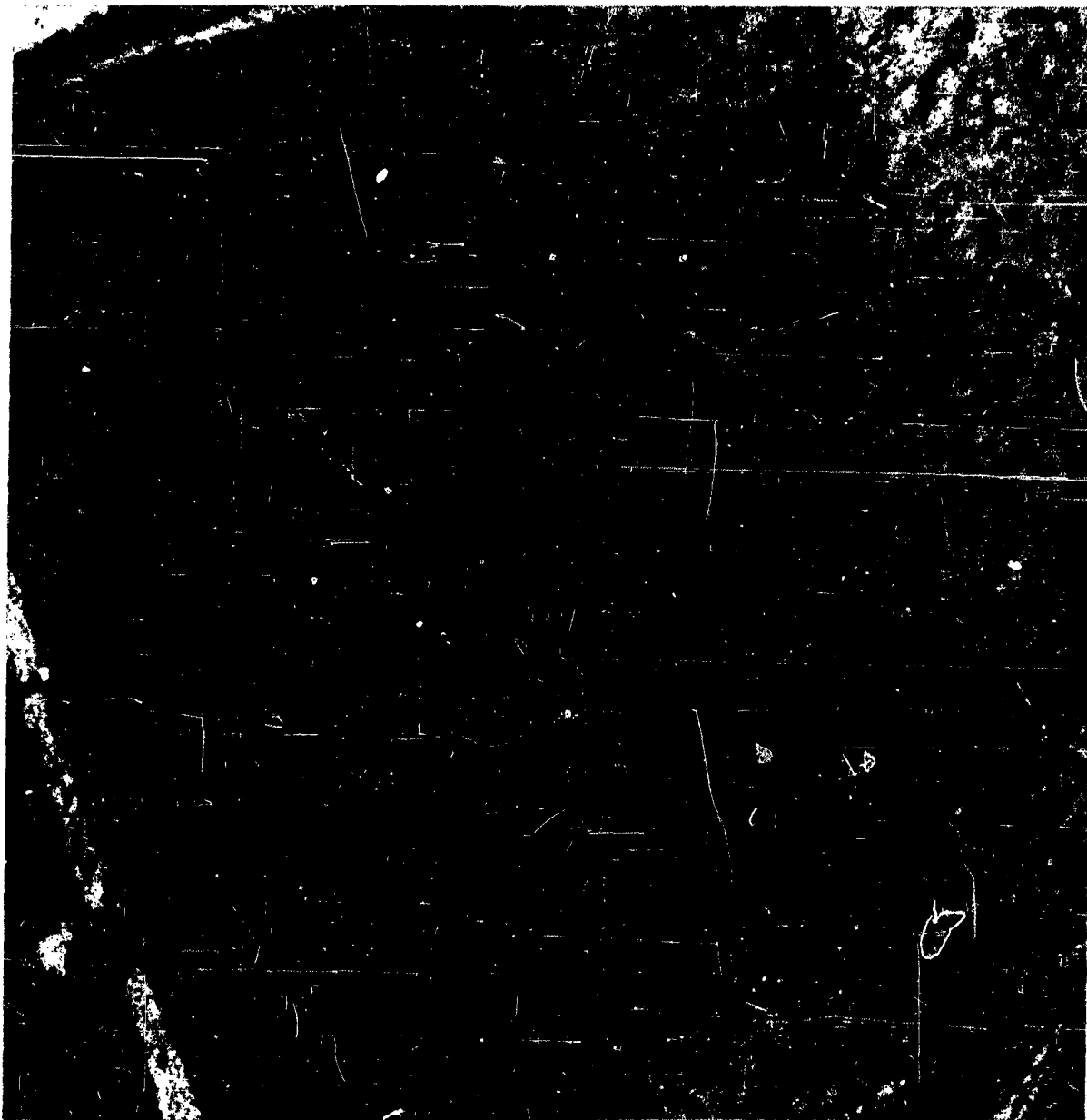


Figure 72

Neg. No. M-1359a

12,000 X

Electronmicrograph of the External Surface of a Dow No. 7 Treatment Film. (Hot molded polystyrene negative - SiO positive replica technique.) Note the apparent collapse of this section of film due to its dehydration in the negative replica process.

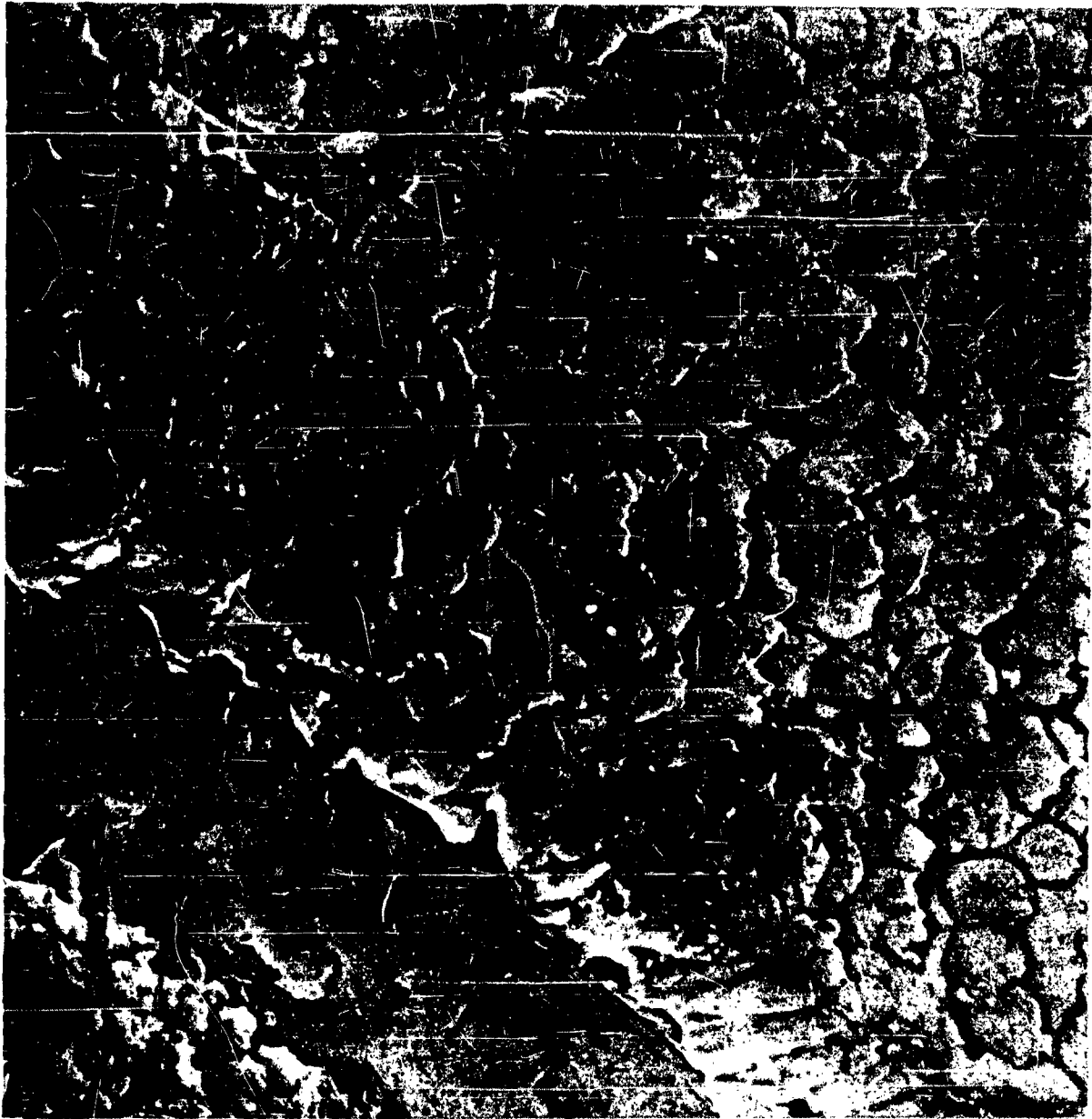


Figure 73

Neg. No. M-1349e

12,000 X

Electronmicrograph of the External Surface of a Dow No. 7 Treatment Film. (Hot molded polystyrene negative - SiO positive replica technique.) Note that this section appears to have suffered only partial damage due to dehydration. The smooth area at the lower left may be the film deposited over a grain boundary.



Figure 74

Neg. No. M-1349b

34,000 X

Electronmicrograph of the External Surface of a Dow No. 7 Treatment Film. (Hot molded polystyrene negative - SiO positive replica technique.) Note the scale-like appearance of this film and its lack of porosity. It would appear that this section suffered little dehydration.

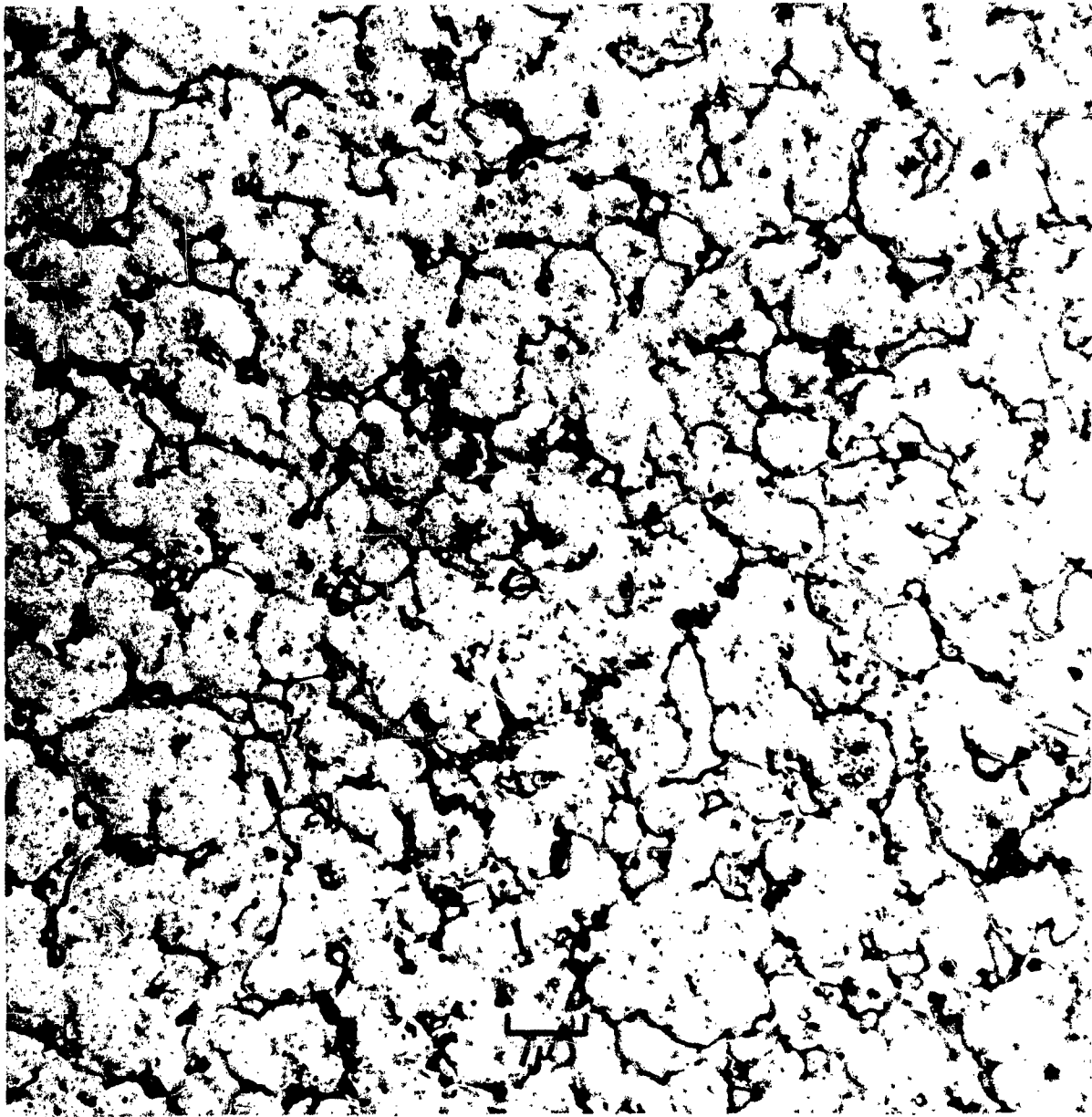


Figure 75

Neg. No. M-1378a

12,000 X

Electronmicrograph of the External Surface of a Dow No. 7 Treatment Film. (Cold polystyrene negative - SiO positive replica technique. This technique should not injure the film. However, the replicas do not appear as sharp as those from the hot molding method.)

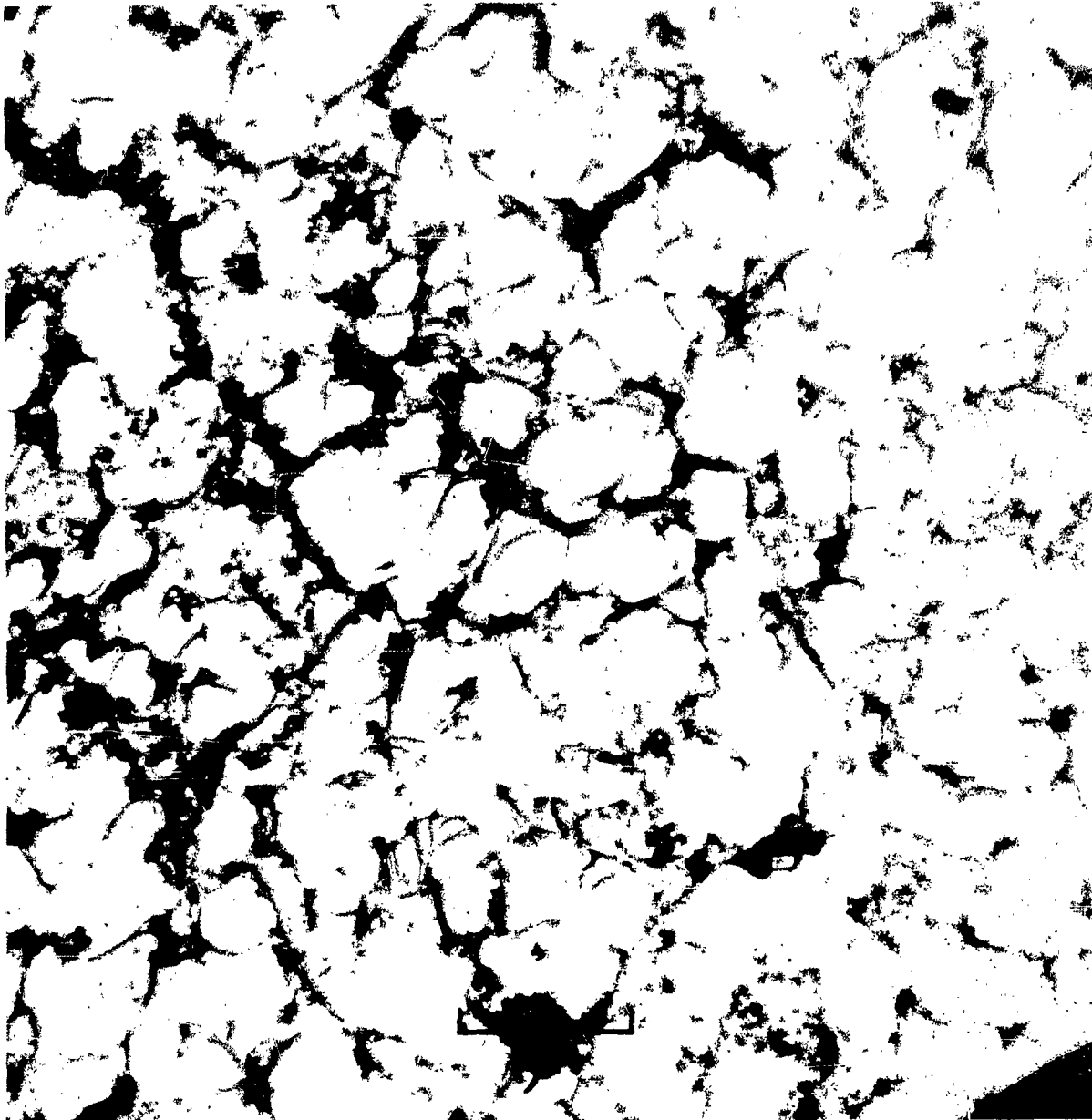


Figure 76

Neg. No. M-1378e

25,600 X

Electronmicrograph of the External Surface of a Dow No. 7 Treatment Film. (Cold polystyrene negative - SiO positive replica technique.) This structure is nearly identical to that found in the upper right of Figure 73.

Profile Views of the Iridite Treatment Film on Magnesium

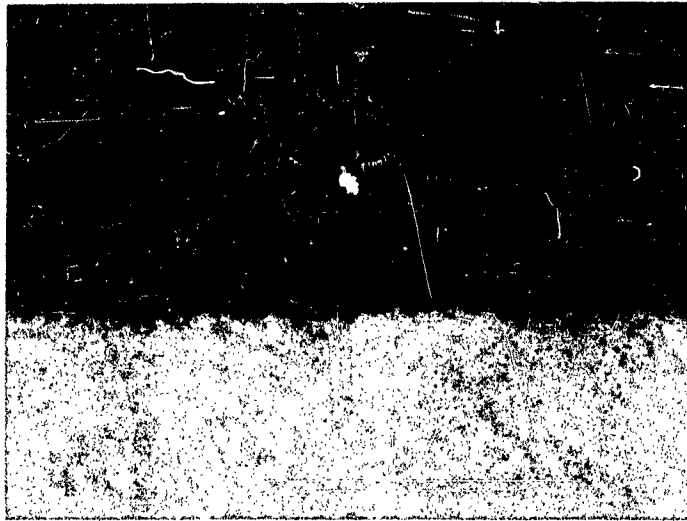


Figure 77a  
Neg. 31972.

500 X  
Oblique Light.

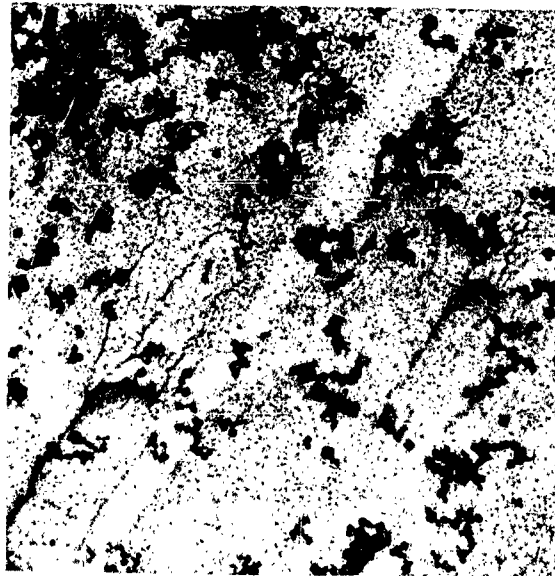
Note that although this film is of the same type as the Dow No. 7 film, it is far less continuous than the latter. Also note the severe etch.



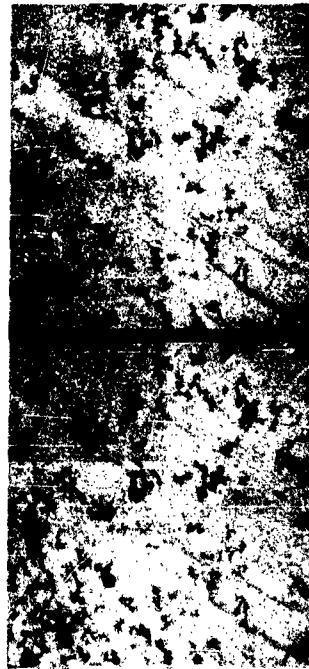
Figure 77b.  
Neg. 32224.

2000 X  
Polarized Light.

Electronmicrographs of the Surface of Very High Purity Magnesium (#67535) after Exposure to Distilled Water. (Fretreatment A. Replica Technique A.)



7200 X



3600 X



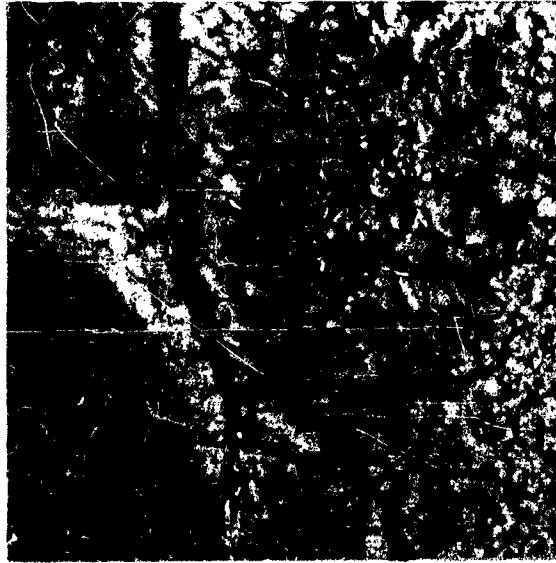
Figure 78 -- Five Minute Exposure  
(Neg. MS-259, Replica 1543)

WADC TR 54-222

Figure 79 -- Twenty Minute Exposure  
(Neg. MS-258, Replica 1544)

144

Electronmicrographs of the Surface of Very High Purity Magnesium (#b7535) after Exposure to Distilled Water. (Fretreatment A. Replica Technique A.)



7200 X



3600 X



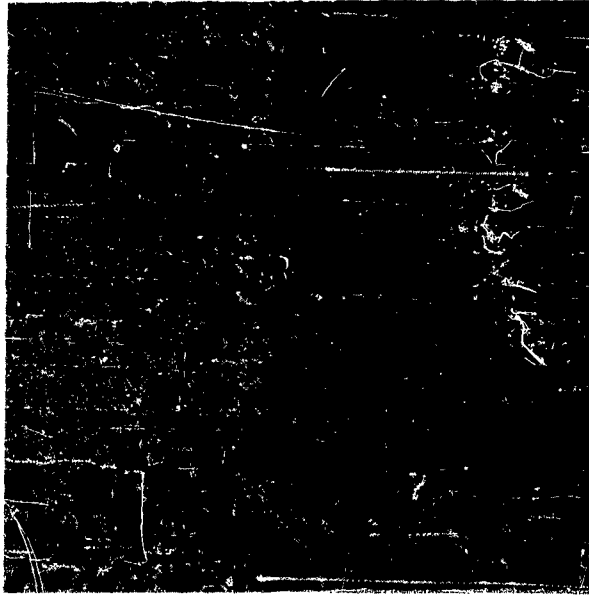
Figure 80-- One Hour Exposure (Neg. MS-253, Replica 1536A)

WADC TR 54-222

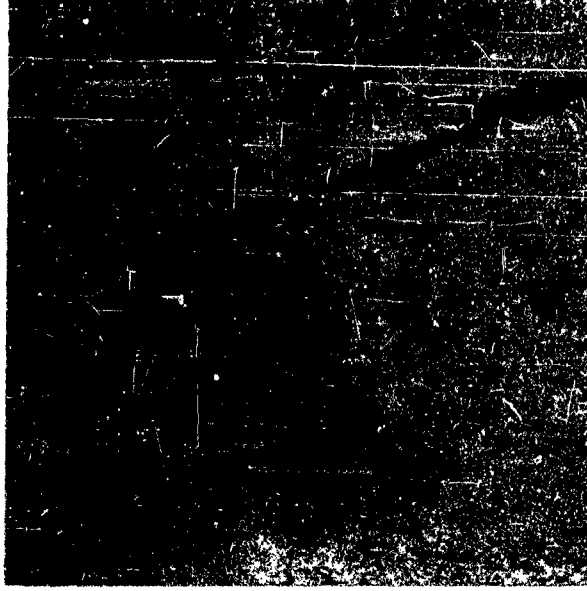
Figure 81-- Two Hour Exposure (Neg. MS-254, Replica 1536B)

145

Electronmicrographs of the Surface of Very High Purity Magnesium (#67535) after Exposure to Distilled Water. (Pretreatment A. Replica Technique A.)



7200 X



3600 X



Figure 82 -- Four Hour Exposure  
(Neg. MS-255, Replica 1539)

WADC TR 54-222

Figure 83 -- Twenty-four Hr. Exposure  
(Neg. MS-248, Replica 1535)

146

Electronmicrographs of the Surface of Very High Purity Magnesium (#67535) after One Hour's Exposure to 0.5N Na<sub>2</sub>CrO<sub>4</sub> Soln. (Film Removal Technique A. Replica Technique A.)

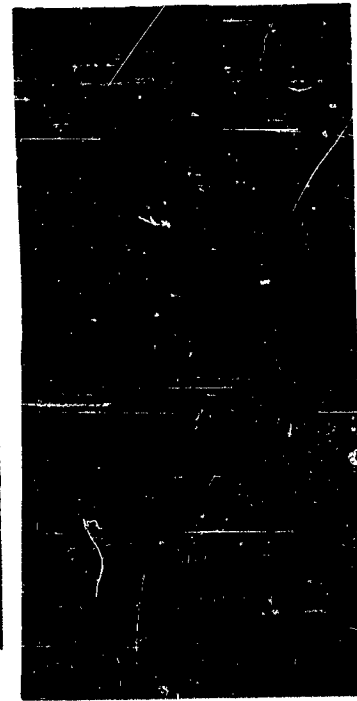
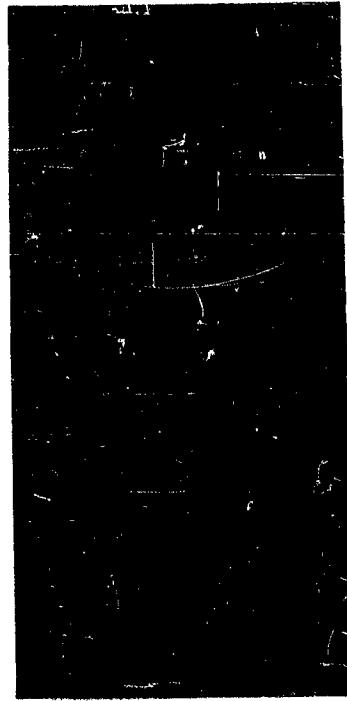
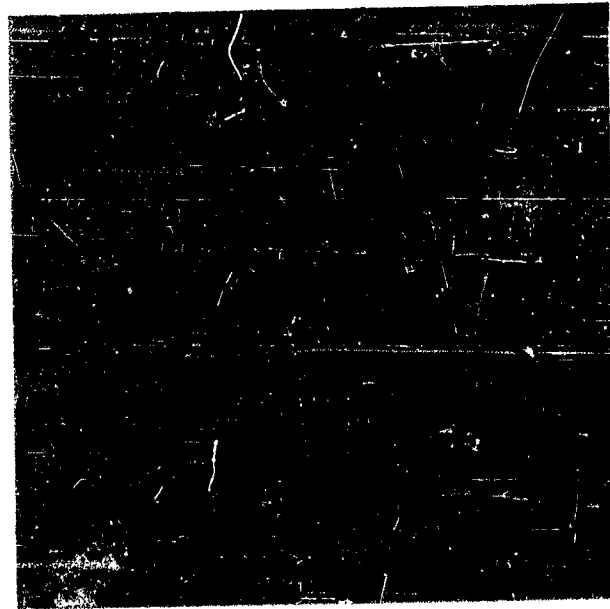
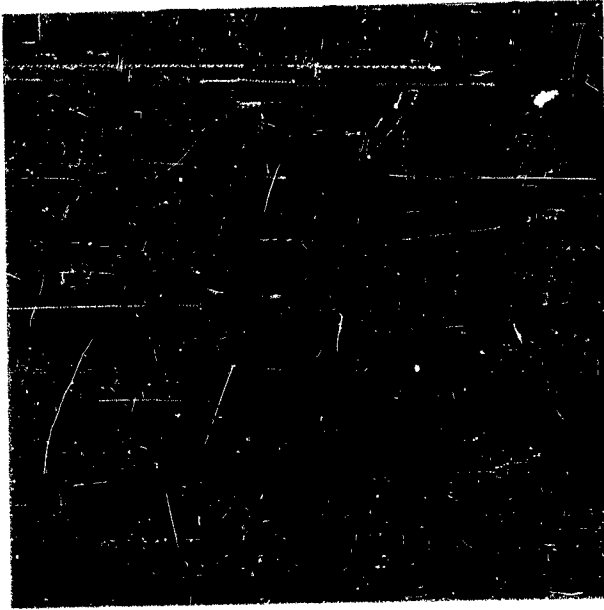


Figure 85 -- (Neg. MS-271, Replica 1545, Specimen Screen 1.)

Figure 84 -- (Neg. MS-270, Replica 1545, Specimen Screen 2.)

WADC TR 54-222

Figure 86

Electronmicrograph of the Surface of Very  
High Purity Magnesium (#67535) after Exposure  
to 0.01N NaCl-0.49N Na<sub>2</sub>CrO<sub>4</sub> for One Hour  
(Negative MS-297, Replica 1560)



14,400X



3,600X

Figure 87

Electronmicrograph of the Surface of Very  
High Purity Magnesium (#67535) after Exposure  
to 0.2N NaCl-0.3N Na<sub>2</sub>CrO<sub>4</sub> for One Hour  
(Negative MS-292, Replica 1558)



14,400X



3,600X

FIGURE 88

Electronmicrograph of the Surface of Very  
High Purity Magnesium (#67535) after Exposure  
to 0.05 N.  $\text{Na}_2\text{CrO}_4$  - 0.45 N. NaCl for One Hour  
(Negative MS-317, Replica 1579)



10,800 X



3,600 X

FIGURE 89

Electronmicrograph of the Surface of Very High Purity Magnesium (#67535) after Exposure to 0.01 N.  $\text{Na}_2\text{CrO}_4$  - 0.49 N. NaCl for One Hour (Negative MS-315, Replica 1580)



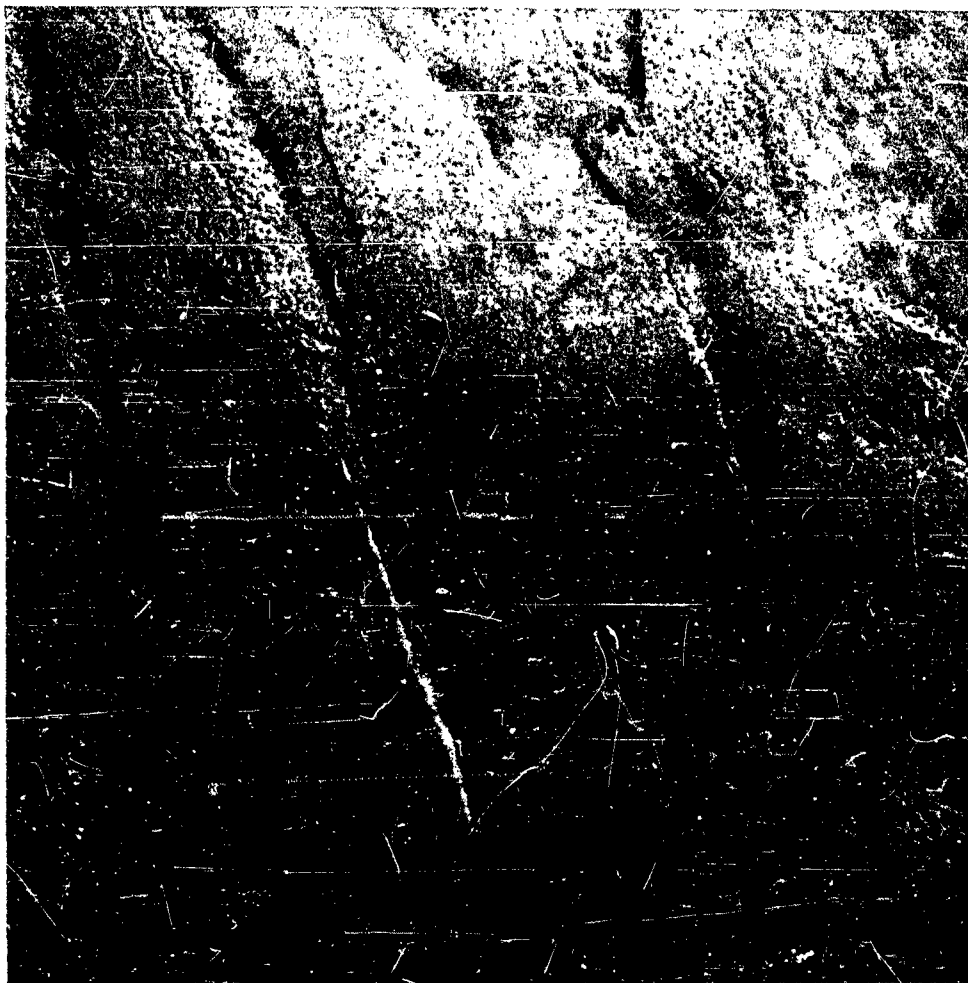
10,800 X



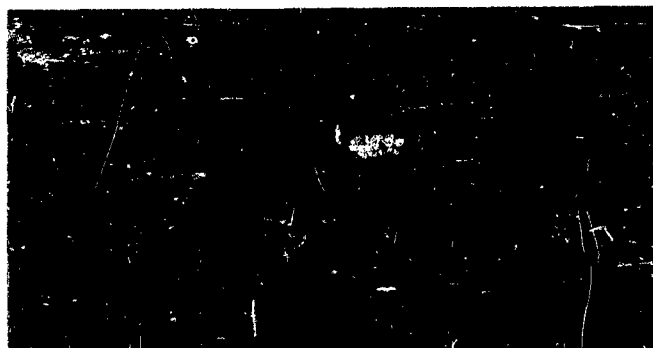
3,600 X

FIGURE 90

Electronmicrograph of the Surface of Very  
High Purity Magnesium (#67535) after Exposure  
to 0.001 N.  $\text{Na}_2\text{CrO}_4$  - 0.499 N. NaCl for One Hour  
(Negative MS-316, Replica 1581)



10,800 X



3,600 X

Electronmicrographs of the Surface of Very High Purity Magnesium (#67535) after One Hour's Exposure to 0.5N NaCl Solution. (Pretreatment A. Replica Technique A.)



7200 X



3600 X



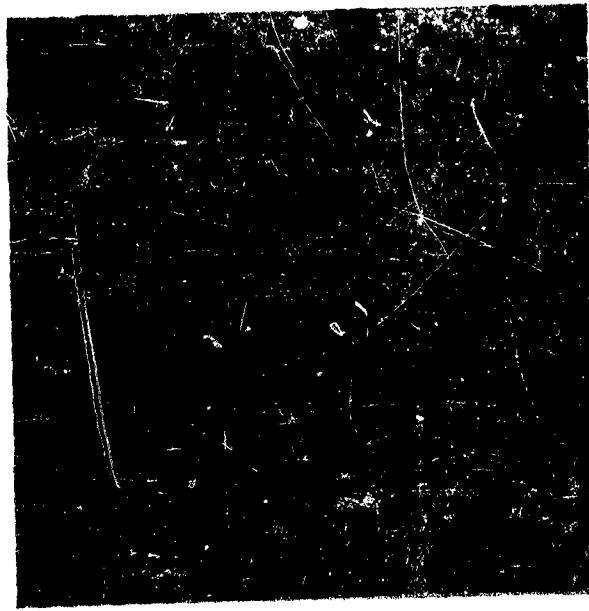
Figure 91 -- (Neg. MS-265, Replica 1546, Specimen Screen 3.)

WADC TR 54-222

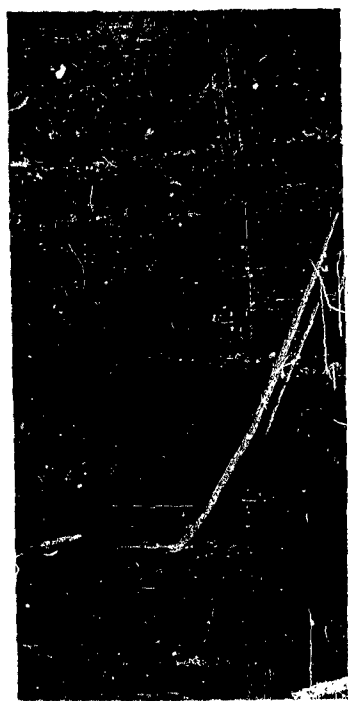
Figure 92 -- (Neg. MS-268, Replica 1546, Specimen Screen 4.)

153

Electronmicrographs of the Surface of Very High Purity Magnesium (#67535) after One Hour's Exposure to 0.5N NaCl Solution. (Pretreatment A. Replica Technique A.)



7200 X



3600 X

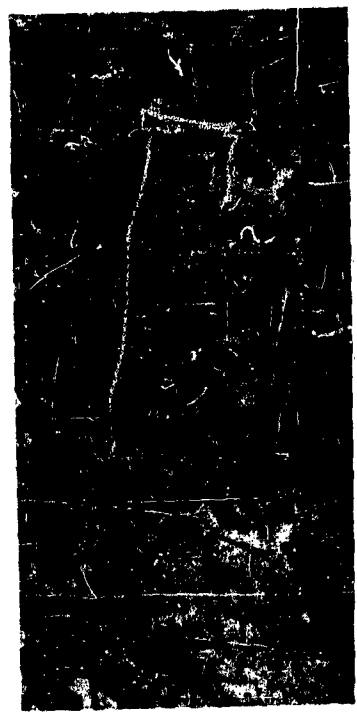


Figure 93 - (Neg. MS-267, Replica 1546, Specimen Screen 1.)

Figure 94 - (Neg. MS-261, Replica 1546, Specimen Screen 2.)

WADC TR 54-222

154